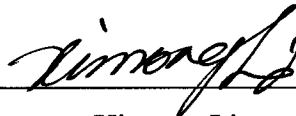


Super-Resolution TOA Estimation with Diversity Techniques for Indoor Geolocation Applications

A Dissertation
Submitted to the Faculty
of the
WORCESTER POLYTECHNIC INSTITUTE
in partial fulfillment of the requirements for the
Degree of Doctor of Philosophy
in
Electrical and Computer Engineering

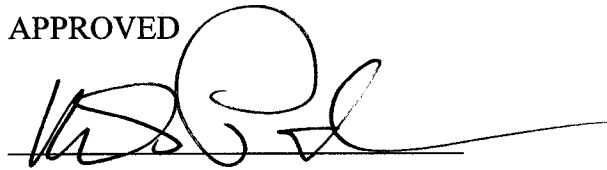
by



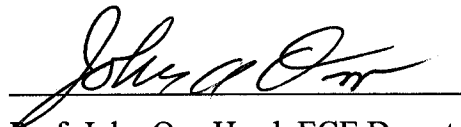
Xinrong Li

April 2003

APPROVED



Prof. Kaveh Pahlavan, Advisor



Prof. John Orr, Head, ECE Department

To my wife

Abstract

Recently, there are great interests in the location-based applications and the location-awareness of mobile wireless systems in indoor areas, which require accurate location estimation in indoor environments. The traditional geolocation systems such as the GPS are not designed for indoor applications, and cannot provide accurate location estimation in indoor environments. Therefore, there is a need for new location finding techniques and systems for indoor geolocation applications.

In this thesis, a wide variety of technical aspects and challenging issues involved in the design and performance evaluation of indoor geolocation systems are presented first. Then the TOA estimation techniques are studied in details for use in indoor multipath channels, including the maximum-likelihood technique, the MUSIC super-resolution technique, and diversity techniques as well as various issues involved in the practical implementation. It is shown that due to the complexity of indoor radio propagation channels, dramatically large estimation errors may occur with the traditional techniques, and the super-resolution techniques can significantly improve the performance of the TOA estimation in indoor environments. Also, diversity techniques, especially the frequency-diversity with the CMDCS, can further improve the performance of the super-resolution techniques. The CRLB derived with the single-path AWGN channel model for the traditional applications is not applicable in indoor

multipath channels. In this thesis, computer simulations based on the frequency-domain channel measurement data, collected with a standard channel measurement system in typical indoor application environments, are employed to evaluate the performance of various TOA estimation techniques. Our simulation results provide a clear insight into the achievable performance in indoor application environments. The simulation method presented in this thesis can be used in practice to conveniently establish empirical performance benchmarks when designing the super-resolution TOA estimation systems for indoor applications.

Acknowledgements

I am deeply indebted to my advisor Professor Kaveh Pahlavan for a lot more than his help, encouragement, and advice, and for a lot more than skills and knowledge that I learned from him. He has been much more than an advisor to me. His words of wisdom, insight, and philosophy are among the best things that I have learned.

Thanks are due to Professor Allen Levesque for his kind help over the last few years, to Professor Kevin Clements, Professor William Michalson, and Dr. Robert Tingley for their valuable comments as my thesis committee members, and to many professors at WPI from whom I have learned greatly.

I am also thankful to many friends for their help in the last few years, especially those in the CWINS, including Dr. Jacques Beneat, Duan Wang, Jeff Feigin, Bardia Alavi, and Emad Zand, who have provided hearty help in many different ways and shared numerous pleasant hours in the lab.

Words cannot express my gratefulness to my dear family for their care and support, especially to my grandma, my parents, and my wife, whose love is the source of my happiness and strength.

Table of Contents

Abstract	i
Acknowledgements	iii
Table of Contents	iv
List of Figures	vii
Chapter 1 Introduction	1
1.1 Indoor Geolocation	1
1.2 Objectives of the Thesis	4
1.3 Contributions of the Thesis	7
1.4 Outline of the Thesis	10
Chapter 2 Technical Aspects of Indoor Geolocation	13
2.1 Introduction	14
2.1.1 Geolocation Methods	14
2.1.2 System Architecture	18
2.2 Channel Characteristics for Indoor Geolocation	22
2.2.1 Impacts of Channel Characteristics	22
2.2.2 Measurement and Modeling of Indoor Channels	24
2.3 Location Sensing Techniques	28
2.3.1 Received Signal Strength (RSS)	29
2.3.2 Angle of Arrival (AOA)	31
2.3.3 Time of Arrival (TOA)	33
2.4 Positioning Algorithms	37
2.4.1 Traditional Techniques	38
2.4.2 Pattern Recognition Techniques	39
2.5 Summary and Conclusions	42

Chapter 3	TOA Estimation for Indoor Geolocation	45
3.1	Maximum Likelihood Estimation of TOA	46
3.2	Cramer-Rao Lower Bound for TOA Estimation	52
3.3	TOA Estimation in Multipath Channels	58
3.4	Estimation of TDOA	65
3.5	TOA/TDOA Measurement Methods	69
3.5.1	TOA/TDOA Measurement Methods for Overlaid Systems	72
3.6	Summary and Conclusions	77
Chapter 4	Super-resolution TOA Estimation Techniques	80
4.1	Introduction	81
4.2	Super-resolution Techniques	83
4.3	Issues in Practical Implementation	90
4.3.1	Improved Estimation of Correlation Matrix with Limited Measurement Data	94
4.3.2	Determination of Parameters L and L_p	99
4.3.3	Eigenvector Method	100
4.4	Diversity Techniques	101
4.5	Summary and Conclusions	108
Appendix 4.A	Derivations of Correlation Coefficients	111
4.A.1	Correlation Coefficients using Forward Estimation Method	111
4.A.2	Correlation Coefficients using Forward-backward Estimation Method	112
4.A.3	Correlation Coefficients with Frequency Diversity	114
Chapter 5	Performance Evaluation Based on Channel Measurements	116
5.1	Frequency-Domain Channel Measurement	117
5.2	Performance Evaluation Method	120
5.3	Performance of Super-resolution Techniques	123
5.4	Comparison of Super-resolution and Conventional Techniques	127
5.5	Effects of Time Diversity	133
5.6	Effects of Frequency Diversity	135
5.7	Summary and Conclusions	139

Appendix 5.A Measurement Sites and Scenarios	142
5.A.1 Descriptions of Measurement Sites	142
5.A.2 Descriptions of Measurement Scenarios	145
Appendix 5.B Cumulative Distribution Functions of the Ranging Errors	149
Chapter 6 Conclusions and Future Work	158
6.1 Conclusions	158
6.2 Future Work	163
Bibliography	165

List of Figures

2.1	Distance-based geolocation method. The radius of the dotted-line circle is the real distance between the MT and the RP; the radius of the solid-line circle is the estimated distance between the MT and the RP.	15
2.2	Direction-based geolocation method. The accuracy of the direction measurement is $\pm\theta_s$.	16
2.3	Functional block diagram of wireless geolocation systems.	18
2.4	Simulation result of indoor radio propagation using ray-tracing software. The location of transmitter is designated by a circle mark, and the location of receiver by a cross mark.	23
2.5	Multipath profile of indoor radio propagation channel.	26
2.6	Radio transmission in the environment of (a) macrocell and (b) microcell. All primary scatters, which cause multipath transmission, are assumed located inside the region of scatters.	32
2.7	Phasor diagram for narrowband signaling on a multipath channel.	35
3.1	The ML estimation of time delay by cross-correlation.	52
3.2	Numerical results of the CRLB of TOA estimation errors with different values of bandwidth and the product of bandwidth and observation time with respect to signal-to-noise power ratio (SNR). The carrier frequency is zero.	57
3.3	Power delay profiles with different channel profiles. (a) Single-path channel with propagation delay $D = 2 \times T_c$; (b) two-path channel with signal attenuation parameters $\alpha_0 = \alpha_1$, and propagation delays $\tau_0 = 2 \times T_c$ and $\tau_1 = 5 \times T_c$; (c) two-path channel with signal attenuation parameters $\alpha_0 = 0.6 \times \alpha_1$, and propagation delays $\tau_0 = 2 \times T_c$, and $\tau_1 = 2.5 \times T_c$.	61
3.4	Inter-frame spacing and medium access priorities.	72

3.5	Unicast data transfer mode for IEEE 802.11.	74
3.6	GRP-based TDOA method for IEEE 802.11 wireless LAN.	76
3.7	Fragmentation mode of IEEE 802.11.	77
4.1	The functional block diagram of the receiver of super-resolution TOA estimation systems. $\hat{H}(f)$ is the estimated channel frequency response, which is defined in (4.4).	88
4.2	The time-domain MUSIC pseudospectrum, obtained with a sample frequency-domain channel measurement data. The estimate of the TOA corresponds to the first peak of the pseudospectrum, marked by a small circle sign as shown on the plot.	89
4.3	The functional block diagram of super-resolution TOA estimation algorithms. $\hat{\mathbf{R}}_{xx}$ is the estimated correlation matrix, L_p is the estimated total number of multipath components defined in (4.1), and $S(\tau)$ is the time-domain pseudospectrum defined in (4.11).	92
4.4	Correlation coefficients of forward and forward-backward correlation matrices, with $\Delta f = 1\text{MHz}$, $(\tau_i - \tau_j) = 15\text{ns}$, $(\theta_i - \theta_j) = 0$, $f_0 = 900\text{MHz}$, and $L = 13$.	97
4.5	Correlation coefficients of forward and forward-backward correlation matrices, with the parameters $M = 9$, $\Delta f = 1\text{MHz}$, $(\theta_i - \theta_j) = 0$, $f_0 = 900\text{MHz}$, and $L = 13$.	98
4.6	General structure of TOA estimation with diversity techniques, general diversity combining scheme (GDCCS).	102
4.7	Estimation of correlation matrix with diversity techniques for super-resolution TOA estimation, correlation matrix based diversity combining scheme (CMDCCS).	103
4.8	Correlation coefficient with frequency diversity, with parameters $(\tau_i - \tau_j) = 15\text{ns}$, $(\theta_i - \theta_j) = 0$, and $f_c = 1\text{GHz}$.	106
4.9	Correlation coefficients of FCM and FBCM with and without frequency diversity, with parameters $\Delta f = 1\text{MHz}$, $(\tau_i - \tau_j) = 15\text{ns}$, $(\theta_i - \theta_j) = 0$, $f_c = 1\text{GHz}$, $L = 13$, and $\Delta F = 100\text{MHz}$.	107
4.10	Correlation coefficients of FCM and FBCM with and without frequency diversity, with parameters $M = 9$, $\Delta f = 1\text{MHz}$, $(\theta_i - \theta_j) = 0$, $f_c = 1\text{GHz}$, $L = 13$, and $\Delta F = 100\text{MHz}$.	108

5.1	Block diagram of the frequency-domain channel measurement system.	118
5.2	Frequency-domain channel measurement data obtained using the measurement system in Fig. 5.1.	125
5.3	Mean of ranging errors using the MUSIC and EV algorithms with the forward (FCM) and forward-back (FBCM) estimation of correlation matrix. The vertical line corresponds to plus and minus one standard deviation of the ranging errors about the mean.	126
5.4	Normalized time-domain channel responses obtained using three different techniques. The vertical dash-dot line denotes the expected TOA. The estimated TOA is marked on the time-domain channel response for each of the three techniques.	129
5.5	Mean of the estimation errors using three different techniques. The vertical line corresponds to plus and minus one standard deviation.	131
5.6	Percentages of the measurement locations where absolute ranging errors are smaller than 3 meters with three different TOA estimation techniques.	132
5.7	Mean and standard deviation of ranging errors without time diversity (EV/FBCM), with time diversity using the CMDCS (EV/FBCM/TD4-CMDCS) and GDCS schemes (EV/FBCM/TD-GDCS).	133
5.8	Cumulative distribution function of the absolute ranging errors for a bandwidth of 20MHz with frequency diversity.	138
5.A.1	A snapshot of Plant 7, Norton Co., Worcester, MA.	143
5.A.2	A snapshot of the Fuller Laboratories, WPI, Worcester, MA.	144
5.A.3	A snapshot of Schussler house, WPI, Worcester, MA.	144
5.A.4	Building layout with transmitter and receiver locations at the ground level of Plant 7, Norton Co., Worcester, MA.	146
5.A.5	Building layout with transmitter and receiver locations at Fuller Laboratories, WPI, (a) for indoor-to-indoor and outdoor-to-indoor scenarios, (b) for outdoor-to-second floor scenarios.	147
5.A.6	Building layout with transmitter and receiver locations at Schussler house, WPI, (a) for indoor-to-indoor and outdoor-to-indoor scenarios, (b) for outdoor-to-second floor scenarios.	148

Chapter 1

Introduction

1.1 Indoor Geolocation

In recent years, with the fast advancement of wireless communication technologies and the ever increasing penetration level of mobile computing devices into the people's daily life, there are increasing interests in the location-based applications and the location finding systems for indoor areas, that is, inside and around building environments [Bac97, Wer98, Bah00, Wan01, Pah02b]. The availability of the location information of mobile computing devices will enable the creation of a large number of new location-based applications. In commercial applications, there is an increasing need for location finding systems in indoor areas to track people with special needs, such as the elderly and children who are away from visual supervision, to navigate the blind, to locate in-demand personnel and equipments in hospitals, and to find people and specific items in large building complex, such as shopping mall and warehouses, among many other similar application scenarios. In public safety and military applications, location finding systems are needed to track inmates in prisons and to navigate policemen, firefighter, and soldiers to complete their missions inside and around buildings. In addition, location-awareness has been widely accepted as a key

feature of the next generation wireless systems. With the accurate location information of the users of mobile devices, such as laptop computers, cellular phones, and handheld PDAs, service providers may provide location-sensitive billing, location-specific advertisement, and the like location-aware services. The next generation location-aware mobile devices, being a powerful communication and/or computing devices carried by users at all time, will be often used in indoor environments. Therefore, it is important to employ the location finding techniques that can perform accurate location estimation in indoor environments.

The existing geolocation systems such as the Global Positioning System (GPS) and wireless enhanced 911 service system (E-911) also address the issue of location finding [[Kap96, Caf98], but these technologies are not designed for indoor applications, and they cannot provide accurate location information in indoor environments. For example, the GPS is designed for location finding applications in the open environments where direct visual contact exists between the GPS receiver device and at least four GPS satellites, and the GPS signals are not designed to penetrate into most of the constructions on the ground. Also, indoor geolocation systems are very different from the traditional location finding systems such as the GPS and the E-911 in many aspects, including application scenarios, operating environments, system requirements, and performance requirements. Therefore, there is a need for new location finding techniques to provide accurate location estimation in indoor environments, which are specifically designed for indoor applications to cope with the unique challenges and to

exploit the unique features therein. The indoor geolocation is emerging as a new important field for research and development.

In the past a few years, many researchers have worked on various aspects of the indoor geolocation. With the wide spread use of the traditional geolocation systems such as the GPS, location finding techniques have been studied for many years and now there is a rather rich literature on this subject. But very few of the existing studies on the location finding techniques are specific to indoor applications. Also, a large amount of research work has been conducted on the application layer aspects of indoor geolocation in the context of location-awareness and context-awareness of mobile computing devices by researchers with computer science background without too much concern about the underlying location finding systems, such as [Bac97, Ban02]. Many relevant references in the literature related to various aspects of the indoor geolocation will be surveyed in details and referred in later chapters where it is appropriate. In addition to the ever increasing interests in indoor geolocation in research community, a variety of the first generation indoor location finding products have been emerging into the market, such as those reported in [Wer98, Fon01] (search with Google for more relevant products with key words such as *indoor geolocation* and *local positioning*). In [Pah98], it was shown that the radio propagation channel characteristics have tremendous effects on the accuracy of the location estimation in indoor environments, which necessitates a devoted study on the location finding techniques for indoor applications. To help the growth of the emerging industry of the indoor geolocation,

there is a need for a scientific framework to lay a foundation for the design and performance evaluation of such systems.

This thesis is concerned with accurate location finding techniques and systems for applications in indoor environments, where the traditional geolocation systems cannot operate properly to provide accurate location estimation. In this thesis, we intend to conduct an in-depth study of the location finding techniques and systems, especially the time-of-arrival (TOA) estimation techniques, in order to provide a fundamental understanding of various issues related to indoor geolocation, and to provide a basic foundation for the design and performance evaluation of indoor geolocation systems. Detailed description of the objectives of this thesis is presented in the next section.

1.2 Objectives of the Thesis

As discussed in last section, the indoor geolocation system has different application scenarios and different system requirements than the traditional systems, and the traditional geolocation systems such as the GPS do not work properly in indoor environments. Also some unique features of indoor applications can be exploited to develop new techniques, which can be used to significantly improve the performance of the location finding systems in indoor environments. Therefore, there is a need for new and innovative techniques to handle the location finding problems in indoor environments. However, the indoor geolocation is a new emerging research field, and there is still no scientific framework to apply for the design of indoor location finding

systems. As part of the research project *Indoor Geolocation Science* funded by the National Science Foundation (NSF), the principal goal of this work is to provide a fundamental understanding of the issues related to the indoor geolocation techniques and systems, and to establish a foundation for the design and performance evaluation of indoor geolocation systems.

More specifically, three objectives are identified for this research work as explained in details in the following. The first objective is to conduct a systematic study of the location finding techniques and systems to identify the unique features and the challenging issues related to indoor geolocation, and to provide a fundamental understanding of this new emerging field. The research work presented in this thesis is only concerned with radiolocation systems. In radiolocation systems, the location coordinate of a target mobile unit is estimated from the location related characteristics of the radio signals communicated between spatially separated units. As a result the radio propagation channel has significant impacts on the performance of the location finding techniques and systems. To achieve the first objective, the system architectures and radiolocation techniques that can be used for indoor applications will be studied as well as the effects of indoor radio propagation channel characteristics on the performance of the location finding techniques and systems.

As we will present in Chapter 2, a location finding system consists of three functional modules, including location sensing, positioning, and display elements (or location-based applications). The location sensing devices measure the location metrics such as the time of arrival (TOA) and the angle of arrival (AOA) directly from the

received radio signals, which are related to the relative position of a mobile terminal with respect to a remotely located reference point with known location coordinate. As the second objective of this thesis, we intend to conduct comprehensive study of the technical aspects of the TOA-based location sensing techniques and their applicability to indoor applications. The TOA estimation techniques have been widely used in a number of traditional location finding systems such as radar, sonar, and the GPS. In this thesis, we first examine the existing TOA estimation techniques and study the applicability of these techniques to indoor applications. As we will present in this thesis, the unique characteristics of indoor radio propagation channels make it very challenging to accurately estimate the TOA with the traditional estimation techniques in indoor environments. Therefore, significant amount of efforts have been devoted in this thesis to explore new signal processing techniques to accurately estimate the TOA in indoor environments, including super-resolution techniques and diversity techniques. The super-resolution TOA estimation techniques are designed by applying the super-resolution spectrum estimation algorithms to the estimated frequency response of the multipath indoor radio propagation channels. The diversity techniques are used to further improve the performance of the super-resolution TOA estimation techniques in indoor environments.

Performance study, including comparative performance study and performance benchmarking among others, is one of the most important issues encountered in the design of signal processing techniques and systems. The performance study of the TOA estimation techniques in the realistic application scenarios provides an insight into the

achievable accuracy of indoor geolocation system. Therefore, as another objective we explore the channel measurement data based simulation methods to compare the performance of various TOA estimation techniques presented in this thesis and to provide a performance benchmark of various techniques that can be achieved in typical indoor application environments. The channel frequency response can be readily measured with a frequency-domain channel measurement system so that the channel measurement data based simulation method presented in this thesis provides a convenient means to establish performance benchmarks when designing super-resolution TOA estimation based indoor location finding systems.

1.3 Contributions of the Thesis

The indoor geolocation is a new emerging research field, and is concerned with accurate location finding techniques and systems in indoor environments, where the traditional geolocation systems do not work properly. The original work presented in this thesis has made contributions to the literature of this new emerging field in the following aspects. First, an overview of a wide variety of technical aspects and challenging issues of indoor geolocation is presented, which provides a basic foundation for the design and performance evaluation of indoor geolocation systems, and forms a basis for further research work in this field. The original work in this regard is presented in Chapter 2 and has been published in [Pah02b].

Second, the traditional TOA and TDOA (time-difference-of-arrival) estimation techniques are presented, and the impacts of indoor radio propagation channels on the

performance of traditional techniques are studied in details. It is shown that due to the complexity of the multipath indoor radio propagation channels, dramatically large estimation errors may occur with the traditional estimation techniques, and the Cramer-Rao lower bound (CRLB) derived for the traditional application scenarios is no longer applicable in indoor environments. Our research provides a fundamental understanding of the challenging issues involved in the TOA estimation in indoor environments. Relevant results are presented in Chapter 3, and have been published in [Li02].

Third, for the dedicated geolocation systems, the TOA can be easily measured with a synchronized transceiver method or a round-trip TOA method, but direct application of these simple methods is difficult for overlaid systems. A non-synchronized method is designed to measure TOA/TDOA with the WLAN (wireless local-area network) signals, which is presented in Chapter 3 and has been published in [Li00a, Li00b]. Such a method can be used to overlay the geolocation functionality onto the existing wireless LANs without significant modification to the existing infrastructure and signaling formats.

Forth, the super-resolution spectral estimation techniques are applied to the TOA estimation in the multipath channels on the basis of the frequency-domain representation of the multipath channel models. The issues in the practical implementation of the super-resolution TOA estimation techniques are studied and several improvement techniques including diversity techniques are proposed to improve the performance of the super-resolution techniques. Diversity techniques and two diversity combining schemes are presented and studied for use with the super-resolution

techniques. The effects of the frequency diversity techniques are analyzed, and it is shown that frequency diversity can further improve the performance of the super-resolution techniques. The original work in this regard is presented in Chapter 4, and has been published in [Li01a, Li01b].

Fifth, a channel measurement data based performance evaluation method is proposed and employed in this thesis to compare and benchmark various TOA estimation techniques in typical indoor application environments. There is no suitable indoor radio propagation channel model available in the literature to evaluate the performance of the TOA estimation techniques in indoor environments. In our research, the super-resolution and the diversity techniques are evaluated and compared with the traditional techniques using the computer simulations based on the empirical channel measurement data. Our simulation results provide a clear insight into the achievable performance of various TOA estimation techniques in the realistic indoor application environments, while the CRLB performance bound obtained for the traditional applications cannot be used to benchmark the performance of the TOA estimation techniques in indoor environments due the existence of the no-line-of-sight (NLOS) situations. The measurement data based simulation method that we employed can be used in practice to establish empirical performance benchmarks for the real implementation of the super-resolution TOA estimation based indoor geolocation systems. The relevant results in this regards are presented in Chapter 5 and have been published in [Li01b, Li02].

1.4 Outline of the Thesis

The rest of the thesis is organized as follows. In Chapter 2, we present a brief overview of a wide variety of the technical aspects and challenging issues involved in the design and performance evaluation of indoor geolocation systems, which provides a fundamental understanding of indoor geolocation systems, and forms a basis for the research work presented in the later chapters. In Section 2.1, an introduction of geolocation methods and system architectures is first presented. Then the technical aspects, challenging issues, and potential research topics related to radio propagation channels, location sensing techniques, and positioning algorithms for indoor geolocation applications are discussed in details in the following three sections, respectively.

This thesis is mainly concerned with the TOA-based radiolocation techniques and systems for indoor applications so that starting from Chapter 3 we will focus on the TOA estimation techniques. In Section 3.1 and 3.2, we first present the maximum likelihood TOA estimation techniques and the CRLB, respectively, which are derived for the traditional applications by modeling the radio propagation channel as the single-path AWGN channels. Since the indoor radio propagation channel is known as severe multipath channel, in Section 3.3 we study the effects of the multipath propagation on the performance of the TOA estimation techniques in indoor environments. The TDOA is another time delay-based location metrics that can be used in place of the TOA. In traditional applications both location metrics have similar estimation techniques and performance. Therefore, in Section 3.4 we also briefly study the estimation techniques

as well as the performance of the TDOA estimation in single-path and multipath channels. Our preliminary analysis will show that the TDOA becomes less appropriate than the TOA in the multipath channels. At last, in Section 3.5, the issues involved in the practical measurement of the TOA with spatially separated mobile units are discussed and the techniques for synchronizing and coordinating the remotely located transmitter and receiver to measure the TOA/TDOA are presented for both dedicated and overlaid location finding systems.

In Chapter 4, we study the super-resolution techniques that can be used in the multipath indoor radio propagation channels to more accurately estimate the TOA than the traditional techniques. In this chapter, the background and theoretical development of the MUSIC super-resolution TOA estimation technique are first presented in Section 4.1 and 4.2, respectively. Then in Section 4.3 we present the issues in the practical implementation of the super-resolution techniques, and analyze the effects of several techniques that can be used in practice to improve the performance of the super-resolution techniques. At last, in Section 4.4 diversity techniques and diversity combining schemes are introduced and analyzed. From the analysis it is shown that the frequency diversity technique can significantly enhance the performance of the super-resolution TOA estimation techniques. To keep the presentation of this chapter concise and easy to follow, some detailed mathematical derivation is omitted from the main content, but presented in the appendix at the end of the chapter.

In Chapter 5, we evaluate the performance of various TOA estimation techniques presented in Chapter 3 and 4 with the computer simulations based on

channel measurement data, which is collected in typical indoor application environments. The channel measurement system is first introduced in Section 5.1, followed by a description of the performance evaluation method employed in this thesis. In Section 5.3, several super-resolution techniques presented in Chapter 4 are evaluated and compared with simulation results. In Section 5.4, to demonstrate the usefulness of the super-resolution techniques, the super-resolution techniques are compared with two conventional TOA estimation techniques. At last, the effects of the time and frequency diversity techniques are evaluated in Section 5.5 and 5.6, respectively. A description of the measurement sites and scenarios are presented in Appendix 5.A, and the cumulative distribution functions of the ranging errors with different TOA estimation techniques are presented in Appendix 5.B for the reference purposes.

At last, the thesis is concluded with conclusions and a discussion of future work in Chapter 6.

Chapter 2

Technical Aspects of Indoor Geolocation

In recently years, there are increasing interests in location-based applications in indoor environments. Location finding systems such as the GPS have been widely used for many years. The traditional geolocation systems are not designed for indoor application, and they cannot provide accurate location estimation in indoor environments. As compared with the traditional systems, the indoor geolocation systems have different application scenarios, operating environments, system requirements, and performance requirements, among many others. Currently, there exists a rich literature on location finding techniques. But unfortunately, very few of the existing studies on this subject are specific to indoor applications. The indoor geolocation is emerging as a new important field for research, which deserves a devoted in-depth study. In this chapter we present a brief overview of a wide variety of the technical aspects and challenging issues involved in the design and performance evaluation of indoor geolocation systems, which provides a fundamental understanding of indoor geolocation systems, and forms a basis for the research work presented in the

later chapters. In Section 2.1, we first present an introduction of geolocation methods and system architectures. Then technical aspects, challenging issues, and potential research topics related to radio propagation channels, location sensing techniques, and positioning algorithms for indoor geolocation applications are discussed in details in the following three sections, respectively.

2.1 Introduction

2.1.1 Geolocation Methods

The geolocation method, that is, the method used by geolocation systems to find the location of a mobile terminal (MT), can be classified into three categories: dead-reckoning, proximity method, and radiolocation method [Caf99]. The dead-reckoning method is based on accurate measurement of the MT's acceleration, velocity, and direction of movements using various inertial sensors of the MT, including gyroscopes, accelerometers, and magnetic compasses among others. Given a known starting position of the MT, the trajectory of the MT can be easily determined with continuous accurate measurement of the acceleration, velocity, and movement direction of the MT. Since the dead-reckoning method relies on accurate update of the MT's location coordinates with respect to the previous location estimates, the estimation error tends to accumulate. With proximity location method, the MT's location is roughly determined to the proximity of the nearest fixed reference points (RP). The detection of proximity to a fixed RP can be accomplished through a large variety of techniques including magnetic sensors and conventional radio transmitters and receivers. The performance

of the proximity method depends on the coverage of each fixed RP as well as the density of the RP infrastructure network. The radiolocation system estimates the MT's location by measuring various characteristics, such as received signal strength (RSS), angle of arrival (AOA), and time of arrival (TOA) that we will discuss later in this chapter, of the radio signals transmitted between the MT and a number of fixed RPs. This thesis is mainly focused on the radiolocation related techniques and systems for indoor geolocation applications.

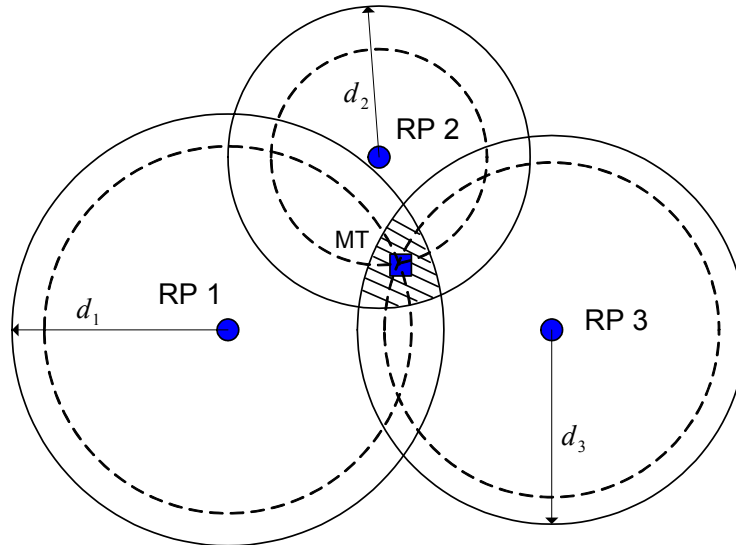


Figure 2.1: Distance-based geolocation method. The radius of the dotted-line circle is the real distance between the MT and the RP; the radius of the solid-line circle is the estimated distance between the MT and the RP.

The radiolocation method can be further categorized into two classes: distance-based method and direction-based method. The distance-based method relies on the

estimation of the distance between the MT and a number of fixed RPs. As shown in Fig. 2.1, each distance measurement will geometrically determine a circle, centered at the RP, which indicates possible location of the MT. Accurate distance measurements from the MT to a minimum of three RPs provide a position fix and given the location coordinates of the RPs, the MT's location coordinate can be easily determined. Usually, the distance estimates based on the TOA measurements in radiolocation system are larger than the true distance between the transmitter and the receiver [Mor95], in which case three distance measurements determine a region of the possible MT locations as depicted in Fig. 2.1, which is known as the region of uncertainty [Tek98]. Otherwise, if the estimated distance is smaller than the real distance, three distance measurements may not be able to provide a position fix nor a region of uncertainty. As a result, more than three RPs are normally needed to improve the location accuracy.

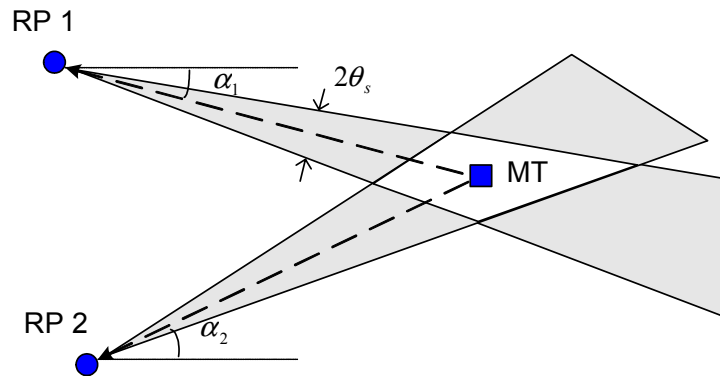


Figure 2.2: Direction-based geolocation method. The accuracy of the direction measurement is $\pm\theta_s$.

The direction-based radiolocation method uses simple triangulation to locate the transmitter as shown in Fig. 2.2. Each RP measures the arrival direction of the received signals, *i.e.*, the angle of arrival (AOA), from the MT, which is indicated by the dashed line connecting the MT and the RP in the diagram in Fig. 2.2. Accurate direction measurements from the MT to a minimum of two RPs provide an exact position fix and given the location coordinates of the RPs, the MT location coordinate can be easily determined. If the accuracy of the direction measurement is $\pm\theta_s$, AOA measurement at the RP receiver will restrict the MT position inside the beam around the dashed line-of-sight (LOS) signal path with an angular spread of $2\theta_s$. The AOA measurements at two RP receivers will provide a position fix within the overlapping region of the two beams as illustrated in Fig. 2.2. We can clearly observe that given the accuracy of the AOA measurement, the accuracy of position estimation degrades with increasing distance between the RP and the MT. On the other hand, the accuracy of the position estimation depends upon the MT position with respect to the RPs. For example, when the MT lies between the two receivers, two AOA measurements will not be able to provide a position fix. As a result, more than two RPs are normally needed to improve the location accuracy. The techniques and the performance of the TOA-based distance estimation and the AOA-based direction estimation will be further discussed later in this chapter in Section 2.3.

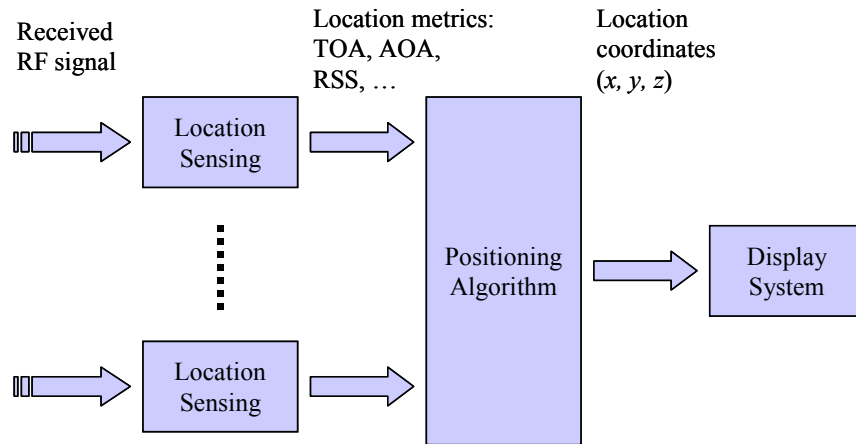


Figure 2.3: Functional block diagram of wireless geolocation systems.

2.1.2 System Architecture

Figure 2.3 illustrates the functional block diagram of a wireless geolocation system. The main elements of the system are a number of location sensing devices that measure/estimate the metrics related to the relative position of a given MT with respect to a known RP, a positioning algorithm that processes the metrics reported by location sensing elements to estimate the location coordinate of the MT, and a display system that illustrates the location of the MT to users. The location metrics may indicate the approximated arrival direction of the signal or the approximated distance from the MT to the RP to be used in the direction-based or the distance-based geolocation methods, respectively, which are discussed in the previous section. The angle of arrival is the common metric used in the direction-based systems. The received signal strength, the carrier signal phase, and the time of arrival of the received signal are the metrics used for the estimation of the distance. As the measurement of the metrics becomes less reliable, the complexity of the positioning algorithm increases. The display system can

simply show the coordinates of the MT or it may identify the relative location of the MT in the layout of an area. This display system could be a software residing in a private PC or a mobile location-finding unit, or a locally accessible software in a local area network (LAN) or a universally accessible service on the web. Obviously, as the horizon of the accessibility of the information increases the design of display systems becomes more complex.

The overall architectures of geolocation systems can be generally grouped into two categories: mobile-based architecture and network-based architecture. For both cases, multiple RPs are needed to geometrically locate a MT based on the measurements of relative distance or direction from the MT to the RPs as we presented in the previous section. With mobile-based architecture, the MT performs all three functions shown in Fig. 2.3, *i.e.*, location sensing, positioning, and display. The MT extracts location metrics from the received radio signals that are transmitted by the RPs, calculates its own location coordinate, and then displays it to the MT user. The mobile-based architecture is used when the location information is mainly used by the MT user as in most of the GPS-based applications. But if needed, the MT's location coordinate can also be forwarded to a central site, such as Geolocation Control Station (GCS), to provide other location-based applications and services. With network-based architecture, the RP performs location sensing by measuring received radio signal from the MT. Then the RPs report location metrics to the GCS, where the MT's location coordinate is estimated using a positioning algorithm. The selection of the geolocation system architecture depends on where the geolocation information is needed, *i.e.*, in the

MT or in the GCS, and some other implementation considerations for specific application scenarios. For example, with network-based architecture, the MT can be implemented much simpler than with mobile-based architecture since the MT does not need to perform location sensing and positioning functions with the network-based architecture.

There are two basic approaches to design a wireless geolocation system. The first approach is to develop new signaling system and network infrastructure of the location sensors focused primarily on location-finding applications. The second approach is to use an existing wireless network infrastructure to locate the MT. The advantage of the first approach is that physical specification, and consequently the quality of the location sensing results, is under the control of designers. With this approach, the MT can be designed as a very small wearable tag or a sticker and the density of sensor infrastructure can be adjusted to the required accuracy of location-finding applications. The advantage of the second approach is that it avoids the expensive and time-consuming deployment of the sensor infrastructure, and no significant change to the physical layer hardware component is needed. Such a system, however, needs to use more intelligent positioning algorithms at the application layer to compensate for the low accuracy of the measured location metrics. Both approaches have their own markets, and design work on both technologies has been pursued in the past a few years [Caf98, Pah02a, Wer98, Bah00].

From the Fig. 2.3, we can observe that the performance of wireless geolocation systems, that is the accuracy of the estimate of location coordinates, are determined by

the quality of the received radio signal, the performance of the location sensing elements, and the performance of the positioning algorithms in sequence. The indoor radio propagation channel characteristics are very different from that of the channels encountered by the traditional wireless geolocation systems including the GPS, sonar, radar, and etc. Thus the location sensing techniques used in the traditional wireless geolocation systems may not provide the optimum performance in indoor environments and on the other hand, the radio propagation channel models used in developing location sensing techniques for the traditional applications are not suitable for indoor applications. To design optimum location sensing techniques and to examine the performance of different signaling techniques and geolocation approaches, the indoor radio propagation channel needs to be studied and modeled through empirical channel measurements.

As we just mentioned, the performance of location sensing elements is largely determined by the radio propagation channel characteristics. Thus in indoor application environments the estimates of location metrics, that is the output of location sensing elements, show different statistical characteristics as compared with the traditional geolocation systems. As a result, traditional positioning algorithms may not provide optimum performance in indoor environments, which necessitates the design of new positioning algorithms for indoor geolocation systems. In the next three sections, we address with more details the technical issues related to channel measurement and modeling, location sensing techniques, and positioning algorithms, respectively, for wireless indoor geolocation systems.

2.2 Channel Characteristics for Indoor Geolocation

In order to design better techniques and evaluate system performance, we need to study, by measurement and modeling, how channel characteristics would affect the accuracy of location sensing elements and positioning algorithms. In this section we briefly review the effects of indoor radio propagation channel characteristics on the estimation of location metrics, and the methods for measurement and modeling of indoor radio propagation channels for geolocation applications. More detailed discussion about the effects of channel characteristics on the estimation of location metrics is deferred and will be presented in Section 2.3.

2.2.1 Impacts of Channel Characteristics

The indoor radio propagation channel is normally characterized as severe multipath, low availability of line of sight (LOS) signal propagation path between the transmitter and the receiver, and site-specific [Pah95].

Figure 2.4 shows a simulation result of indoor radio propagation using ray-tracing software. In ray-tracing simulations of radio propagation channels, the radio signal is modeled as rays as in the study of optics. Rays of radio signal emanated from the transmitter reach the receiver after transmission through and reflection from walls, or other signal scattering objects, while scattering objects have different signal attenuation parameters for transmission and reflection. As a result a large number of rays of radio signal will arrive at the receiver with varying arrival time and signal power

through different propagation path. This propagation phenomenon is known as multipath propagation.

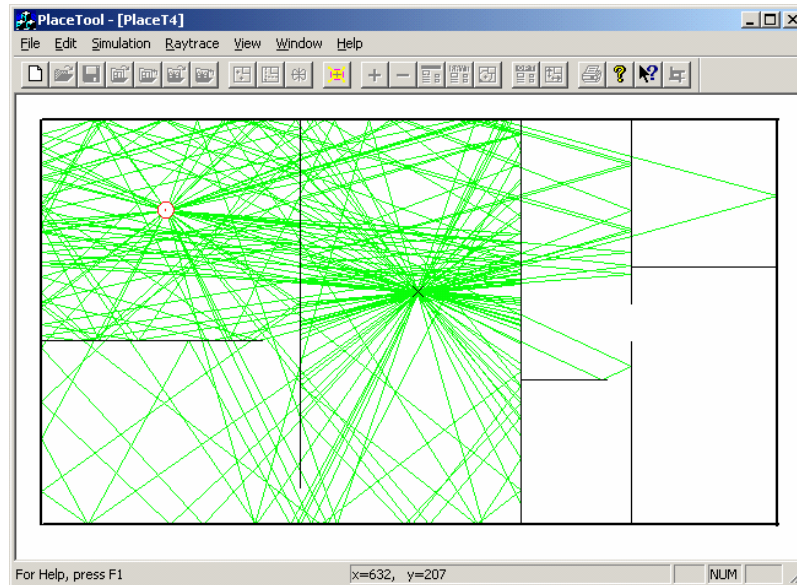


Figure 2.4: Simulation result of indoor radio propagation using ray-tracing software. The location of transmitter is designated by a circle mark, and the location of receiver by a cross mark.

In geolocation application, we are only interested in estimating the arrival time or the arrival direction of the signal arriving through the direct line-of-sight (DLOS) radio propagation path for distance-based or direction-based geolocation methods, respectively, which were discussed in Section 2.1. But in severe multipath propagation conditions, the multipath components will interfere with the DLOS signal, which makes the accurate measurement of location metrics a very challenging task. Normally large estimation errors of location metrics are resulted from multipath interferences. When

the DLOS is not detectable, which is known as no-LOS (NLOS) situations, dramatically large errors occur in location sensing results since the arrival time of a multipath component is detected erroneously as the arrival time of the DLOS signal. The NLOS situation can be resulted from a number of different conditions. For example, if the DLOS signal path between the transmitter and the receiver is obstructed when measuring the TOA, low receiver sensitivity and small receiver dynamic range may easily result in the NLOS situation [Pah98]. Thus two major sources of errors in the measurement of location metrics in indoor environment are the multipath interference and the NLOS situation.

In addition, the site-specific nature and the time dependent fading effect, which is caused by random movement of scattering objects (such as people) in the application environment, of the indoor radio propagation channels make it difficult to model and simulate the channel and also makes the geolocation sensor network infrastructure ad hoc in nature. The site-specific sensor network infrastructure is generally difficult to deploy, which necessitates an in-depth study of the system architectures and the practical deployment methods and rules for the ad hoc sensor networks in indoor application environment.

2.2.2 Measurement and Modeling of Indoor Channels

Empirical channel measurement is essential to study and model the radio propagation channel and to check the validity of the modeling results. In the literature various measurement results of indoor radio propagation channel have been reported for

frequencies from 1 to 60 GHz for telecommunications applications [Pah95]. The same channel measurement systems can be used for geolocation applications, but the measurement results collected for telecommunications applications cannot be used directly for geolocation applications because they do not have a well-calibrated estimate of the AOA, RSS, and/or TOA of the DLLOS signal, and an accurate measurement of the physical direction and/or distance from the transmitter to the receiver. A new set of short-range wide-band measurement data of indoor radio propagation channel has been collected and calibrated in CWINS for the TOA-based geolocation applications [Ben99], which is used in this thesis to evaluate the performance of the TOA estimation techniques. More indoor radio propagation channel measurements are needed to study and model the channel for wireless indoor geolocation systems using different location sensing techniques including the RSS, TOA, and AOA as well as different combinations of these techniques.

Radio propagation channel models are developed to provide a means to analyze the performance of a wireless receiver. Performance criteria for telecommunication and geolocation systems are quite different as discussed in [Pah98]. The performance criterion for telecommunication systems is the bit error rate (BER) of the received data stream while for geolocation systems performance measure is the accuracy of the estimated location coordinates. The accuracy of location estimation is a function of the accuracy of location sensing and the accuracy of positioning. Thus channel models for geolocation applications have to reflect the effects of channel behavior on the estimated

value of the location metrics at receivers, such as the RSS, TOA, AOA, or any combination of these metrics.

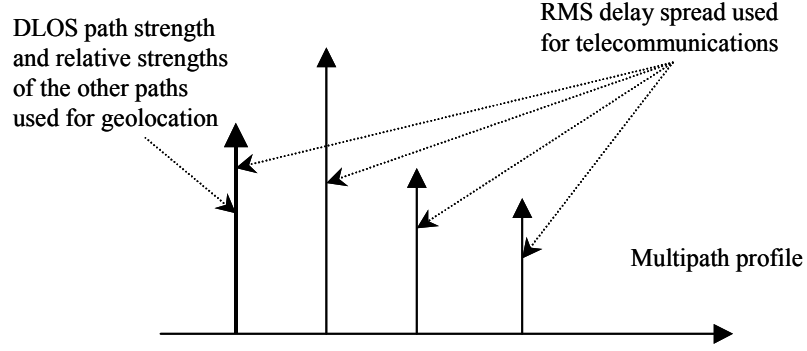


Figure 2.5: Multipath profile of indoor radio propagation channel.

While we do not have any good models for the multipath characteristics of the indoor radio propagation channels for geolocation applications, three classes of recent statistical modeling approaches can be employed to develop reliable models in the future, which are the wideband 2D multipath modeling, the 3D geometrical statistical modeling, and the 3D measurement-based statistical modeling [Pah02b]. In the measurement-based 2D statistical modeling, the measurement data are used to define a discrete multipath profile similar to the one shown in Fig. 2.5, which is expressed mathematically in the following form

$$h(\tau) = \sum_{k=0}^{L_p-1} \alpha_k \delta(\tau - \tau_k), \quad (2.1)$$

where L_p is the number of multipath components, and $\alpha_k = |\alpha_k| e^{j\phi_k}$ and τ_k are the complex amplitude and the propagation delay of the k th path, respectively. The

measurement systems for this approach are the same as the measurement systems used for telecommunication applications [Pah98, Ben99]. However, these systems are calibrated for accurate measurement of the arrival time of the DLOS signal path and for each measurement the physical distance between the transmitter and the receiver is accurately recorded. Preliminary measurement and modeling work in this field is reported in [Kri99, Ben99]; larger calibrated measurement databases and more practical multipath models need further investigation.

In the 3D modeling, the mathematical model of the multipath radio propagation channel is represented by

$$h(\tau, \theta) = \sum_{k=0}^{L_p-1} \alpha_k \delta(\tau - \tau_k, \theta - \theta_k), \quad (2.2)$$

where θ_k is the arrival direction of the k th path [Tin01]. While in the 2D modeling each path was associated with an arrival time, in the 3D modeling each path is associated with an arrival time and an arrival direction. The 3D models can be developed either based on the geometrical statistical analysis of the arrival paths from different directions or based on empirical 3D channel measurement data. The 3D geometrical statistical models, developed for smart antenna applications, use an analytical approach to relate propagation parameters to the structure of scattering in the application environment [Has02]. In this approach, a mathematical description of radio propagation based on statistical building features and a geometric optics approximation of Maxwell's equations is employed to derive the relevant radio propagation models such as the distributions of the arrival time, direction, and strength of arriving paths. Further research in this area is needed to develop statistical models for the arrival time of the

DLOS path and its relation with respect to other paths to make them useful for the performance analysis of geolocation systems.

In the 3D measurement-based statistical modeling, results of the measured characteristics of radio propagation channels are used to develop models suitable for the performance evaluation of the geolocation systems based on the AOA, TOA and RSS. The major challenge for this approach is the implementation of a system to measure the 3D characteristics of radio channels. Recently, two techniques have been studied for this purpose. Using the first technique, a directional antenna is mechanically rotated to measure the strength of the signal arriving from different directions, while using the second technique, a set of eight channel impulse responses are measured using an antenna array and the AOA are calculated using signal processing techniques [Tin01]. Preliminary 3D modeling of an indoor radio propagation channel using a limited database in a building is available in [Tin01]. More extensive measurement and modeling in this field are needed to develop reliable channel models for indoor geolocation applications.

2.3 Location Sensing Techniques

As we discussed in Section 2.1, the location sensing elements measure the RSS, AOA and TOA as location metrics. The indoor radio propagation channel suffers from severe multipath propagation and heavy shadow fading condition so that the measurements of the RSS and AOA provide a less accurate metrics than that of the TOA [Pah02a]. As a result, similar to the GPS systems, independent systems designed

for indoor geolocation normally employ the more accurate TOA as the location metric. Systems using existing infrastructures installed for wireless LAN or the 3G indoor systems may use the measurements of RSS, AOA, TOA, or any combination of these metrics to fully exploit the existing hardware/software implementation designed for the traditional telecommunication applications [Bah00]. For example, in wireless communication systems, the RSS information is usually easily accessible, thus it makes sense to find ways to exploit the RSS information to further improve the geolocation performance. As a result, although this thesis is focus on the TOA-based geolocation techniques, issues related to the estimation of the RSS and AOA are briefly discussed in the following together with the issues related to the estimation of the TOA.

2.3.1 Received Signal Strength (RSS)

The received signal strength (RSS), *i.e.*, the received signal power, can be easily measured at the receiver. The RSS is related to the distance between the transmitter and the receiver mathematically in the form of path loss models [Pah95]. The path loss model characterizes the signal power attenuation level as the signal travels from the transmitter to the receiver. Assuming the path loss model is known *a priori*, with the knowledge of the transmitted signal power at the receiver the distance between the transmitter and the receiver can be calculated at the receiver from the known path loss model by measuring the received signal strength. Such a distance estimation method is known as the RSS-based ranging technique. The same as the TOA-based geolocation method that we presented in Section 2.1, the RSS-based estimation of the distances

between a mobile terminal and a minimum of three reference points can be employed to estimate the position of the mobile terminal.

A wide variety of path loss models have been developed for different environments, each with different values of model parameters or different parameters and mathematical function forms [Pah95]. In indoor environment the path loss model is highly site-specific. For example, the value of power-distance gradient, which is a parameter of path loss models, vary in a wide range between 15-20 dB/decade and a value as high as 70 dB/decade [Pah95]. Also the received signal strength of radio signals demonstrates fast-fading phenomenon caused by multipath propagation with for example as large as 30 dBm fluctuation in small local movement, and time-dependent fading phenomenon caused by dynamically changing channel conditions, such as random movement of people over time in the application environments, with for example as large as 20 dBm fluctuation in seconds [Ber99]. As a result of the complexity of the indoor radio propagation channel, in practice using the RSS-based geolocation method necessitates the estimation of the path loss model of the specific application environment during the system installation or the initialization phase to compensate for the site-specific nature of the indoor radio propagation channel, and frequent reestimation of the path loss model to cope with the dynamically changing environment. Thus an immediate conclusion is that the RSS-based geolocation method is not a suitable choice for accurate indoor location finding systems.

Some authors have studied various techniques to improve the performance of the RSS-based geolocation method including the fuzzy logic algorithms [Son94] and

the premeasurement-based pattern recognition techniques [Bah00]. In essence, all these improvement techniques try to improve the location accuracy by designing more intelligent yet more complex positioning algorithms to combat the large distance estimation errors resulted from the RSS-based ranging technique. More details on the intelligent RSS-based geolocation methods will be presented later in this chapter in the context of positioning algorithms.

2.3.2 Angle of Arrival (AOA)

The AOA is usually measured using directional antennas or more often times using antenna arrays. In mobile radio systems, the antenna arrays are typically located only at base stations (BS), because of the difficulties to employ antenna arrays in a mobile station or mobile handset. Therefore, the AOA location metric is normally employed in network-based location finding systems. A variety of signal processing techniques are available for AOA estimation using antenna arrays, including maximum likelihood estimator, minimum variance method, and super-resolution sub-space techniques; details of these techniques can be found in [Caf99, Tin00] and many other references therein.

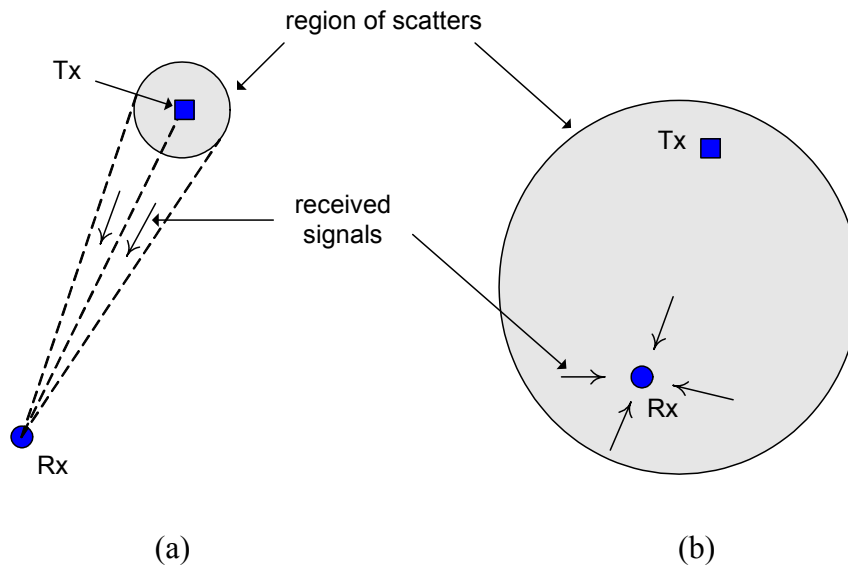


Figure 2.6: Radio transmission in the environment of (a) macrocell and (b) microcell. All primary scatters, which cause multipath transmission, are assumed located inside the region of scatters.

In general, the accuracy of the AOA estimation largely depends upon the radio propagation environments. Figure 2.6 illustrates two scenarios of radio transmission, *i.e.*, the transmission in macrocell environment and the transmission in microcell environment, respectively. The primary scattering objects, *i.e.*, the scatters, which cause multipath transmission, are assumed all located inside the *region of scatters* shown in the diagram [Jak94]. Then for macrocell environment where the primary scatters are located around the transmitter and far away from the receivers, the AOA method can provide acceptable location accuracy [Caf99] since the received signal roughly all coming from the direction of the transmitter. But in microcell situation where the primary scatters are located around the receiver, received signals could be

coming from any direction around the receiver. Thus in microcell environment, dramatically large AOA estimation errors will occur if the LOS signal path is blocked and a scattered signal component is used for the AOA estimation. The indoor radio propagation environment, where the LOS signal path is usually blocked by surrounding objects or walls, can be readily modeled as the microcell environment. Even when a strong LOS signal is detectable in indoor environments, strong multipath signals may introduce considerable interference to the AOA estimation, resulting in large AOA estimation errors. As a result, the AOA-based geolocation method is not preferred in indoor severe multipath environments for accurate indoor location finding systems.

2.3.3 Time of Arrival (TOA)

In indoor areas, due to the obstruction and the scattering of radio signals by walls, ceilings, or other objects, the DLOS propagation path is not always the strongest path and even in some occasions, for example the NLOS conditions, the DLOS signal may not be detectable with a specific receiver implementation [Pah98]. In such cases, dramatically large errors occur in the TOA estimation. To accurately estimate the TOA in indoor areas, we need to resort to different and more complex signaling formats, frequency of operation, and signal processing techniques that can resolve the problems.

The TOA-based systems measure the distance based on an estimate of the signal propagation delay, *i.e.*, the TOA, between a transmitter and a receiver since in free space or in air, radio signals travel at the constant speed-of-light (see Section 3.1 for more rigorous definition of the TOA estimation problem). The TOA can be measured either

by measuring the phase of the received narrowband carrier signal or by directly measuring the arrival time of a wideband pulse. The wideband pulses for measuring the TOA can be generated either directly with the ultra-wide band signals [Fon01] or by using spread spectrum signals [Wer98]. In the following subsections, we present these techniques in three classes: narrowband, wideband, and ultra wideband techniques.

2.3.3.1 Narrowband Signals and Phase Measurement for TOA Estimation

In narrowband ranging technique, the phase difference between the received and the transmitted carrier signals is used to measure the distance between the transmitter and the receiver. The phase of a received carrier signal, ϕ , and the TOA of the signal, τ , are related by $\tau = \phi / \omega_c$, where ω_c is the carrier frequency in radian. In application scenarios of the GPS where the DLOS signal path is always present, measurement of carrier phase may be helpful to improve the location accuracy. But in the indoor geolocation environments, the severe multipath propagation condition causes substantial errors in the narrowband phase measurements. When a narrowband carrier signal is transmitted in a multipath environment, the composite received carrier signal is the sum of a number of carriers, arriving along different paths, of the same frequency but different amplitude and phase. The frequency of the composite received signal remains unchanged but the phase will be different from that of the DLOS signal as shown in Fig. 2.7 [Pah95]. An immediate conclusion is that the phase-based distance measurement using narrowband carrier signal cannot provide accurate estimate of the distance in the heavy multipath indoor environments.

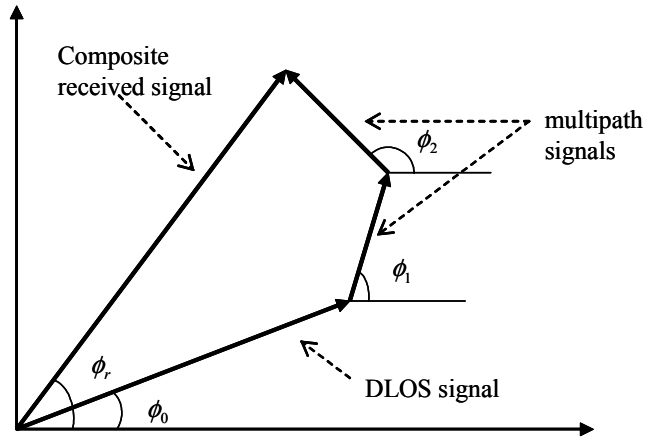


Figure 2.7: Phasor diagram for narrowband signaling on a multipath channel.

2.3.3.2 Wideband Signals and Super-resolution Techniques for TOA Estimation

The direct-sequence spread-spectrum (DSSS) wideband signal has been used in ranging systems for many years [Kap96]. In such a system, a signal coded by a known pseudo-random (PN) sequence is transmitted by a transmitter. Then a receiver crosscorrelates the received signal with a locally generated PN sequence using a sliding correlator or a matched filter [Wer98, Kap96]. The distance between the transmitter and the receiver is determined from the arrival time of the first correlation peak. Because of the processing gain of the correlation process at the receiver, the DSSS ranging system performs much better than other competing systems in suppressing interference from other radio systems operating in the same frequency band. More details of the wideband signal-based TOA estimation techniques will be presented in Chapter 3.

Due to the scarcity of the available bandwidth in practice, in some indoor geolocation applications, the DSSS ranging systems may not be able to provide adequate accuracy. On the other hand, it is always desirable to achieve higher ranging accuracy using the same bandwidth. Inspired by high resolution spectrum estimation techniques, a number of researchers have studied super-resolution techniques for time-domain analysis such as [Pal91]. A frequency-domain super-resolution technique can be used to determine the TOA with high resolution from the estimated frequency channel response. In this thesis, Chapter 4 is devoted to the super-resolution TOA estimation techniques including the basic theories and the issues in practical implementation.

2.3.3.3 Ultra Wideband (UWB) Approach for TOA Estimation

As we mentioned earlier, the signal bandwidth is one of the key factors that affect the TOA estimation accuracy in the multipath propagation environments. The larger the bandwidth, the higher the ranging accuracy. The UWB system, which exploits bandwidths in excess of one GHz, have attracted considerable attention as a means of accurately measuring the TOA for indoor geolocation applications [Fon01]. Due to the high attenuation associated with the high-frequency carrier, the frequency band considered for UWB system is typically focused on 2 - 3 GHz on the unlicensed basis. With results of propagation measurement in a typical modern office building, it has been shown that the UWB signal does not suffer multipath fading [Win98], which is desirable for accurate TOA estimation in indoor areas. The actual deployment of the UWB systems in the US is subject to the FCC approval. The main concern of the FCC

authorities is the interference of the UWB devices to, among other licensed services, the GPS systems that operate approximately at 1.5 GHz frequency band. Similar to the spread spectrum signals, the UWB signal has low, flat, and noise-like power spectrum. But given the weak satellite signals that must be processed by the GPS receivers, the noise-like UWB signal is still harmful to the GPS systems in close vicinity. A significant amount of research work is under way to assess the effect of the UWB interference on the GPS receivers.

2.4 Positioning Algorithms

As we discussed before, the measurement accuracy of the location metrics in indoor areas depends on the accuracy of the location sensing technologies and the site-specific indoor radio propagation channel conditions. Due to the imperfect implementation of the location sensing techniques, the lack of bandwidth, and the complexity of the multipath indoor radio propagation channels among other factors, there are always varying errors associated with the measurements of the location metrics. To achieve high positional accuracy when the measurements of location metrics are unreliable, the errors encountered in the location sensing process have to be mitigated in the positioning process. In the next two subsections we discuss the traditional positioning algorithms used with the reliable measurements of the location metrics and the more intelligent pattern recognition techniques that can be used to improve the positioning performance when the measurements of the location metrics are unreliable.

2.4.1 Traditional Techniques

In indoor radio propagation channels, it is difficult to accurately measure the AOA, RSS and carrier signal phase so that most of the independent indoor positioning systems mainly use the TOA-based techniques. With the reliable TOA-based distance measurements, simple geometrical triangulation methods can be used to find the location of the MT as presented in Section 2.1 [Caf98]. But due to the estimation errors of the distances at the RP receivers, caused by the inaccurate TOA measurement, the geometrical triangulation technique can only provide a region of uncertainty, instead of a single fix of position coordinates, for the estimated location of the MT. To obtain an estimate of the location coordinates in the presence of the measurement errors of the location metrics, a variety of direct and iterative statistical positioning algorithms have been developed to solve the problem by formulating it into a set of non-linear equations [Caf98].

In some indoor geolocation applications, the purpose of the positioning systems is to provide a visualization of the possible mobile locations instead of an estimate of the location coordinates [Wer98]. On the other hand, the positional accuracy is not constant across the area of coverage and the poor geometry of relative position of the MT and the RP can lead to a high geometric dilution of precision [Tek98]. The output of the statistical methods is an estimate of the mobile location coordinates, and the changes of the shape of the region of uncertainty are not revealed by this method.

When the region of uncertainty information as well as the estimate of the location is needed, both the geometric and the statistical triangulation algorithms are used [Tek98].

For the traditional outdoor geolocation systems, the intelligent techniques, such as the Kalman filter based techniques for tracking and fusion of multiple metrics, are normally used to improve the positioning performance [Kap96]. In essence, these techniques are readily applicable to indoor geolocation systems. However, indoor application environments have some unique features, discussed in the next section, which makes the traditional positioning algorithms less attractive. On the other hand, the unique features of indoor applications enable the design of the intelligent positioning algorithms that can significantly improve the positioning performance in indoor areas.

2.4.2 Pattern Recognition Techniques

For indoor geolocation applications, the service area is restricted to the inside and the close vicinity of a building while nowadays the building floor plan is normally accessible as an electronic document. The availability of electronic building floorplan is one of the features of indoor applications that can be exploited in the positioning algorithms. For example, while tracking a mobile terminal in buildings, with the aid of the building floorplan, the situations involving crossing the walls or jumping through the floors can be easily identified and eliminated. Another unique feature of indoor applications is that the size of the coverage area is much smaller than outdoor applications. This makes it possible to conduct comprehensive study and planning of

the deployment of the sensor infrastructure network. Careful planning of the sensor infrastructure network can significantly reduce the estimation errors of the location metrics caused by the NLOS propagation condition. The structural information of the sensor network can also be easily employed in the intelligent positioning algorithms in a way similar to the use of building floorplans. The small coverage of indoor geolocation systems, as compared with outdoor systems, also makes it possible to conveniently conduct extensive pre-measurement in the areas of interest for deployment. As a result, the pre-measurement based location pattern recognition, also known as location fingerprinting, technique is attracting significant attention for indoor applications [Bah00]. On the other hand, in most of the indoor applications, including finding the equipments in-demand or locating the personnel in critical condition such as unconscious firefighter inside the building on fire, the MT to be located is usually in quasi-stationary situations. For such quasi-stationary application scenarios, the pattern recognition algorithms are more promising than the traditional techniques and the Kalman filter based tracking techniques.

The basic operation of the pattern recognition positioning algorithms is simple. Each building is unique in its signal propagation characteristics; each location spot in a building would have a unique signature in terms of the RSS, TOA, and/or AOA, observed from different sensors in the building. A pattern recognition system determines the unique pattern features, *i.e.*, the location signature, of the area of interest in an initial training process, and then this knowledge is used to develop the rules for recognition. The challenge for such algorithms is to distinguish the locations with

similar signature. To build the signature database, a terminal is carried through the service area transmitting signals to a monitoring site through the location sensing elements of all reference points. The service area is divided into the non-overlapping zones or grids, and a pattern recognition training algorithm analyzes and compiles the received signal patterns in terms of the RSS, TOA, AOA, or any combination of these metrics to derive a unique location signature for each zone.

For quasi-stationary applications, the simplest way for pattern recognition is using the nearest-neighbor method on the basis of premeasurement and training. With such a method, a location signature database is first developed; then in regular operation the Euclidean distance measure is calculated between the measured metrics, RSS, TOA, or AOA and all entities in the signature database. The location estimate is determined to be the one associated with the minimum Euclidean distance [Bah00]. Experimental results are available in the references [Bah00, Pah02b]. A simple experiment conducted in the Center for Wireless Communications, the University of Oulu, Finland, shows that the standard deviation of the positioning errors, using the nearest-neighbor pattern recognition method, is 2.4 m and at about 80% locations the positional error was less than 3 m [Pah02b]. But it is worth to note that due to the site-specific and the dynamically varying nature of indoor radio propagation environments as we discuss in Section 2.2, the performance result reported may not applied to other application environments or for other time period in the same building.

When the area of coverage becomes large and a large number of sensors are involved, the size of the location signature database increases dramatically, which

makes the use of the simple nearest-neighbor pattern recognition technique computationally cumbersome. More complex algorithms, including the fuzzy logic, neural network, subspace techniques, and hidden Markov model based techniques among others, are being investigated to reduce the overall computational complexity and to improve the performance. When the 3G systems using the spread spectrum signals and the RAKE receivers are employed for indoor geolocation, it's possible to use the measured time and signal strength of all fingers in place of RSS to improve the positioning performance. Even though building and updating the signature database are much easier in indoor environments than in wide urban areas, the major drawback of the pattern recognition techniques still lies in the substantial efforts needed in the generation and maintenance of the signature database in the view of the fact that the application environments of indoor geolocation systems are dynamically changing constantly.

2.5 Summary and Conclusions

Indoor geolocation is an emerging research and engineering field that needs a scientific foundation. In this chapter we presented a brief overview of a wide variety of the technical issues involved in the design and performance evaluation of indoor geolocation systems. To provide a scientific foundation for indoor geolocation, significant research work needs to be conducted in all aspects of this new field. We need to characterize the indoor radio propagation channels that impact the performance of the indoor geolocation systems, based on the RSS, AOA, TOA, or any combination

of these location metrics, through empirical channel measurement and modeling; we need to design new location sensing techniques to provide accurate estimate of the location metrics in the complex indoor multipath environments; we need to design new positioning algorithms to compensate for the erroneous estimates of the location metrics resulted from the multipath propagation, to fuse the measurements of several location metrics to improve the positioning performance, and to exploit the unique features of indoor applications; we also need to study the system architectures and the practical deployment methods and rules for location sensor infrastructure networks to achieve the optimum system performance in the ad hoc indoor application environments.

Two classes of indoor geolocation systems are emerging nowadays. The first class has the dedicated infrastructure for location finding applications, employ complex signaling formats, location sensing techniques and positioning algorithms, such as the wideband and the UWB signals, and the super-resolution techniques. The challenge for such systems is to develop a signaling system and infrastructure that is inexpensive to design and deploy, complies with the frequency regulations, and provides a comprehensive coverage for the accurate ranging. The second class system overlays the location finding functionality onto the existing wireless systems deployed for the telecommunication and broadband data applications, including the wireless LAN systems and the cellular networks. The overlaid system can only obtain less reliable estimate of location metrics using the existing physical layer signaling format and infrastructure networks, but improves positioning performance by employing the pre-measurement data and the complex positioning algorithms at the higher application

layer such as the pattern recognition techniques. In general, both techniques demonstrate promising positioning performance for emerging markets for indoor geolocation applications. In the next chapter we present the TOA estimation techniques in details.

Chapter 3

TOA Estimation for Indoor Geolocation

The TOA estimation techniques have been widely used for many well-known traditional location finding applications, including the GPS, radar, and sonar systems. In essence the same TOA estimation techniques developed for the traditional applications can be applied to the emerging indoor location finding systems. However, because the severe multipath indoor application environment is very different from that of the GPS, radar, or sonar systems, the performance of the traditional TOA estimation techniques degrades significantly when applied to indoor systems. In this chapter we first present the maximum likelihood technique for the TOA estimation, which was derived for the traditional location finding applications, and the Cramer-Rao lower bound for the TOA estimation errors, which provides a means to predict and bound the accuracy of the TOA estimation techniques. Then we will study in details the impacts of indoor multipath radio propagation channel on the performance of the TOA estimation techniques. The time-difference-of-arrival (TDOA) is another time delay based location metric that can be used in place of the TOA in location finding systems.

In traditional applications, the estimation techniques as well as the performance of the TDOA and the TOA are very similar, but in the multipath indoor radio propagation channels the TDOA location metric becomes less appropriate than the TOA due to an inherent ambiguity in the estimation technique. So we will briefly look into this issue by studying the impacts of multipath propagation on the TDOA estimation techniques. At last, the issues in the practical measurement of the TOA location metric with spatially separated mobile units are discussed and techniques for synchronizing and coordinating the remotely located transmitter and receiver to measure the TOA and the TDOA are presented.

3.1 Maximum Likelihood Estimation of TOA

The time delay estimation problem is defined as follows. A known radio signal is emanated from a transmitter and the signal is monitored at a spatially separated receiver. The receiver estimates the arrival time of the radio signal, *i.e.*, the time-of-arrival (TOA), arriving from the transmitter. Assuming the transmitter and the receiver are synchronized in time and the transmission time of the radio signal is known to the receiver, the receiver can easily convert the arrival time estimation to the time delay estimation, *i.e.*, the propagation delay of the signal from the transmitter to the receiver. Then since in free space the radio signal propagates at the well-known constant speed-of-light, the propagation delay of the radio signal can be easily converted to the distance between the transmitter and receiver, which is used in the distance-based geolocation method, presented in Section 2.1, for location finding purposes. In the literature as well

as in this thesis for the ease of analysis it is usually assumed that the spatially separated transmitter and receiver are synchronized, and the transmission time of the radio signal is known to the receiver if not declared otherwise, even though it needs special treatment to achieve in practice. Thus the acronym TOA, which is the arrival time of radio signal in strict sense, often also refers to the propagation delay of radio signal from transmitter to receiver where actual meaning should be clear from the context. Issues and techniques to synchronize or coordinate the spatially separated transmitter and receiver to measure the TOA location metric are discussed in Section 3.5.

The estimation of TOA falls into the field of signal parameter estimation. The signal parameter estimation concerns with finding the optimum measurement of a set of unknown parameters $\boldsymbol{\psi} = [\psi_1, \psi_2, \dots, \psi_M]$ contained in a signal $s(t; \boldsymbol{\psi})$ by observing the signal in the presence of the additive noise $n(t)$. Usually, for the ease of analysis, the additive noise $n(t)$ is assumed to be additive white Gaussian noise (AWGN) with two-sided power spectral density $N_0 / 2$. The observed signal $x(t)$ is expressed as,

$$x(t) = s(t; \boldsymbol{\psi}) + n(t). \quad (3.1)$$

There are basically two criteria that are widely used in signal parameter estimation: maximum-likelihood (ML) criterion and maximum *a posteriori* probability (MAP) criterion. In the MAP criterion, the signal parameter vector $\boldsymbol{\psi}$ is modeled as a vector of random variables, and characterized by a joint *a priori* probability density function (PDF) $p(\boldsymbol{\psi})$. In the ML criterion, the signal parameter vector $\boldsymbol{\psi}$ is treated as deterministic but unknown [Pro95].

By performing an orthonormal expansion of $x(t)$ using N orthonormal functions $\{f_l(t), 1 \leq l \leq N\}$, we may represent $x(t)$ by a vector of coefficients $\mathbf{x} = [x_1, x_2, \dots, x_N]$. The joint PDF of the random variables $\{x_1, x_2, \dots, x_N\}$ in the expansion can be expressed as $p(\mathbf{x} | \boldsymbol{\psi})$. Then the ML estimate of $\boldsymbol{\psi}$ is the value that maximizes $p(\mathbf{x} | \boldsymbol{\psi})$. On the other hand, the MAP estimate is the value of $\boldsymbol{\psi}$ that maximizes the *a posteriori* PDF of $\boldsymbol{\psi}$

$$p(\boldsymbol{\psi} | \mathbf{x}) = \frac{p(\mathbf{x} | \boldsymbol{\psi})p(\boldsymbol{\psi})}{p(\mathbf{x})}. \quad (3.2)$$

We note that if there is no prior knowledge of the parameter vector $\boldsymbol{\psi}$, we may assume that it is uniformly distributed over a given range of the values of the parameters. In such a case, the value of $\boldsymbol{\psi}$ that maximizes $p(\mathbf{x} | \boldsymbol{\psi})$ also maximizes $p(\boldsymbol{\psi} | \mathbf{x})$ so that the MAP and the ML estimates are identical.

In our treatment of the parameter estimation given below, we view the parameters as unknown, but deterministic. Hence, we adopt the ML criterion for estimation of these parameters. In the ML estimation of the signal parameters, we require that the receiver extract the estimate by observing the received signal over a time interval T_0 , which is called the observation interval. The estimates obtained from a single observation interval are sometimes called one-shot estimates. In practice, however, the estimation is performed on a continuous basis by using tracking loops (either analog or digital) that continuously update the estimates.

If we assume the additive noise $n(t)$ is white and zero-mean Gaussian

$$n(t) \sim N(0, \sigma_n^2), \quad (3.3)$$

the joint PDF $p(\mathbf{x} | \boldsymbol{\psi})$ can be expressed as

$$\begin{aligned} p(\mathbf{x} | \boldsymbol{\psi}) &= \prod_{l=1}^N p(x_l | \boldsymbol{\psi}) \\ &= \left(\frac{1}{\sqrt{2\pi\sigma_n}} \right)^N \exp \left\{ -\frac{1}{2\sigma_n^2} \sum_{l=1}^N [x_l - s_l(\boldsymbol{\psi})]^2 \right\} \end{aligned} \quad (3.4)$$

where

$$\begin{aligned} x_l &= \int_{T_0} x(t) f_l(t) dt \\ s_l(\boldsymbol{\psi}) &= \int_{T_0} s(t; \boldsymbol{\psi}) f_l(t) dt \end{aligned} \quad (3.5)$$

and T_0 represents the integration interval in the expansion of $x(t)$ and $s(t; \boldsymbol{\psi})$. We note that by substituting (3.5) into (3.4), we can easily derive that

$$\frac{1}{2\sigma_n^2} \sum_{l=1}^N [x_l - s_l(\boldsymbol{\psi})]^2 = \frac{1}{N_0} \int_{T_0} [x(t) - s(t; \boldsymbol{\psi})]^2 dt \quad (3.6)$$

where $N_0/2 = \sigma_n^2$ is the two-sided power spectral density of the white noise $n(t)$.

Now, the maximization of $p(\mathbf{x} | \boldsymbol{\psi})$ with respect to the signal parameter $\boldsymbol{\psi}$ is equivalent to the maximization of the likelihood function

$$\Lambda(\boldsymbol{\psi}) = \exp \left\{ -\frac{1}{N_0} \int_{T_0} [x(t) - s(t; \boldsymbol{\psi})]^2 dt \right\} \quad (3.7)$$

or the log-likelihood function

$$\ln \Lambda(\boldsymbol{\psi}) = -\frac{1}{N_0} \int_{T_0} [x(t) - s(t; \boldsymbol{\psi})]^2 dt. \quad (3.8)$$

To apply the ML estimator to the time delay estimation, we first assume that the radio propagation channel between the transmitter and receiver is single-path and

disturbed only by additive white Gaussian noise, which is usually referred to as the AWGN channel. This means that the received signal encounters a constant propagation delay D , which is the TOA to be estimated, and a constant signal strength attenuation α so that the radio propagation channel between the transmitter and receiver is modeled by

$$h(t) = \alpha \delta(t - D), \quad (3.9)$$

and the received signal is given by

$$\begin{aligned} x(t) &= s(t) \otimes h(t) + n(t) \\ &= \alpha s(t - D) + n(t) \end{aligned} \quad (3.10)$$

where $n(t)$ is additive white Gaussian noise.

To obtain the maximum likelihood time delay estimate, the function to be maximized is the likelihood function given in (3.7) or equivalently (3.8) with the time delay parameter τ substituted for $\boldsymbol{\psi}$, that is

$$\ln \Lambda(\tau) = -\frac{1}{N_0} \int_{T_0} [x(t) - s(t - \tau)]^2 dt. \quad (3.11)$$

Following the necessary condition for a maximum

$$\left. \frac{d \ln \Lambda(\tau)}{d\tau} \right|_{\tau=\hat{\tau}_{ML}} = 0, \quad (3.12)$$

we can obtain that

$$\begin{aligned} \frac{d}{d\tau} \left(\int_{T_0} x(t) s(t - \tau) dt \right) \Big|_{\tau=\hat{\tau}_{ML}} &= \frac{d}{d\tau} \left(\frac{1}{2} \int_{T_0} s^2(t - \tau) dt \right) \Big|_{\tau=\hat{\tau}_{ML}} \\ &= \frac{1}{2} \frac{d}{d\tau} \left(\int_{T_0} s^2(t') dt' \right) \Big|_{\tau=\hat{\tau}_{ML}} \\ &= 0 \end{aligned} \quad (3.13)$$

reflecting the fact that the translation of the integrand on the right-hand side does not render the integral a function of τ and hence the right-hand side equals to zero. The correlation function of the received signal and the transmitted signal is defined as

$$\begin{aligned} r_{xs}(\tau) &= \int_{T_0} x(t)s(t-\tau) dt \\ &= \alpha r_{ss}(\tau-D) + v(\tau) \end{aligned} \quad (3.14)$$

where $r_{ss}(\tau)$ is the auto-correlation function of the transmitted signal and $v(\tau)$ is the additive noise term given by

$$\begin{aligned} r_{ss}(\tau) &= \int_{T_0} s(t)s(t-\tau) dt \\ v(\tau) &= \int_{T_0} n(t)s(t-\tau) dt. \end{aligned} \quad (3.15)$$

By substituting (3.14) into (3.13)

$$\left. \frac{d}{d\tau} r_{xs}(\tau) \right|_{\tau=\hat{D}_{ML}} = 0, \quad (3.16)$$

we can observe that the ML estimate of the propagation delay can be obtained by finding the value of τ that maximizes the correlation function $r_{xs}(\tau)$ as shown in Fig. 3.1. The received signal is cross-correlated with a delayed version of the transmitted signal and a variety of possible delay values \hat{D} are tried until the peak detector detects a peak.

The correlation function $r_{xs}(\tau)$, which is a function of delay, is referred to as delay profile while the function $|r_{xs}(\tau)|^2$ is referred to as power delay profile. In practice, the delay profile can be measured at receiver using a sliding correlator or a matched filter [Pah95]. If the transmitter and the receiver are synchronized to the same

time reference, the propagation delay can be estimated by measuring the delay of the peak of the delay profile or the power delay profile with respect to the time reference. Time delay estimation can also be accomplished using tracking loops, which continuously update the estimates [Pro95]. The time synchronization between spatially separated transmitter and receiver is hard to achieve in practice. The alternatives of the TOA measuring methods are presented in Section 3.5. The next section discusses the performance of the TOA estimation in the AWGN channels.

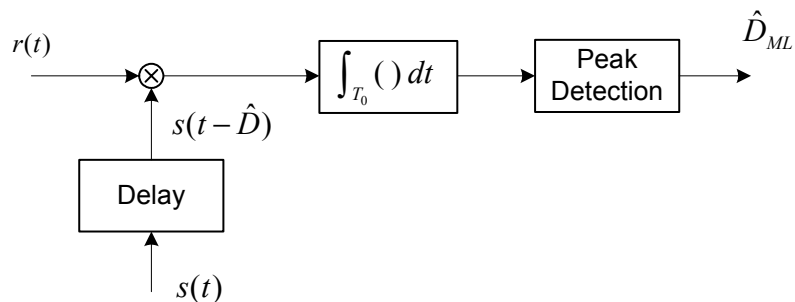


Figure 3.1: The ML estimation of time delay by cross-correlation.

3.2 Cramer-Rao Lower Bound for TOA Estimation

The quality of a signal parameter estimate is usually measured in terms of the estimate bias and its variance. In order to define these terms, we assume that there is a data vector $\mathbf{x} = [x_1, x_2, \dots, x_N]^T$, with the conditional PDF $p(\mathbf{x} | \psi)$, from which we extract an estimate of a parameter ψ . The bias of an estimate $\hat{\psi}$ is defined as

$$\text{bias} = E[\hat{\psi}(\mathbf{x})] - \psi, \quad (3.17)$$

where ψ is the true value of the parameter. When $E[\hat{\psi}(\mathbf{x})] = \psi$, we say that the estimate is unbiased. The variance of the estimate $\hat{\psi}(\mathbf{x})$ is defined as

$$\begin{aligned}\sigma_{\hat{\psi}}^2 &= E[(\hat{\psi}(\mathbf{x}) - E[\hat{\psi}(\mathbf{x})])^2] \\ &= E[\hat{\psi}(\mathbf{x})^2] - \{E[\hat{\psi}(\mathbf{x})]\}^2.\end{aligned}\tag{3.18}$$

In general $\sigma_{\hat{\psi}}^2$ may be difficult to compute. However, a well-known result in parameter estimation is the Cramer-Rao Lower Bound (CRLB) on the mean square error defined as [Van68]

$$E[(\hat{\psi}(\mathbf{x}) - \psi)^2] \geq \left[\frac{d}{d\psi} E[\hat{\psi}(\mathbf{x})] \right]^2 / E \left[\left(\frac{d}{d\psi} \ln p(\mathbf{x} | \psi) \right)^2 \right].\tag{3.19}$$

When the estimate is unbiased, that is $E[\hat{\psi}(\mathbf{x})] = \psi$, the numerator of (3.19) is unity and the bound becomes a lower bound on the variance $\sigma_{\hat{\psi}}^2$ of the estimate $\hat{\psi}(\mathbf{r})$, *i.e.*,

$$\begin{aligned}\sigma_{\hat{\psi}}^2 &\geq 1 / E \left[\left(\frac{d}{d\psi} \ln p(\mathbf{x} | \psi) \right)^2 \right] \\ &= -1 / E \left[\frac{d^2}{d\psi^2} \ln p(\mathbf{x} | \psi) \right]\end{aligned}\tag{3.20}$$

since $E \left[\left(\frac{d}{d\psi} \ln p(\mathbf{x} | \psi) \right)^2 \right] = -E \left[\frac{d^2}{d\psi^2} \ln p(\mathbf{x} | \psi) \right]$ [Van68]. To further simplify (3.20)

consider that $\ln p(\mathbf{x} | \psi)$ differs from the log-likelihood function $\ln \Lambda(\psi)$ by a constant factor independent of ψ . Thus it follows that

$$\begin{aligned}
\sigma_{\hat{\psi}}^2 &\geq 1 / E \left[\left(\frac{d}{d\psi} \ln \Lambda(\psi) \right)^2 \right] \\
&= -1 / E \left[\frac{d^2}{d\psi^2} \ln \Lambda(\psi) \right].
\end{aligned} \tag{3.21}$$

This lower bound provides a benchmark for the variance of any practical estimate. Any estimate that is unbiased and whose variance attains the lower bound is called an efficient estimate. In general, efficient estimate is rare. When they exist, they are maximum likelihood estimates.

The Cramer-Rao lower bound (CRLB) of the variance of TOA estimation errors about the true time delay can be derived by assuming $T_0 \rightarrow \infty$ as follows,

$$\begin{aligned}
&E \left[\frac{d^2}{d\tau^2} \ln \Lambda(\tau) \right] \\
&= E \left[\frac{d^2}{d\tau^2} \left(-\frac{1}{N_0} \int_{T_0} [x(t) - s(t - \tau)]^2 dt \right) \right] \\
&= \frac{2}{N_0} \int_{T_0} E[x(t)] \frac{d^2}{d\tau^2} s(t - \tau) dt \\
&= \frac{2}{N_0} \int_{T_0} s(t - \tau) \frac{d^2}{d\tau^2} s(t - \tau) dt \\
&= \frac{2}{N_0} \left(\frac{j}{2\pi} \right)^2 \int_{T_0} \int_{-\infty}^{\infty} \int_{-\infty}^{\infty} w_2^2 S(w_1) S(w_2) e^{j(w_1 + w_2)(t - \tau)} dw_1 dw_2 dt \\
&= -\frac{2}{N_0} \left(\frac{1}{2\pi} \right)^2 \int_{-\infty}^{\infty} \int_{-\infty}^{\infty} 2\pi \delta(w_1 + w_2) w_2^2 S(w_1) S(w_2) dw_1 dw_2 \\
&= \frac{-1}{\pi N_0} \int_{-\infty}^{\infty} w^2 S(w) S(-w) dw \\
&= \frac{-1}{\pi N_0} \int_{-\infty}^{\infty} w^2 |S(w)|^2 dw
\end{aligned} \tag{3.22}$$

where $S(w)$ is the Fourier transform of the signal $s(t)$. For the ease of analysis, here we assume $\alpha = 1$ in the signal model in (3.10), or equivalently assume the signal attenuation factor are estimated before the cross-correlation operation so that the signal $s(t)$ is the signal at the input of the receiver instead of the transmitted signal. Thus,

$$\begin{aligned}\sigma_{\hat{D}}^2 &\geq -1 / E \left[\frac{d^2}{d\tau^2} \ln \Lambda(\tau) \right] \\ &= \frac{\pi N_0}{\int_{-\infty}^{\infty} w^2 |S(w)|^2 dw} \\ &= \frac{1}{\rho_0^2 \beta_\tau^2}\end{aligned}\tag{3.23}$$

where

$$\begin{aligned}\rho_0^2 &= \frac{E_s}{N_0 / 2} \\ \beta_\tau^2 &= \frac{\int_{-\infty}^{\infty} w^2 |S(w)|^2 dw}{\int_{-\infty}^{\infty} |S(w)|^2 dw}\end{aligned}\tag{3.24}$$

and $E_s = \frac{1}{2\pi} \int_{-\infty}^{\infty} |S(w)|^2 dw = \int_{-\infty}^{\infty} s^2(t) dt$ is the energy of the signal. As shown in [Rae97], it can be proved that the variance of the ML estimate of the delay estimation in the neighborhood of the true delay value attains the CRLB as the observation time T_0 tends to infinity.

If we assume that the signal spectrum is two sided and extends from f_1 to f_2 Hz (and also from $-f_1$ to $-f_2$ Hz) with constant energy spectral density $S_0 / 2$ W/Hz, the CRLB in (3.23) can be simplified as follows [Qua81]. With the aforementioned assumptions,

$$\begin{aligned}\beta_\tau^2 &= \frac{2 \int_{f_1}^{f_2} (2\pi f)^2 \pi S_0 df}{2 \int_{f_1}^{f_2} \pi S_0 df} \\ &= \frac{4\pi^2}{3} (f_2^2 + f_1 f_2 + f_1^2)\end{aligned}\quad (3.25)$$

and

$$\sigma_b^2 \geq \frac{3}{8\pi^2 T_0} \frac{1}{\text{SNR}} \frac{1}{f_2^3 - f_1^3}, \quad (3.26)$$

where the signal energy $E_s = P_s T_0$, P_s is the mean signal power, T_0 is the observation time, the mean noise power, *i.e.*, the variance of the noise, $\sigma_n^2 = N_0(f_2 - f_1)$ since the power spectral density of the white noise is $N_0/2$, and the signal-to-noise power ratio (SNR) $\text{SNR} = P_s / \sigma_n^2$. Equation (3.26) may also be written in terms of the signal bandwidth B and the center frequency f_0 as

$$\sigma_b^2 \geq \frac{1}{8\pi^2} \frac{1}{\text{SNR}} \frac{1}{BT_0} \frac{1}{f_0^2 + B^2/12} \quad (3.27)$$

where $B = f_2 - f_1$ and $f_0 = (f_2 + f_1)/2$. We can observe that the bound is inversely proportional to the SNR, the product of signal bandwidth, and the observation time, and is inversely related to the square of the carrier frequency and the signal bandwidth.

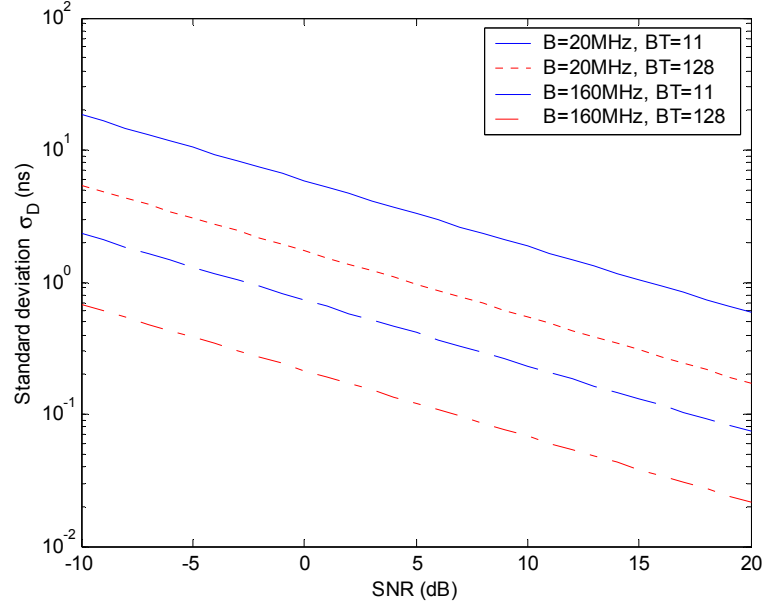


Figure 3.2: Numerical results of the CRLB of TOA estimation errors with different values of bandwidth and the product of bandwidth and observation time with respect to signal-to-noise power ratio (SNR). The carrier frequency is zero.

Figure 3.2 shows some numerical results of the CRLB of the TOA estimation errors obtained from (3.27) with different values of bandwidth and the product of bandwidth and observation time with respect to the signal-to-noise power ratio while assuming the frequency is zero, *i.e.*, the cross-correlation is performed in baseband. The ML estimate of the TOA is unbiased and the variance of the estimation errors is lower bounded by the CRLB.

So far the maximum likelihood estimation of time delay, determined by (3.16), and the CRLB of the variance of time delay estimation errors given by (3.23) and (3.26) are all derived for the single-path AWGN channels. But the indoor radio propagation

channel is multipath channel. As shown in the next section, the multipath propagation of radio signals has tremendous impacts on the performance of the TOA estimation. In indoor multipath environments, the TOA estimation techniques derived for the single-path AWGN channel model can no longer achieve good performance and the CRLB presented in this section no longer closely bounds the TOA estimation errors in multipath channels.

3.3 TOA Estimation in Multipath Channels

In deriving the ML estimation method, we assumed the radio propagation channel between the transmitter and the receiver is single-path and disturbed only by the additive white Gaussian noise. In such a channel, the received signal is given by (3.10), which is

$$x(t) = \alpha s(t - D) + n(t), \quad (3.28)$$

where the parameter D is the signal propagation delay, α is the complex signal strength attenuation parameter, and $n(t)$ is the additive white Gaussian noise. And the delay profile is given by (3.14)

$$r_{xs}(\tau) = \alpha r_{ss}(\tau - D) + v(\tau), \quad (3.29)$$

where $r_{ss}(\tau)$ is the auto-correlation function of the transmitted signal and $v(\tau)$ is the additive noise term given by (3.15). However, when the signal is transmitted through a multipath channel which is mathematically modeled as

$$h(t) = \sum_{k=0}^{L_p-1} \alpha_k \delta(t - \tau_k), \quad (3.30)$$

where L_p is the number of multipath components, α_k and τ_k are the complex amplitude and propagation delay of the k th path, respectively, the received signal becomes

$$\begin{aligned} x(t) &= s(t) \otimes h(t) + n(t) \\ &= \sum_{k=0}^{L_p-1} \alpha_k s(t - \tau_k) + n(t). \end{aligned} \quad (3.31)$$

For geolocation applications, the propagation delay of the DLOS path τ_0 needs to be estimated. So that in this thesis the term TOA is used to only refer to the propagation delay of the DLOS path in multipath channels if not declared otherwise.

Using the same correlation receiver shown in Fig. 3.1, the delay profile measured in multipath channels is given by

$$\begin{aligned} r_{xs}(\tau) &= \frac{1}{T_0} \int_{T_0} x(t) s(t - \tau) dt \\ &= \sum_{k=0}^{L_p-1} \alpha_k r_{ss}(\tau - \tau_k) + v(\tau) \end{aligned} \quad (3.32)$$

We note that in contrast to that in the single-path channels, in the multipath channels the measured delay profile is a weighted sum of multiple shifted auto-correlation functions of the transmitted signal. In general, the same correlation technique can be used for the TOA estimation in multipath channels. As discussed in [Pah98], whether the propagation delay of the DLOS is detectable or not largely depends on the instantaneous channel profile between the transmitter and the receiver and the characteristics of the ranging systems such as the signal bandwidth, the receiver sensitivity, and the receiver dynamic range. The receiver sensitivity specifies the minimum power level of a signal that can be detected and the receiver dynamic range

defines the difference in the power level of the strongest and the weakest detectable signals. According to the detectability of the DLOS path, the radio propagation channel profiles are classified into three categories for the TOA estimation in indoor geolocation applications [Pah98]. The first category is the dominant direct path (DDP) case, in which the DLOS path is detectable by measurement systems and it is the strongest path in the channel profile. The second category is the non-dominant direct path (NDDP) case, where the DLOS path is detectable by measurement systems but it is not the dominant path in the channel profile. The third category is the undetected direct path (UDP) case where measurement systems cannot detect the DLOS path. The channel profiles can also be grouped simply into DLOS and NLOS (no-LOS) cases according to whether the DLOS path is detectable or not [Pah02].

In general, signals of any format can be employed for the TOA estimation using the ML estimation technique. But the wideband DSSS signal is widely used for the TOA-based ranging systems because of several advantages as compared with other alternatives. From (3.27), we note that the performance of the TOA estimation improves as the bandwidth increases. As a result, one advantage of using the DSSS signal for the TOA estimation is its large bandwidth, which also helps to resolve multipath signals as we present in the following. Another advantage is that because of the processing gain of the correlation process in the receivers, the DSSS signal-based ranging system performs much better than the competing systems in suppressing interference from other radio systems operating in the same frequency band. The same ML estimator can be used in the implementation of the TOA estimation systems using

DSSS signaling, where the delay profile is first measured and then the TOA is determined by finding the delay value that maximizes the measured delay profile.

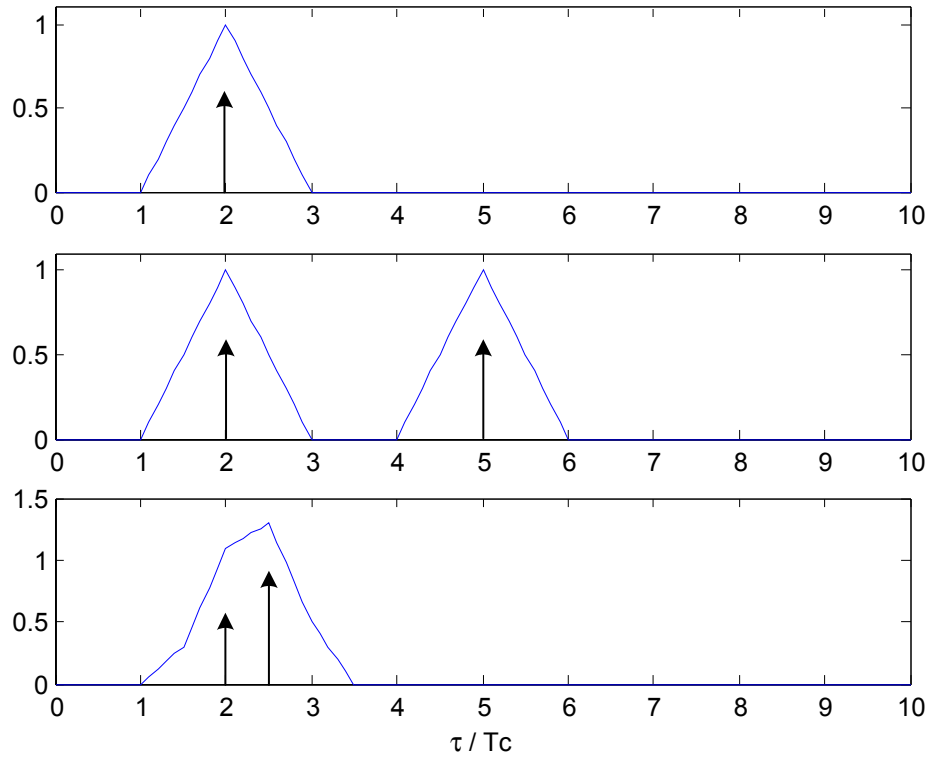


Figure 3.3: Power delay profiles with different channel profiles. (a) Single-path channel with propagation delay $D = 2 \times T_c$; (b) two-path channel with signal attenuation parameters $\alpha_0 = \alpha_1$, and propagation delays $\tau_0 = 2 \times T_c$ and $\tau_1 = 5 \times T_c$; (c) two-path channel with signal attenuation parameters $\alpha_0 = 0.6 \times \alpha_1$, and propagation delays $\tau_0 = 2 \times T_c$, and $\tau_1 = 2.5 \times T_c$.

Figure 3.3 presents the power delay profiles obtained using DSSS signals with three different channel profiles. In measuring the delay profiles using DSSS signals, a

maximal-length shift register sequence (*m*-sequence) is commonly used as a PN sequence. The auto-correlation function of the *m*-sequence is a triangular function similar to the one shown in Fig. 3.3a with a spread of $\pm T_c$ around the correlation peak, where T_c is the chip interval of the sequence. The spread of the correlation peak depends on the signal bandwidth since the bandwidth of the baseband DSSS signals equals to $1/T_c$ without pulse shaping. When the channel has a single-path profile given by (3.9), the propagation delay D can be determined using the ML estimator by finding the delay value that corresponds to the peak of the power delay profile shown in Fig. 3.3a and the variance of the estimate is bounded by the CRLB in (3.23).

When a radio signal is passed through a multipath channel, the delay profile consists of multiple copies of the delayed version of the auto-correlation function of the transmitted signal as given by (3.32). Figure 3.3b shows the power delay profile obtained in a two-path channel. We can observe that when the difference between the adjacent path delays is greater than $2 \times T_c$, clearly separated correlation peaks appear in the power delay profile so that the delay of the DLOS can be determined by finding the delay value that corresponds to the first peak. When the first peak is the strongest one of the delay profile, the channel belongs to the DDP category. When the first peak is not the strongest one but it is detectable with the given receiver sensitivity and receiver dynamic range, it falls into the NDDP case. If the strength of the first peak is below the receiver sensitivity or the difference between the strength of the first peak and the strongest peak exceeds the receiver dynamic range, the DLOS path is not detectable so

that the channel profile falls into the UDP category. In this case, dramatically large TOA estimation errors may occur.

When the difference between the adjacent delays is smaller than $2 \times T_c$, the two delayed correlation functions overlap. Due to the construction and deconstruction effects between the two overlapped correlation functions, as shown in Fig. 3.3c large delay estimation error occurs if the TOA is estimated by detecting the first peak of the power delay profile. Increasing signal bandwidth reduces the spread of the correlation peak and helps to resolve the DLOS path. However, it is practically impossible to increase the signal bandwidth freely due to the regulations on frequency spectrum usage posed by the FCC. An alternative way of increasing the resolution lies in the application of advanced signal processing techniques, which is the main subject of Chapter 4.

From the previous discussion we can conclude that if the same ML estimator designed for the AWGN channels is used in the multipath channels, the performance of the TOA estimation degrades significantly, depending on the characteristics of the ranging system and the instantaneous channel profile that the radio signal encounters. In summary, the following general principles can be used to improve the TOA estimation in multipath channels:

- Increase the receiver dynamic range and the receiver sensitivity,
- Increase the resolution of estimation techniques by increasing the signal bandwidth or by employing advanced signal processing techniques,

- Place the ranging transmitter and receiver, or deploy the reference points of indoor geolocation systems, in a way to minimize the occurrence of the NLOS propagation scenarios between the transmitter and the receiver.

The CRLB in (3.23) is derived for the single-path AWGN channel and it is the variance of the ML delay estimate in the neighborhood of its true value. However, in multipath channels the CRLB is not directly applicable because dramatically large TOA estimation errors occur when the DLOS path is undetectable. There are no suitable indoor radio propagation channel models for performance evaluation of the TOA estimation techniques. Consequently, in the literature, in designing the TOA estimation techniques for multipath channels, the performance evaluation is usually conducted by studying the resolution of the estimation techniques based on computer simulations with a simple two-path channel model [Pal91]. As we discussed previously, in addition to the resolution of the estimation techniques, the radio channel characteristics has tremendous effects on the performance of the TOA-based ranging systems in real application scenarios. So that in indoor areas, performance of TOA estimation techniques can be measured more appropriately by computer simulations based on channel measurements, by conducting field measurement using prototype systems, or by using the ray-tracing software to simulate the site-specific indoor radio channels. Due to the complexity of the indoor radio propagation channels, the performance study based on these methods reveals much more realistic statistical results than the resolution study of the estimation techniques with the simple theoretical channel models.

3.4 Estimation of TDOA

The time-difference-of-arrival (TDOA) is an alternative location metric, which is a time delay based location metric similar to the TOA. Instead of measuring the arrival time, or equivalently the distance, as in the TOA-based approach, in the TDOA-based approach the time difference of arrival, or equivalently the distance difference, from a MT to two RPs are measured. A minimum of two TDOA measurements, which requires a minimum of three RPs, can be used to provide a position fix of the MT similar to the distance-based geolocation method presented in Section 2.1. In this thesis details of TDOA-based location method is not discussed; interested readers are referred to [Caf99, Kap96] and references therein. In traditional location finding applications, the estimation techniques as well as the performance of the TDOA and the TOA are closely related and very similar, but in the multipath indoor radio propagation channels the TDOA location metric becomes less appropriate than the TOA due to an inherent ambiguity in the estimation technique. In this section we will briefly look into this issue by studying the impacts of multipath propagation on the TDOA estimation techniques, which is closely related to the delay estimation technique used for the TOA estimation.

The problem of the TDOA estimation is generally modeled as follows. A signal is transmitted from a remote source and is monitored at two spatially separated receivers. When the radio propagation channel between the transmitter and the receiver is assumed to be single-path and disturbed only by the additive white Gaussian noise, the received signals at the two receivers can be mathematically represented by

$$\begin{aligned}x_1(t) &= s(t) + n_1(t) \\x_2(t) &= \alpha s(t + D) + n_2(t)\end{aligned}\tag{3.33}$$

where α is the amplitude ratio of the signals observed at the two receivers and D is the difference in the arriving time of the signals observed at the two receivers. The noises $n_1(t)$ and $n_2(t)$ are jointly independent stationary random process, and the transmitted signal $s(t)$ is assumed to be uncorrelated with the noises. The receivers are synchronized in time so that the TDOA to be estimated is the time delay D . Normally a cross-correlation technique, similar to the one that is used in estimating the TOA, is used to estimate the TDOA. First the delay profile, which is the cross-correlation function of the two received signals, is obtained,

$$\begin{aligned}r_{12}(\tau) &= \frac{1}{T_0} \int_{T_0} x_1(t)x_2(t - \tau) dt \\ &= \alpha r_{ss}(\tau - D) + v(\tau)\end{aligned}\tag{3.34}$$

where the T_0 represents the observation time interval, the auto-correlation function of the transmitted signal $r_{ss}(\tau)$ is the same as in (3.15), and the additive noise term is given by

$$\begin{aligned}v(\tau) &= \frac{1}{T_0} \int_{T_0} n_1(t)n_2(t - \tau) dt + \\ &\quad \frac{1}{T_0} \int_{T_0} s(t)n_2(t - \tau) dt + \frac{1}{T_0} \int_{T_0} \alpha n_1(t)s(t + D - \tau) dt.\end{aligned}\tag{3.35}$$

Then the TDOA is estimated by finding the value of the delay that maximizes the delay profile in (3.34). A generalized correlation method can also be used in estimating the TDOA, where each of the two received signals is pre-filtered. With proper choice of

the pre-filters, the estimation of the TDOA can be improved using the generalized correlation method presented in [Kna76].

The CRLB can be derived for the variance of the TDOA estimate about the true value [Kna76, Qua81]. With some simplification assumptions similar to those used in deriving (3.26), at low SNR ($\text{SNR} \ll 1$) the CRLB for the TDOA estimation can be determined as [Qua81]

$$\sigma_{\hat{D}}^2 \geq \frac{3}{8\pi^2 T_0} \frac{1}{(\text{SNR})^2} \frac{1}{f_2^3 - f_1^3} \quad (3.36)$$

while at high SNR ($\text{SNR} \gg 1$) it is given by [Qua81]

$$\sigma_{\hat{D}}^2 \geq \frac{3}{4\pi^2 T_0} \frac{1}{\text{SNR}} \frac{1}{f_2^3 - f_1^3}. \quad (3.37)$$

Comparing (3.36) and (3.37) with (3.26), we note that in general the estimate of the TDOA is less accurate than that of the TOA. This observation can be intuitively justified since in the case of the TDOA estimation, both signals are corrupted by noise, but in the case of the TOA estimation a clean reference signal is available for correlation.

When the transmitted signal $s(t)$ is propagated through multipath channels, the received signals at the two receivers are given by,

$$\begin{aligned} x_1(t) &= \sum_{k=0}^{L_{p1}-1} \alpha_{1k} s(t - \tau_{1k}) + n_1(t) \\ x_2(t) &= \sum_{l=0}^{L_{p2}-1} \alpha_{2l} s(t - \tau_{2l}) + n_2(t) \end{aligned} \quad (3.38)$$

where the two sets of parameters $\{L_{p1}, \alpha_{1k}, \tau_{1k}\}$, $0 \leq k \leq L_{p1}$, and $\{L_{p2}, \alpha_{2l}, \tau_{2l}\}$, $0 \leq l \leq L_{p2}$, define the multipath channels between the transmitter and the two receivers, respectively. Then the cross-correlation function of the two received signals becomes

$$r_{12}(\tau) = \sum_{k=0}^{L_{p1}-1} \sum_{l=0}^{L_{p2}-1} \alpha_{1k} \alpha_{2l} r_{ss}(\tau - (\tau_{1k} - \tau_{2l})) + v(\tau) \quad (3.39)$$

where the additive noise term is given by

$$\begin{aligned} v(\tau) = & \frac{1}{T_0} \int_{T_0} n_1(t) n_2(t - \tau) dt + \frac{1}{T_0} \sum_{k=0}^{L_{p1}-1} \alpha_{1k} \int_{T_0} s(t - \tau_{1k}) n_2(t - \tau) dt \\ & + \frac{1}{T_0} \sum_{l=0}^{L_{p2}-1} \alpha_{2l} \int_{T_0} n_1(t) s(t - \tau_{2l} - \tau) dt. \end{aligned} \quad (3.40)$$

We can observe that similar to the case of the TOA estimation in multipath channels, the delay profiles for the TDOA estimation consists of multiple copies of the auto-correlation function of the transmitted signal with different delays. In multipath channels, the TDOA to be measured is the time difference between the propagation delays of the two DLOS paths

$$TDOA = \tau_{10} - \tau_{20}. \quad (3.41)$$

From (3.39) we can observe that the TDOA cannot be detected by finding the delay value that corresponds to the first peak of the delay profile since the first occurring correlation function in the delay axis does not necessarily corresponds to the delay value $(\tau_{10} - \tau_{20})$. On the other hand, following a discussion similar to that in section 3.3, we can deduce that in multipath channels, the delayed copy of the correlation function corresponding to the delay value $(\tau_{10} - \tau_{20})$ is not necessarily the strongest one in the delay profile given by (3.39). This means that in multipath channels there is

ambiguity in detecting the TDOA from the delay profiles since the correlation peak to be detected is neither the strongest one nor the first one for sure. An intuitive conclusion following this fact is that in multipath channels the estimation of the TDOA is much harder than the estimation of the TOA. Moreover, the CRLB in (3.36) and (3.37) are no longer applicable for the estimate of the TDOA for the same reason discussed in Section 3.3 for the TOA estimation, and dramatically large errors occur in the TDOA estimation due to the complexity of the multipath indoor radio propagation channels.

Since in geolocation applications, the ranging signal $s(t)$ transmitted by a MT is usually known to the RPs, a more obvious method of estimating the TDOA for the signal received by two spatially separated RP receivers is to calculate the difference of the TOA estimates measured by the two receivers. This method avoids the ambiguity in estimating the TDOA from the delay profile (3.39) that we just mentioned, but it requires the synchronization between the transmitter and both of the receivers while the direct measurement of TDOA by the cross-correlation method only requires the synchronization between the two receivers. More issues in the measurement methods of the TOA and the TDOA will be discussed in the next section.

3.5 TOA/TDOA Measurement Methods

In essence, the TOA estimation techniques that we discussed in the previous sections, concern with the estimation of the arrival time of a radio signal. To convert the arrival time estimation to the signal propagation delay estimation for the purpose of

geolocation, the spatially separated transmitter and receiver need to be synchronized in time and the transmission time of the radio signal needs to be known to the receiver. Thus the process of the TOA measurement involves coordination between a pair of the spatially separated transmitter and receiver. In this section, we discuss the coordination methods that are needed to form a TOA or a TDOA estimate from the arrival time estimation.

In general, there are two basic measurement methods to measure the TOA from radio signals: the synchronized transceiver method and the round-trip TOA method. To measure the TOA using the synchronized transceiver method, the remotely located transmitter and receiver are synchronized to a common time reference. If the transmission time of the radio signal is sent to the receiver as a timestamp while the arrival time of the signal is estimated at the receiver, the TOA can be easily calculated as the difference of the arrival time and the transmission time of the signal.

The accurate synchronization between remotely located terminals are usually very difficult to achieve in practical application scenarios where they are physically separated and randomly located. To avoid the synchronization requirement, a round-trip TOA method can be employed to measure the TOA. Using the round-trip TOA method, a terminal A sends a radio signal to a second terminal B . Then terminal B simply echoes the received signal back to terminal A using a different carrier frequency, or using the same carrier frequency but after waiting for a known time period, for proper operation of the two RF transceivers. Terminal A measures the arrival time of the signal received from terminal B . The time delay between transmission time t_0 and

the arrival time t_1 of the signal at terminal A includes the round-trip propagation delay 2τ , *i.e.* the round-trip TOA, and a processing delay τ_p that is encountered in the two transceivers. The processing delay τ_p can be easily measured during the system initialization or calibration period and can be readily compensated. Consequently, the TOA estimate is obtained as

$$TOA = \frac{1}{2}[t_1 - t_0 - \tau_p]. \quad (3.42)$$

There are two basic ways to measure the TDOA: the direct cross-correlation method and the indirect TOA-based method. With the direct method, two receivers are synchronized to a common time reference. The synchronized receivers receive a radio signal from a transmitter, then the received signal is digitized and forwarded to a central station to perform cross-correlation to estimate the TDOA as presented in Section 3.4. With the indirect method, transmitter needs to be synchronized to the same time reference of the receivers. Each receiver measures the TOA independently and the estimates of the TOA are forwarded to a central station to form an estimate of the TDOA. It is noted that both methods require the synchronization among several physically separated terminals. In the next section, we present a non-synchronized TDOA measurement method which exploits the architecture and signaling system of wireless LAN (WLAN) systems based on IEEE 802.11 standards.

For the dedicated geolocation systems, the simple approaches that we just discussed can be easily applied. But for the overlaid geolocation systems, the direct application of these methods is challenging because the geolocation function is overlaid

onto a wireless network without significant modifications to the existing infrastructure and hardware as well as the physical layer signaling formats. In the following we explore the TOA/TDOA measurement methods for the overlaid geolocation systems.

3.5.1 TOA/TDOA Measurement Methods for Overlaid Systems

With the wide deployment of the wireless LAN systems in indoor areas, implementing geolocation functions in the WLANs has received considerable attention in the recent years [Pah00b, Li00a, Li00b, Bah00]. The geolocation functions and services can be either integrated into the next generation WLANs or overlaid in the existing systems. In this section we focus on the TOA/TDOA measurement methods that can be used in the overlaid systems without concerning about the signal format and the detailed time delay estimation techniques.

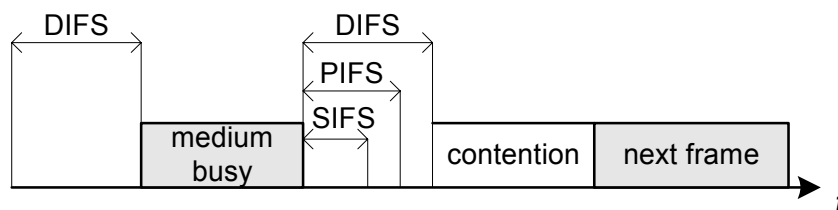


Figure 3.4: Inter-frame spacing and medium access priorities.

As we will describe in details shortly, some features of the MAC layer protocols of the IEEE 802.11 standards can be exploited in measuring the TDOA for geolocation purposes. To ease the discussion, some relevant materials of the standard are briefly reviewed first. Three basic access mechanisms are defined in the 802.11 MAC layer

specifications: the mandatory basic method based on the CSMA/CA, an optional RTS/CTS method to avoid the hidden terminal problem, and a contention-free polling method for the time-bounded service [Iee99]. There are three important parameters for controlling the waiting time before accessing the medium, *i.e.* the SIFS (Short inter-frame spacing), the PIFS (PCF inter-frame spacing) and the DIFS (DCF inter-frame spacing). These three parameters define the priorities of the medium access as shown in Fig. 3.4. The medium can be busy due to the transmission of data frames or other control frames. During a contention phase, several nodes try to access the medium. The parameter SIFS denotes the shortest waiting time and thus the highest priority for medium access. The DIFS is used for asynchronous data service, the PIFS is used for a time-bounded service and the SIFS is defined for the short control messages such as acknowledgements for data packets or polling responses. The unicast data transfer mode defined in the standard is illustrated in Fig. 3.5. A terminal accesses the medium and transmits a data frame. Once the receiver receives the data, it replies directly with a short acknowledgement message ACK after waiting for a short SIFS duration. Since the waiting time SIFS is the shortest and other stations can only access the medium after a longer waiting period, no other stations can access the medium in the meantime to cause a collision. This mechanism ensures the proper transmission and reception of the ACK message.

If the time durations of the SIFS and the data frame are known accurately, the round-trip TOA method can be easily applied by measuring the time interval between the transmission time of a data frame and the arrival time of the ACK frame. However,

according to the standard, in a real implementation, the accuracy of the time spacing between frames that are defined to be separated by a SIFS time is only within $2\mu s$, which corresponds to a maximum ranging error of 600m. Apparently, this method is not appropriate for indoor geolocation applications since the coverage of WLANs is usually below 100m for most of the application scenarios. But if significant modifications are made in the design of mobile terminals and access points to ensure accurate estimate of the time delays, this method is still applicable.

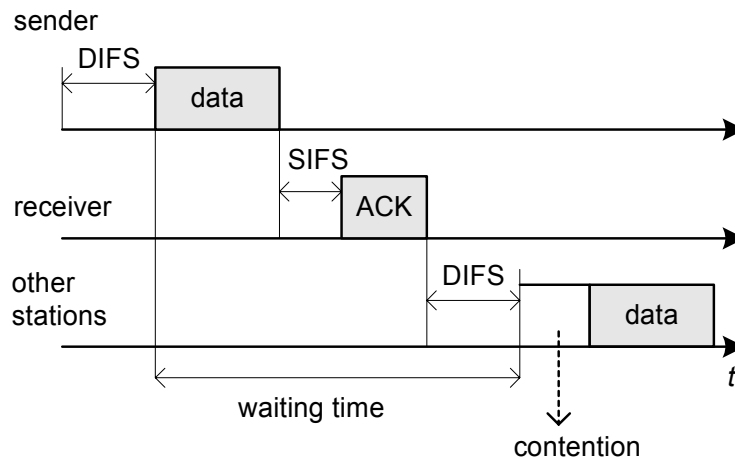


Figure 3.5: Unicast data transfer mode for IEEE 802.11.

Instead of measuring the TOA, the TDOA can be measured in the overlaid systems as shown in Fig. 3.6. Here we assume the overlaid geolocation system consists of a Geolocation Control Station (GCS) and a number of Geolocation Reference Points (GRP) operating around the AP of the WLAN networks. The geolocation service is first initiated by a MT or the GCS. Suppose the AP sends a data frame to the MT at the

time t_0 and MT replies with an ACK message after it receives the data. Meanwhile the GRPs monitor the communication traffic between the AP and the MT to measure the time delays between the arriving time of the data frame and the ACK message, *i.e.*, τ_{11} and τ_{21} shown in Fig. 3.6. The GRP1 and GRP2 receive the data frame at t_{10} and t_{20} , and ACK message at t_{11} and t_{21} , respectively. The durations τ_{10} and τ_{20} denote the propagation delays from the AP to GRP1 and GRP2 while τ_1 and τ_2 denote the propagation delays from the MT to GRP1 and GRP2, respectively. Since the distance from the AP to each of the GRP can be assumed known *a priori*, the propagation delays from the AP to the GRPs, τ_{10} and τ_{20} , can be accurately estimated. Therefore, the TDOA from the MT to the GRP1 and the GRP2 can be obtained as follows:

$$\begin{aligned}
 TDOA_{21} &= \tau_2 - \tau_1 \\
 &= [(\tau_{20} + \tau_{21}) - \tau_{00}] - [(\tau_{10} + \tau_{11}) - \tau_{00}] \\
 &= (\tau_{20} + \tau_{21}) - (\tau_{10} + \tau_{11}).
 \end{aligned} \tag{3.43}$$

Using this method, the GCS acts as a master that collects the measurements of the time delays τ_{11} and τ_{21} to form the estimate of the TDOA. Since the measurement at each GRP is the time delay not the timestamp with respect to a common time reference, the GRPs are not necessarily to be synchronized. Thus this method can also be referred to as non-synchronized TDOA measurement method. But it is worth to note that the GRPs need to be able to estimate time delay accurately.

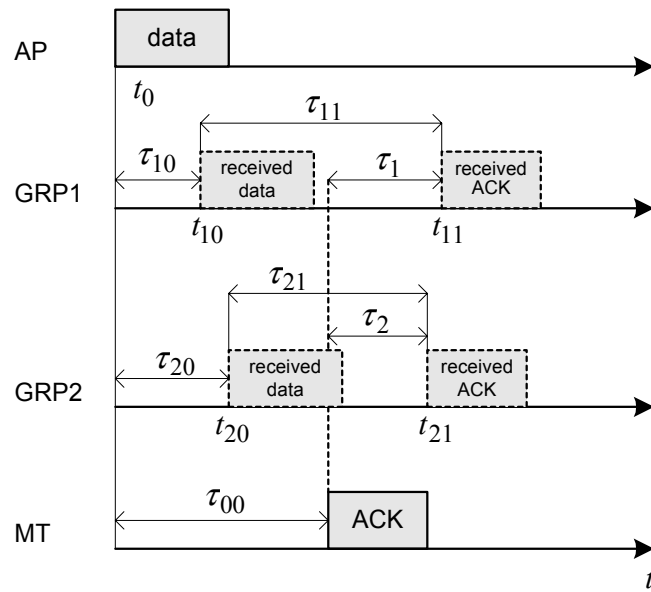


Figure 3.6: GRP-based TDOA method for IEEE 802.11 wireless LAN.

The non-synchronized TDOA measurement method can be used for systems using the optional RTS/CTS mechanism. Utilizing RTS/CTS for geolocation purpose might be a more appropriate choice than using the unicast mode of the mandatory CSMA/CA mechanism since the RTS message can also act as a request for geolocation services to reserve a time period for geolocation only. Furthermore, the fragmentation mode defined by the standard shown in Fig. 3.7 can be used to improve the performance in measuring the TDOA by averaging multiple consecutive measurements.

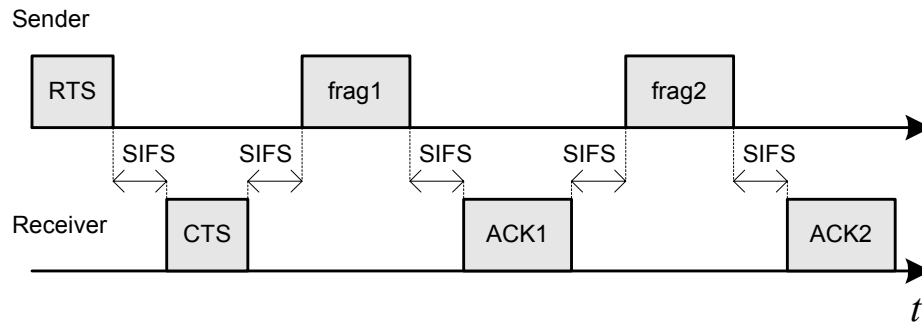


Figure 3.7: Fragmentation mode of IEEE 802.11.

Another major WLAN standard is the HIPERLAN standards, which is a collective reference name to the high performance radio local area networks standards developed by ETSI (European Telecommunications Standards Institute) project BRAN (Broadband Radio Access Networks). The same non-synchronized TDOA measurement method can be used in the overlaid geolocation systems in the HIPERLAN/2 WLANs as discussed in details in [Li00a].

3.6 Summary and Conclusions

The TOA-based radio ranging technique has been widely employed in the traditional location finding (or positioning and tracking) systems, including radar, sonar, and the GPS. As a result, a large amount of research work has been devoted in the study of the TOA estimation techniques. The maximum-likelihood TOA estimation technique was derived for the applications where the radio propagation channel can be simply modeled as single-path AWGN channel. The CRLB of the TOA estimation errors about the true time delay provides a benchmark for the variance of any practical

estimator. In practice, the performance of the ML TOA estimation technique in the traditional location finding systems is quite closely bounded by the CRLB. However, in indoor geolocation applications, due to the complexity of the multipath indoor radio propagation channels, dramatically large TOA estimation errors may occur and the CRLB derived for the traditional application scenarios is no longer suitable for benchmarking the performance of practical indoor geolocation systems. In general, in multipath channels, the performance of the TOA estimation can be improved by increasing the receiver dynamic range and the receiver sensitivity; increasing the time-domain resolution of the estimation techniques; placing the ranging transmitter and receiver in a way to minimize the occurrence of the NLOS scenarios. While the CRLB cannot directly apply to indoor environments, the performance of the TOA estimation can be benchmarked using the computer simulations based on empirical channel measurement data; conducting field measurement with prototype systems; and using the computer simulations based on ray-tracing software to simulate the site-specific indoor radio propagation channels.

The time difference of arrival (TDOA) is another time delay-based location metric that can be used in place of the TOA. In the single-path AWGN channels, the techniques and the performance of the TDOA estimation are very similar to that of the TOA estimation. But as explained in this chapter, in multipath channels, the TOA is more appropriate due to an ambiguity in the TDOA estimation with the ML cross-correlation technique.

For the dedicated geolocation systems, the simple synchronized transceiver method or round-trip TOA method can be easily employed. But for the overlaid geolocation systems, the direct application of these methods is challenging because the geolocation function is overlaid onto a wireless network system without significant modifications to the existing infrastructure and hardware as well as physical layer signaling formats. A non-synchronized TDOA measurement method is designed for overlaying the geolocation functionality onto the existing wireless networks such as the WLAN systems.

In the next chapter, the super-resolution TOA estimation techniques will be presented, which can be used to improve the performance of the TOA estimation in the multipath indoor radio propagation channels.

Chapter 4

Super-Resolution TOA Estimation Techniques

In last chapter we have shown that the TOA estimation techniques derived for the traditional location finding applications is not suitable for indoor applications since the radio propagation channel of the traditional application environment can be readily modeled as the single-path AWGN channel while the application environment of indoor geolocation systems is severe multipath channel. The two major sources of the TOA estimation errors in indoor environment are the multipath interference and the NLOS condition. As discussed in Section 3.3 one way to improve the performance of the TOA estimation in indoor multipath environment is to increase the resolution of the estimation techniques by increasing the signal bandwidth or by employing advanced signal processing techniques. In this chapter, we present an investigation of the frequency-domain super-resolution TOA estimation technique designed by applying the super-resolution spectrum estimation techniques to the frequency-domain channel response, which can be modeled as a harmonic signal model. In the following we first present the theoretical background and the development of the basic algorithm for the

TOA estimation. Then we present and evaluate the issues and techniques, including diversity techniques, which should be considered in the practical implementation of the algorithm for indoor geolocation applications. Two diversity combining schemes for the super-resolution TOA estimation techniques are presented and the effects of the diversity techniques are analyzed based on these two schemes. The quantitative performance evaluation of the super-resolution techniques is deferred until next chapter, where the empirical channel measurement data based computer simulation method is used to compare and evaluate the performance of various TOA estimation techniques presented in this chapter.

4.1 Introduction

With the emergence of the location-based applications and the next generation location-aware wireless systems, location finding techniques are becoming increasingly important [Pah02a]. As discussed in the preceding chapters, location finding based on the TOA is the most popular method for accurate positioning systems. The basic problem in TOA-based techniques is to accurately estimate the propagation delay of the radio signal arriving from the transmitter through the direct line-of-sight (DLOS) radio propagation path. However, as presented in Chapter 2 and 3, in indoor environments due to the severe multipath condition and the complexity of radio propagation, the DLOS signal cannot always be accurately detected [Pah98, Pah02]. Among other techniques presented in Section 3.3, increasing the time-domain resolution of the channel response to resolve the DLOS path improves the performance of the location

finding systems employing the TOA estimation techniques. Thus in this chapter we develop and investigate the super-resolution as well as the diversity techniques that can be used to improve the time-domain resolution of the channel response.

The super-resolution algorithms have been widely studied in the field of the model-based parametric spectral estimation for a variety of applications [Man00]. Recently, a number of researchers have applied the super-resolution spectral estimation techniques to the time-domain analysis for different applications. These applications include electronic devices parameter measurement [Bey01, Yam91] and multipath radio propagation studies [Lo94, Mor98, Pal91, Dum94, Saa97]. In [Lo94], the super-resolution technique was employed in the frequency domain to estimate the multipath time dispersion parameters such as the mean excess delay and the RMS delay spread. A similar method was used in [Mor98] to model indoor radio propagation channels with the parametric harmonic signal models. Here we address the application of the super-resolution techniques to the accurate TOA estimation for indoor geolocation applications. In the literature, the time delay related estimation problems have been studied with a variety of super-resolution techniques, such as the minimum-norm [Pal91], the root-MUSIC [Dum94] and the TLS-ESPRIT [Saa97]. It is worth to note that while the super-resolution techniques can increase the time-domain resolution as well as the location finding performance, it also increases the complexity of the system implementation. But the studies of the complexity and the cost of the practical implementation of the super-resolution techniques are beyond the scope of this research. Here we focus on the development of the theoretical foundation of the super-resolution

TOA estimation techniques, and issues as well as techniques to address the limitations posed by indoor geolocation applications, which is different from the spectral estimation applications. Also in this chapter we study the diversity techniques and the diversity combining schemes for the super-resolution techniques to further improve the performance of the TOA estimation in indoor geolocation applications.

4.2 Super-Resolution Techniques

The multipath indoor radio propagation channel is normally modeled as a complex, low-pass equivalent impulse response given by (2.1), that is

$$h(t) = \sum_{k=0}^{L_p-1} \alpha_k \delta(t - \tau_k), \quad (4.1)$$

where L_p is the total number of multipath components, and $\alpha_k = |\alpha_k| e^{j\theta_k}$ and τ_k are the complex attenuation and the propagation delay of the k th path, respectively. The multipath components are indexed so that the propagation delays τ_k , $0 \leq k \leq L_p - 1$, are in ascending order. As a result, the parameter τ_0 in the model denotes the propagation delay of the shortest path, *i.e.*, the DLOS path, and it needs to be detected for the purpose of the TOA estimation. Taking Fourier transform of (4.1), the frequency-domain channel response can be obtained as

$$H(f) = \sum_{k=0}^{L_p-1} \alpha_k e^{-j2\pi f \tau_k}. \quad (4.2)$$

When modeling the multipath indoor radio propagation channels, the parameters α_k and τ_k are random time-variant functions because of the motion of people and other

objects in and around buildings. However, since the rate of their variations is very slow as compared with the measurement time interval, these parameters can be treated as the time-invariant random variables [Sal87]. The phase of the complex attenuation θ_k is normally assumed random from one snapshot to another with a uniform probability density function (PDF) $U(0, 2\pi)$ [Pah95]. On the other hand, these parameters are frequency-dependent since they are related to the radio signal characteristics such as the transmission and reflection coefficients. However, as shown in [Yan94], for the frequency bands used in this paper these parameters can be assumed frequency-independent.

In practice, the discrete samples of the frequency-domain channel response can be obtained by sweeping the channel at different frequencies [How90], by using a multi-carrier modulation technique such as OFDM, or in a DSSS system by deconvolving the received signal over the frequency band of high signal-to-noise ratio [Pal91, Dum94, Lo94, Saa97]. In this thesis, we consider the super-resolution TOA estimation based on the frequency-domain measurement of indoor channel response. In Chapter 5, we will study the performance of the super-resolution TOA estimation techniques with the computer simulations based on empirical frequency-domain channel measurement data, which were obtained by sweeping the channel at different frequencies with a standard frequency-domain channel measurement system.

If we exchange the role of the time and the frequency variables in (4.2), we can observe that it becomes the harmonic signal model

$$H(\tau) = \sum_{k=0}^{L_p-1} \alpha_k e^{-j2\pi f_k \tau}, \quad (4.3)$$

which is well known in the model-based parametric spectral estimation field [Man00]. Consequently, in essence any spectral estimation techniques that are suitable for the harmonic signal model can be applied to the frequency response of the multipath indoor radio channel to perform the time-domain analysis. In this section, we apply the MUSIC algorithm, which was first introduced in [Sch81], as an example of the super-resolution algorithms, to the TOA estimation for indoor geolocation applications.

The discrete measurement data are obtained by sampling the channel frequency response (or frequency-domain channel response) $H(f)$ at L equally spaced frequencies. Considering the additive white noise in the measurement process and representing the estimated channel frequency response in noise with $\hat{H}(f)$, the sampled discrete frequency-domain channel response is given by

$$\begin{aligned} x(l) &= \hat{H}(f_l) = H(f_l) + w(l) \\ &= \sum_{k=0}^{L_p-1} \alpha_k e^{-j2\pi(f_0+l\Delta f)\tau_k} + w(l), \end{aligned} \quad (4.4)$$

where $l = 0, 1, \dots, L-1$ and $w(l)$ denotes the additive white measurement noise with the mean zero and the variance σ_w^2 . We can then concisely write the signal model in (4.4)

in the following vector form

$$\mathbf{x} = \mathbf{H} + \mathbf{w} = \mathbf{V}\mathbf{a} + \mathbf{w}, \quad (4.5)$$

where

$$\begin{aligned}
\mathbf{x} &= [x(0) \quad x(1) \quad \dots \quad x(L-1)]^T \\
\mathbf{H} &= [H(f_0) \quad H(f_1) \quad \dots \quad H(f_{L-1})]^T \\
\mathbf{w} &= [w(0) \quad w(1) \quad \dots \quad w(L-1)]^T \\
\mathbf{V} &= [\mathbf{v}(\tau_0) \quad \mathbf{v}(\tau_1) \quad \dots \quad \mathbf{v}(\tau_{L_p-1})] \\
\mathbf{a} &= [\alpha_0' \quad \alpha_1' \quad \dots \quad \alpha_{L_p-1}']^T
\end{aligned}$$

and

$$\begin{aligned}
\mathbf{v}(\tau_k) &= [1 \quad e^{-j2\pi\Delta f\tau_k} \quad \dots \quad e^{-j2\pi(L-1)\Delta f\tau_k}]^T \\
\alpha_k' &= \alpha_k e^{-j2\pi f_0\tau_k},
\end{aligned}$$

and the superscript T denotes the matrix transpose operation.

The MUSIC super-resolution techniques are based on the eigen-decomposition of the auto-correlation matrix of the preceding signal model in (4.5),

$$\begin{aligned}
\mathbf{R}_{xx} &= E\{\mathbf{xx}^H\} \\
&= \mathbf{V}\mathbf{A}\mathbf{V}^H + \sigma_w^2\mathbf{I},
\end{aligned} \tag{4.6}$$

where

$$\mathbf{A} = E\{\mathbf{aa}^H\}, \tag{4.7}$$

and \mathbf{I} is the identity matrix while the superscript H denotes the conjugate transpose operation, *i.e.*, the Hermitian, of a matrix. Since the propagation delays τ_k in (4.1) can be readily assumed all different, the matrix \mathbf{V} has full column rank, *i.e.*, the column vectors of \mathbf{V} are linearly independent. If we assume the magnitude of the parameters α_k is constant and the phase is a uniform random variable in $[0, 2\pi]$, the $L_p \times L_p$ covariance matrix \mathbf{A} is non-singular. Then from the theory of linear algebra, it follows that assuming $L > L_p$, the rank of the matrix $\mathbf{V}\mathbf{A}\mathbf{V}^H$ is L_p , or equivalently, the $L - L_p$

smallest eigenvalues of \mathbf{R}_{xx} are all equal to σ_w^2 . The eigenvectors corresponding to $L - L_p$ smallest eigenvalues of \mathbf{R}_{xx} are called noise eigenvectors while the eigenvectors corresponding to the L_p largest eigenvalues are called signal eigenvectors. Thus the L -dimensional subspace that contains the signal vector \mathbf{x} can be split into two orthogonal subspaces, known as signal subspace and noise subspace, by the signal eigenvectors and the noise eigenvectors, respectively. Assuming the eigenvectors are all normalized, we have

$$\mathbf{Q}_w^H \mathbf{Q}_w = \mathbf{I}, \quad (4.8)$$

where

$$\mathbf{Q}_w = [\mathbf{q}_{L_p} \quad \mathbf{q}_{L_p+1} \quad \cdots \quad \mathbf{q}_{L-1}]$$

and \mathbf{q}_k , $L_p \leq k \leq L-1$, are the noise eigenvectors. Then the projection matrix of the noise subspace can be readily determined as (see the definition of the projection matrix in the reference [Man00])

$$\begin{aligned} \mathbf{P}_w &= \mathbf{Q}_w (\mathbf{Q}_w^H \mathbf{Q}_w)^{-1} \mathbf{Q}_w^H \\ &= \mathbf{Q}_w \mathbf{Q}_w^H. \end{aligned} \quad (4.9)$$

Since the vector $\mathbf{v}(\tau_k)$, $0 \leq k \leq L_p - 1$, must lie in the signal subspace and the signal subspace is orthogonal to the noise subspace, we have

$$\mathbf{P}_w \mathbf{v}(\tau_k) = \mathbf{0}, \quad (4.10)$$

that is, the vector $\mathbf{v}(\tau_k)$, $0 \leq k \leq L_p - 1$, must be orthogonal to the noise subspace.

Thus the multipath delays τ_k , $0 \leq k \leq L_p - 1$, can be determined by finding the delay values at which the time-domain MUSIC pseudospectrum, defined as

$$\begin{aligned}
S_{MUSIC}(\tau) &= \frac{1}{\|\mathbf{P}_w \mathbf{v}(\tau)\|^2} = \frac{1}{\mathbf{v}^H(\tau) \mathbf{P}_w^H \mathbf{P}_w \mathbf{v}(\tau)} \\
&= \frac{1}{\mathbf{v}^H(\tau) \mathbf{P}_w \mathbf{v}(\tau)} = \frac{1}{\|\mathbf{Q}_w^H \mathbf{v}(\tau)\|^2} \\
&= \frac{1}{\sum_{k=L_p}^{L-1} |\mathbf{q}_k^H \mathbf{v}(\tau)|^2}
\end{aligned} \tag{4.11}$$

achieves the maximum value. The derivation in (4.11) is apparent by noticing that

$$\begin{aligned}
\mathbf{P}_w^H \mathbf{P}_w &= \mathbf{Q}_w \mathbf{Q}_w^H \mathbf{Q}_w \mathbf{Q}_w^H = \mathbf{Q}_w \mathbf{I} \mathbf{Q}_w^H \\
&= \mathbf{Q}_w \mathbf{Q}_w^H \\
&= \mathbf{P}_w,
\end{aligned}$$

i.e., the projection matrix is *idempotent* [Man00].

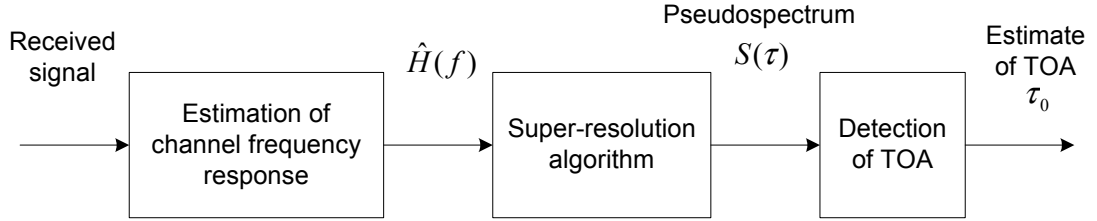


Figure 4.1: The functional block diagram of the receiver of super-resolution TOA estimation systems. $\hat{H}(f)$ is the estimated channel frequency response, which is defined in (4.4).

Figure 4.1 shows a functional block diagram of the receiver of the super-resolution TOA estimation systems. The received signal is first used to estimate channel frequency response, which is modeled as (4.4) and (4.5). Then a super-resolution algorithm, such as the MUSIC algorithm presented in this section, is used to

transform the channel frequency response to the time-domain pseudospectrum, which is defined in (4.11). The estimate of the TOA is then obtained by detecting the first peak of the pseudospectrum along the delay axis.

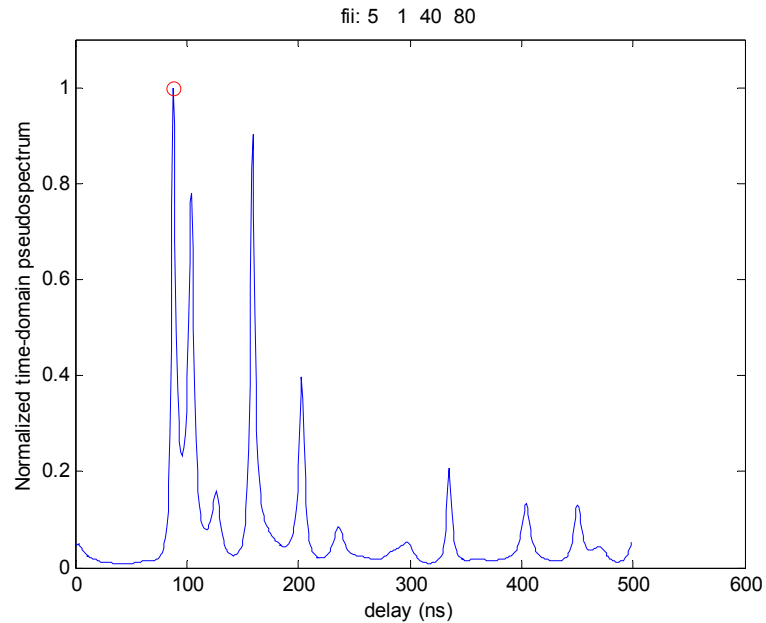


Figure 4.2: The time-domain MUSIC pseudospectrum, obtained with a sample frequency-domain channel measurement data. The estimate of the TOA corresponds to the first peak of the pseudospectrum, marked by a small circle sign as shown on the plot.

Figure 4.2 shows a sample result of the time-domain MUSIC pseudospectrum obtained by applying the MUSIC algorithm to an empirical frequency-domain channel measurement data. The simulation method as well as the descriptions of the channel measurement system and the measurement data is presented in Chapter 5. The TOA is

estimated by searching for the first peak of the pseudospectrum, which corresponds to the arrival time of the signal arriving from the DLOS path. In geolocation applications, we are only interested in the arrival time of the first DLOS signal path, but if needed the arrival times of all the paths in the multipath channel model in (4.1) can be estimated by identifying delay values corresponding to all the significant peaks of the pseudospectrum using peak detection algorithms. It should be emphasized here that there is no quantitative relationship between the magnitude of the peaks of the pseudospectrum and the values of the attenuation parameters of the multipath channel model, that is, the attenuation parameters of the multipath channel model cannot be estimated from the magnitude of the pseudospectrum peaks. The attenuation parameters of the multipath channel model is normally estimated from the measured time-domain or frequency-domain channel response and the estimates of arrival times using least-square algorithms [Pal91, Man94, Mor98]. In the next section issues in the practical implementation of the super-resolution TOA estimation techniques are presented.

4.3 Issues in Practical Implementation

Note that in the analysis in last section, which led to the MUSIC TOA estimation algorithm, we considered the theoretical or the true correlation matrix \mathbf{R}_{xx} . In practice, the correlation matrix must be estimated from the measured data samples. Figure 4.3 illustrates a functional block diagram of the super-resolution TOA estimation algorithms. The input data vector, *i.e.*, the estimate of channel frequency response

given in (4.5), is first used to estimate the correlation matrix \mathbf{R}_{xx} . Then the eigenvalues as well as the corresponding eigenvectors of the correlation matrix are computed. The parameter L_p is determined through the analysis of the eigenvalues and eigenvectors of the correlation matrix, which is discussed in details later in this section. Finally, the pseudospectrum is obtained using (4.11).

If we have P snapshots of the measurement data, the estimate of the correlation matrix is obtained from

$$\hat{\mathbf{R}}_{xx} = \frac{1}{P} \sum_{k=1}^P \mathbf{x}^{(k)} \mathbf{x}^{(k)H} . \quad (4.12)$$

But if only one snapshot of the measurement data of length N is available, the data sequence is divided into M consecutive segments of length L and then the correlation matrix is estimated as

$$\hat{\mathbf{R}}_{xx} = \frac{1}{M} \sum_{k=0}^{M-1} \mathbf{x}(k) \mathbf{x}(k)^H , \quad (4.13)$$

where

$$\mathbf{x}(k) = [x(k) \quad \dots \quad x(k + L - 1)]^T$$

and $M = N - L + 1$. In this section we will focus on the second method, where only one snapshot of measurement data is used in estimating the data correlation matrix as in (4.13). Methods based on multiple snapshots will be discussed in the next section for application with the diversity techniques.

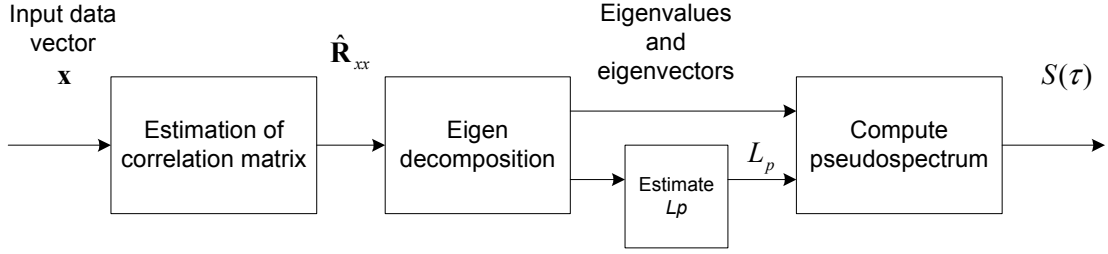


Figure 4.3: The functional block diagram of super-resolution TOA estimation algorithms. $\hat{\mathbf{R}}_{xx}$ is the estimated correlation matrix, L_p is the estimated total number of multipath components defined in (4.1), and $S(\tau)$ is the time-domain pseudospectrum defined in (4.11).

As we mentioned earlier, for the super-resolution TOA estimation techniques, the measurement data vector \mathbf{x} is obtained by sampling channel frequency response uniformly over a given frequency band. In order to avoid aliasing in the time domain, similar to the time-domain Nyquist sampling theorem, the frequency-domain sampling interval Δf is determined so as to satisfy the condition $1/\Delta f \geq 2\tau_{\max}$, where $\tau_{\max} = \max(\tau_{L_p-1})$ is the maximum delay of the measured multipath radio propagation channel. For example, for indoor geolocation applications, the frequency sampling interval Δf is normally set to be 1 MHz, which accommodates application scenarios where the maximum delay τ_{\max} is less than 500 ns or equivalently the maximum length of the multipath signal propagation path is less than 150 m. Thus with a bandwidth of 20 MHz, the length of one measurement data sequence is 21, which is far too short to accurately estimate the correlation matrix. This is very different from the situation in

the spectrum estimation applications, where the super-resolution algorithms are widely used. In the spectrum estimation applications, the super-resolution algorithms are used to convert the time-domain measurement data of a random signal to frequency domain to estimate the spectrum of the signal. Thus in the spectrum estimation applications, more measurement data or longer measurement data vector \mathbf{x} , which is the input of the super-resolution algorithms and is used to estimate the correlation matrix, can be obtained by simply extending the observation time of the random signal. With longer measurement data, the correlation matrix can be estimated more accurately using (4.13), which leads to better performance of the super-resolution algorithm. But in the TOA estimation applications, the super-resolution algorithm is used to convert the measurement data, which is the estimate of channel frequency response, from frequency domain to time domain as illustrated in Fig. 4.1 to estimate the arrival time of the DLOS signal. Thus, in TOA estimation applications, the length of the measurement data equals to the ratio of the measured signal bandwidth and the frequency sampling interval. With the frequency sampling interval fixed, determined by the sampling theorem that we just discussed, increasing the length of the measurement data means an increase in the signal bandwidth. In practice, the national/international frequency usage regulation rules, such as regulations by the Federal Communications Commission (FCC), pose a limitation on available signal bandwidth. As a result, in applying the super-resolution algorithms to the TOA estimation applications we will face the issue of having short limited length measurement data that we cannot increase freely. Thus in the TOA estimation applications it is important to find ways to ensure the proper

operation of the super-resolution algorithms with short limited measurement data. As presented in the following a number of techniques can be used to improve the performance, including the forward-backward estimation method for correlation matrix estimation and the eigenvector method in this section, and the diversity techniques in the next section. In this section methods to estimate the total number of multipath components are also presented in details.

4.3.1 Improved Estimation of Correlation Matrix with Limited Measurement Data

The measurement data \mathbf{x} in (4.5) and Fig. 4.3 are normally assumed stationary. Thus the correlation matrix of the data \mathbf{R}_{xx} is Hermitian, *i.e.*, conjugate symmetric, and Toeplitz, *i.e.*, having equal elements along all diagonals. However, in practice the estimate of the correlation matrix $\hat{\mathbf{R}}_{xx}$ based on the actual measurement data of small finite length N is not Toeplitz. The estimate of the correlation matrix can be improved using the following *forward-backward correlation matrix* (FBCM),

$$\hat{\mathbf{R}}_{xx}^{(\text{FB})} = \frac{1}{2}(\hat{\mathbf{R}}_{xx} + \mathbf{J}\hat{\mathbf{R}}_{xx}^*\mathbf{J}) \quad (4.14)$$

where the superscript $*$ denotes conjugate, superscript FB stands for the forward-backward estimation, and \mathbf{J} is the $L \times L$ exchange matrix, defined as

$$\mathbf{J} = \begin{bmatrix} 0 & \cdots & 0 & 1 \\ \vdots & \ddots & 1 & 0 \\ 0 & \ddots & \ddots & \vdots \\ 1 & 0 & \cdots & 0 \end{bmatrix}.$$

It can be easily shown that the matrix $\hat{\mathbf{R}}_{xx}^{(\text{FB})}$ is persymmetric, that is

$$\mathbf{J}\hat{\mathbf{R}}_{xx}^{(\text{FB})}\mathbf{J} = \hat{\mathbf{R}}_{xx}^{(\text{FB})*}, \quad (4.15)$$

and its elements are conjugate symmetric about both main diagonals. This technique is widely used in the spectral estimation applications with the name *modified covariance method* [Man00], in the linear least-square signal estimation with the name *forward-backward linear predication* (FBLP) [Man00], and in the antenna array signal processing with the name *modified spatial smoothing preprocessing* [Wil88, Yam91]. In contrast to the forward-backward correlation matrix in (4.14), here we call the correlation matrix in (4.13) the *forward correlation matrix* (FCM).

In our development of the basic theories, we assumed that the magnitude of the parameters α_k , $0 \leq k \leq L_p - 1$, in (4.1) are constant and the phase θ_k , $0 \leq k \leq L_p - 1$, are independent uniformly distributed random variables. With such assumptions it can be shown that the correlation matrix \mathbf{A} , defined in (4.6), is full-rank, *i.e.*, non-singular. But if the phase θ_k , $0 \leq k \leq L_p - 1$, are non-random, which is true if only one snapshot of the measurement data is used in estimating the correlation matrix \mathbf{R}_{xx} , the rank of the correlation matrix \mathbf{A} tends to degrade to 1 and the matrix tends to singular. In such a situation, the MUSIC algorithm does not work properly. But fortunately, for the signal model in (4.4), the estimation of data correlation matrix using (4.13) has decorrelation effects as explained below. The decorrelation effects in forward and forward-backward correlation matrices were analyzed in [Red87, Wil88, Yam91]. Following the definition in [Red87], the correlation coefficient for the forward

estimation method in (4.13) between α_i' and α_j' , *i.e.*, the i th and j th element of the multipath model parameter vector \mathbf{a} defined in (4.5), can be derived as

$$\rho_{ij}^{(\text{FCM})} = \frac{A_{ij}}{\sqrt{A_{ii}A_{jj}}} = Ke^{-j\phi}, \quad (4.16)$$

where

$$K = \frac{\sin[M\pi\Delta f(\tau_i - \tau_j)]}{M \sin[\pi\Delta f(\tau_i - \tau_j)]}$$

$$\phi = -(\theta_i - \theta_j) + 2\pi f_0(\tau_i - \tau_j) + \pi(M-1)\Delta f(\tau_i - \tau_j),$$

and A_{ij} is the (i, j) th element of the parameter correlation matrix \mathbf{A} defined in (4.7).

From (4.16) it is noted that the decorrelation effects of the forward estimation method depend on the number of segments M , the frequency sampling interval Δf , and time delay difference $(\tau_i - \tau_j)$. Similarly, the correlation coefficient of the forward-backward estimation method in (4.14) can be readily derived as

$$\rho_{ij}^{(\text{FBCM})} = K \cos(\phi + \psi/2)e^{j\psi/2}, \quad (4.17)$$

where

$$\psi = 2\pi(L-1)\Delta f(\tau_i - \tau_j),$$

and K and ϕ are the same as in (4.16). Detailed derivation of (4.16) and (4.17) can be found in the Appendix 4.A. From (4.17) it is clear that the correlation coefficient of the forward-backward estimation method depends on the length of the segments L , the phase difference of parameters $(\theta_i - \theta_j)$, and the lowest frequency of the spectrum f_0 , in addition to M , Δf , and $(\tau_i - \tau_j)$ as in (4.16).

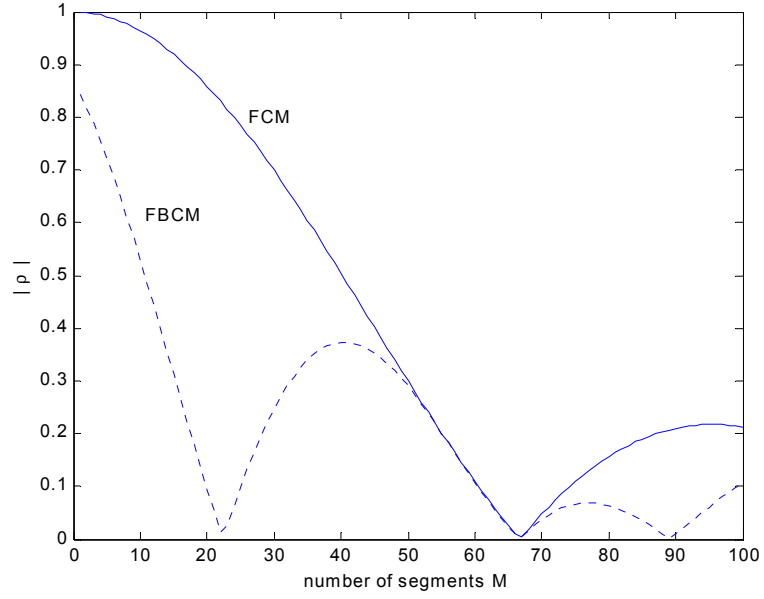


Figure 4.4: Correlation coefficients of forward and forward-backward correlation matrices, with $\Delta f = 1\text{MHz}$, $(\tau_i - \tau_j) = 15\text{ns}$, $(\theta_i - \theta_j) = 0$, $f_0 = 900\text{MHz}$, and $L = 13$.

From (4.16) and (4.17) it can be readily shown that

$$|\rho_{ij}^{(\text{FBCM})}| = |\rho_{ij}^{(\text{FCM})}| \times |\cos(\phi + \psi/2)|. \quad (4.18)$$

Thus we can clearly observe that the forward-backward correlation matrix has better decorrelation effect than the forward correlation matrix, that is,

$$|\rho_{ij}^{(\text{FBCM})}| \leq |\rho_{ij}^{(\text{FCM})}| \quad (4.19)$$

since $|\cos(\phi + \psi/2)| \leq 1$. Figure 4.4 and Fig. 4.5 show examples of the decorrelation effects, calculated from (4.16) and (4.17), versus the number of segments and the delay difference, respectively. The results in Fig. 4.4 and 4.5 clearly verify the relation in

(4.19), that is, the forward-backward correlation matrix has better decorrelation effect than the forward correlation matrix. The better decorrelation effect leads to potentially better performance of the super-resolution algorithm. In Chapter 5 we compare the performance of the forward and the forward-backward estimation methods with computer simulation results. In next section we address the issue of the estimation of L_p in practice, *i.e.*, the total number of the multipath components.

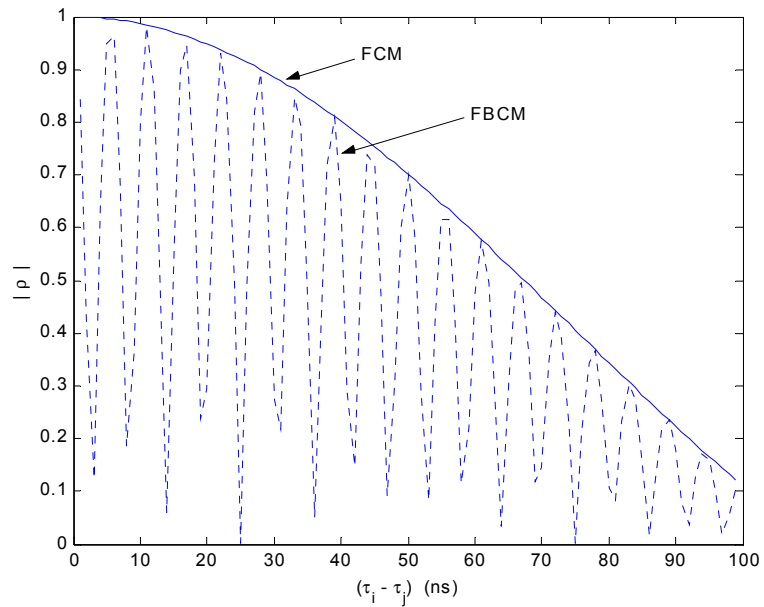


Figure 4.5: Correlation coefficients of forward and forward-backward correlation matrices, with the parameters $M = 9$, $\Delta f = 1\text{MHz}$, $(\theta_i - \theta_j) = 0$, $f_0 = 900\text{MHz}$, and $L = 13$.

4.3.2 Determination of Parameters L and L_p

If we use only one measurement data snapshot of N samples to estimate the TOA using super-resolution algorithms, the first step is to determine the value of L for the estimation of $\hat{\mathbf{R}}_{xx}$ as in (4.13). With large values of L , the potential for higher resolution of the MUSIC algorithm increases, which is similar to that in array signal processing where increasing L means an increase in subarray aperture and thus an increase in resolution capability [Tuf82, Kri96]. On the other hand, from (4.13), we can see that for a fixed value of N , the value of M decreases as L increases. The decrease in M increases fluctuations in the matrix $\hat{\mathbf{R}}_{xx}$ resulting in large perturbations of the eigenvalues and eigenvectors of $\hat{\mathbf{R}}_{xx}$, and reduces the number of coherent α_k that can be detected [Kri96, Lib99]. Consequently, the value of L needs to be selected so that it provides a balance between resolution and stability of the algorithm. Different values of L have been used in the literature, for example [Lan80] used $N/2$ and $N/3$, [Tuf82] used $3N/4$, and [Pal91] adopted $3N/5$. In this paper we use a value of $2N/3$, which was determined through computer simulations.

Another parameter that needs to be determined in using a super-resolution technique is the total number of multipath components L_p . If the true correlation matrix \mathbf{R}_{xx} is available, L_p can be easily determined by observing eigenvalues of the correlation matrix since in theory, the $L - L_p$ smallest eigenvalues of \mathbf{R}_{xx} are all equal to σ_w^2 , and the remaining L_p eigenvalues are all larger than σ_w^2 . But in practical

implementation, especially when the correlation matrix is estimated from a limited number of data samples, the noise eigenvalues are all different, which makes it challenging to clearly distinguish signal eigenvalues and noise eigenvalues. In [Wax85], the information theoretic criteria for model selection, including Akaike information theoretic criteria (AIC) and Rissanen Minimum Descriptive Length criteria (MDL), are applied to this problem. The MDL criterion for estimation of L_p is used in this paper, which is given in [Wax85]

$$MDL(k) = -\log \left(\frac{\prod_{i=k}^{L-1} \lambda_i^{1/(L-k)}}{\frac{1}{L-k} \sum_{i=k}^{L-1} \lambda_i} \right)^{M(L-k)} + \frac{1}{2} k(2L-k) \log M, \quad (4.20)$$

where λ_i , $0 \leq i \leq L-1$, are the eigenvalues of correlation matrix in descending order. The estimate of L_p is determined as the value of $k \in [0, L-1]$ for which the MDL is minimized. In the reference [Xu94], authors showed that when the forward-backward estimation method is used, the MDL criteria in (4.17) cannot directly apply and the second term of the criteria must be modified to $(1/4)k(2L-k+1) \log M$, that is

$$MDL(k)^{(FB)} = -\log \left(\frac{\prod_{i=k}^{L-1} \lambda_i^{1/(L-k)}}{\frac{1}{L-k} \sum_{i=k}^{L-1} \lambda_i} \right)^{M(L-k)} + \frac{1}{4} k(2L-k+1) \log M. \quad (4.21)$$

4.3.3 Eigenvector Method

One implicit assumption in the MUSIC method is that the noise eigenvalues are all equal, *i.e.*, $\lambda_k = \sigma_w^2$ for $L_p \leq k \leq L-1$, that is, the noise is white. However, as we just discussed, when the correlation matrix is estimated from a limited number of data

samples in practice, the noise eigenvalues are not equal. A slight variation on the MUSIC algorithm, known as the Eigenvector (EV) method, can be used to account for the potentially different noise eigenvalues [Man00, Joh82]. The pseudospectrum of the EV algorithm is defined as

$$S_{EV}(\tau) = \frac{1}{\sum_{k=L_p}^{L-1} \frac{1}{\lambda_k} |\mathbf{q}_k^H \mathbf{v}(\tau)|^2}, \quad (4.22)$$

where λ_k , $L_p \leq k \leq L-1$, are the noise eigenvalues. In effect, the pseudospectrum of each eigenvector is normalized by its corresponding eigenvalue. If the noise eigenvalues are equal, the EV method and the MUSIC method are identical. The performance of the MUSIC and EV methods were compared in [Joh82] and it was shown that the EV method is less sensitive to inaccurate estimate of the parameter L_p , which is highly desirable in a practical implementation. As presented in the next chapter, the EV method is shown by computer simulations to have slightly better performance than the MUSIC method. In the next section, we investigate diversity techniques that can be used to further improve the performance of super-resolution TOA estimation techniques.

4.4 Diversity Techniques

Diversity techniques such as time diversity, space diversity, and frequency diversity are widely utilized in wireless communication systems to improve link performance [Pah95, Rap96, Pah02a]. Diversity techniques take advantage of the

random nature of the radio propagation channel by finding and combining uncorrelated signal paths. In essence, all diversity techniques used for wireless communication systems can be used for TOA estimation systems with the general structure shown in Fig. 4.6, where the diversity system has P diversity branches. The TOA is estimated independently at each diversity branch of receiver, and then a combining algorithm is used to process the TOA estimates from all branches to obtain an optimum estimate. A variety of different combining algorithms can be designed for different diversity techniques. The simplest one is the equal-gain combining algorithm given by

$$\hat{\tau}_0 = \frac{1}{P} \sum_{k=1}^P \hat{\tau}_0^{(k)}. \quad (4.23)$$

In some cases, more complex variable-gain combining is also possible, where the estimate of each diversity branch is weighted with a coefficient that reflects the quality of time delay estimation at each branch. More research work is needed to design optimum combining algorithms for diversity techniques for TOA estimation applications.

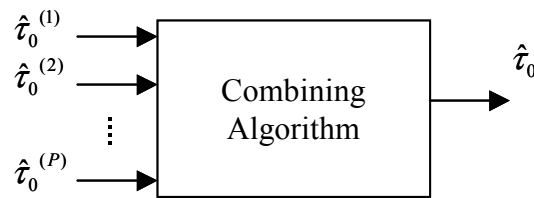


Figure 4.6: General structure of TOA estimation with diversity techniques, general diversity combining scheme (GDCCS).

For the super-resolution TOA estimation techniques presented in this paper, diversity techniques can also be applied as shown in Fig. 4.7. Instead of combining independent time delay estimates as in Fig. 4.6, the measurement data at diversity branches are combined to estimate the correlation matrix using the formula in (4.12). For the convenience of referencing, we call the structure in Fig. 4.6 a *general diversity combining scheme* (GDCS), and the structure in Fig. 4.7 a *correlation matrix-based diversity combining scheme* (CMDCS). In super-resolution TOA estimation techniques, the major computational load is in the eigen-analysis, *i.e.*, computation of the eigenvalues and eigenvectors, of the correlation matrix. As a result, CMDCS is computationally superior to GDCS since the CM-based scheme performs eigen-analysis only once, but the general scheme needs to perform independent eigen-analysis P times.

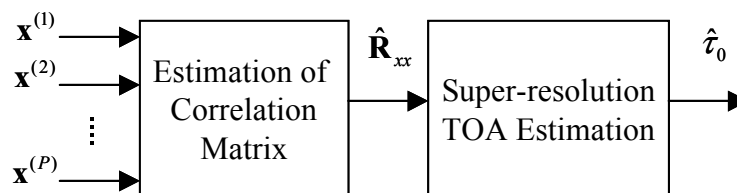


Figure 4.7: Estimation of correlation matrix with diversity techniques for super-resolution TOA estimation, correlation matrix based diversity combining scheme (CMDCS).

On the other hand, by applying the CMDCS scheme, the underlying assumption concerning the radio propagation channel is that the amplitude attenuation and the time

delay for each path, and the number of signal paths are the same from the transmitter to all diversity branches of the receiver. This restricts CMDCS to only quasi-stationary scenarios, where the channel structure remains unchanged while the P diversity measurement data are collected. This is one disadvantage of the CM-based scheme as compared with the general scheme, which has no such restriction in application. This condition for applicability also makes it challenging to use CMDCS for space diversity since in space-diversity situations, the radio propagation channel from the transmitter and diversity branches of the receiver are most likely not the same. Similarly, CMDCS is not suitable for time diversity. As we discussed in the preceding section, the super-resolution technique cannot work properly when the phase of each signal path remains unchanged together with the amplitude attenuation and time delay for each path, and the total number of signal paths. For quasi-stationary scenarios, it is unknown whether the phase is random or not for repeated measurements while the number of signal paths and the amplitude attenuation and time delay for each path all remain unchanged. But simulation results based on measurement data collected on indoor radio channels, which will be presented in the next chapter, show that time-diversity with CMDCS yields almost no improvement over non-diversity techniques. In contrast, frequency-diversity can be well fitted into CMDCS. By using frequency-diversity, the k th measurement data vector $\mathbf{x}^{(k)}$, $1 \leq k \leq P$, are obtained using k th carrier frequency. A quantitative relationship between the improvement of TOA estimation accuracy and frequency diversity is not known, but the effects of frequency diversity can be conveniently

analyzed using the correlation coefficients similar to the way by which we analyzed the forward and the forward-backward correlation methods in the last section.

For frequency diversity, if the carrier frequency f_0 is uniformly distributed, *i.e.*

$$f_0 \sim U(f_c - \Delta F / 2, f_c + \Delta F / 2), \quad (4.24)$$

where f_c is center frequency and ΔF is the range of the frequency distribution, the correlation coefficient between α_i' and α_j' can be derived as

$$\begin{aligned} \rho_{ij}^{(\text{FD})} &= \frac{\sin(\pi \Delta F (\tau_i - \tau_j))}{\pi \Delta F (\tau_i - \tau_j)} e^{j[(\theta_i - \theta_j) - 2\pi f_c (\tau_i - \tau_j)]} \\ &= \text{sinc}(\pi \Delta F (\tau_i - \tau_j)) e^{j[(\theta_i - \theta_j) - 2\pi f_c (\tau_i - \tau_j)]} \end{aligned} \quad (4.25)$$

where the superscript FD stands for frequency diversity, and the *sinc* function is defined as $\text{sinc}(x) = \sin(x)/x$. Similarly, if the frequency diversity method is used for the forward correlation matrix, the correlation coefficient becomes

$$\rho_{ij}^{(\text{FCM, FD})} = K' e^{-j\phi'}, \quad (4.26)$$

where

$$\begin{aligned} K' &= K \frac{\sin(\pi \Delta F (\tau_i - \tau_j))}{\pi \Delta F (\tau_i - \tau_j)} = K \text{sinc}(\pi \Delta F (\tau_i - \tau_j)) \\ &= |\rho_{ij}^{(\text{FD})}| |\rho_{ij}^{(\text{FCM})}| \end{aligned}$$

$$\phi' = -(\theta_i - \theta_j) + 2\pi f_c (\tau_i - \tau_j) + \pi(M-1)\Delta f (\tau_i - \tau_j)$$

and that for forward-backward correlation matrix becomes

$$\rho_{ij}^{(\text{FBCM, FD})} = K' \cos(\phi' + \frac{\psi}{2}) e^{j\psi/2}, \quad (4.27)$$

where K' and ϕ' are the same as in (4.26). Details of the derivation of (4.25), (4.26), and (4.27) are presented in Appendix 4.A. We notice that by using the frequency diversity method, the coherence between multipath components is decorrelated according to the *sinc* function as ΔF and absolute value of delay difference ($\tau_i - \tau_j$) increase.

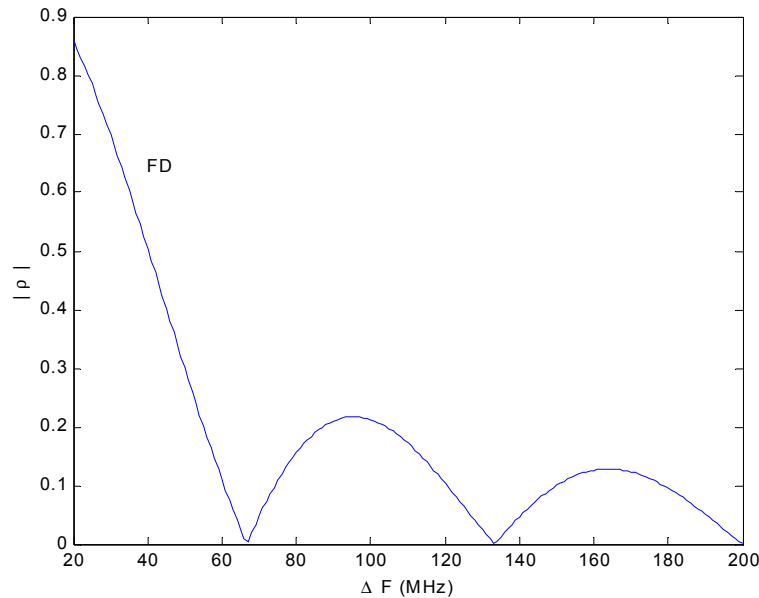


Figure 4.8: Correlation coefficient with frequency diversity, with parameters $(\tau_i - \tau_j) = 15\text{ns}$, $(\theta_i - \theta_j) = 0$, and $f_c = 1\text{GHz}$.

Figure 4.8 shows an example of the decorrelation effect of frequency diversity, calculated from (4.25), versus the range of the frequency distribution. Figure 4.9 and Fig. 4.10 shows correlation coefficients of forward and forward-backward correlation matrices with frequency diversity, calculated from (4.26) and (4.27), using the same

parameters as in Fig. 4.4 and Fig. 4.5. We can clearly observe that the frequency diversity technique further improves the decorrelation effects in both forward and forward-backward correlation matrices. In Chapter 5, we compare and evaluate the performance of diversity techniques using computer simulations based on empirical frequency-domain indoor radio propagation channel measurement data.

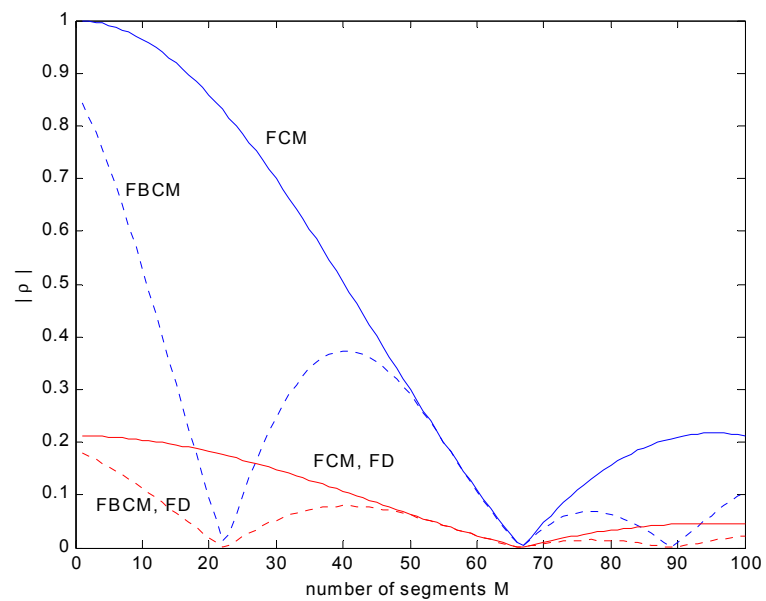


Figure 4.9: Correlation coefficients of FCM and FBCM with and without frequency diversity, with parameters $\Delta f = 1\text{MHz}$, $(\tau_i - \tau_j) = 15\text{ns}$, $(\theta_i - \theta_j) = 0$, $f_c = 1\text{GHz}$, $L = 13$, and $\Delta F = 100\text{MHz}$.

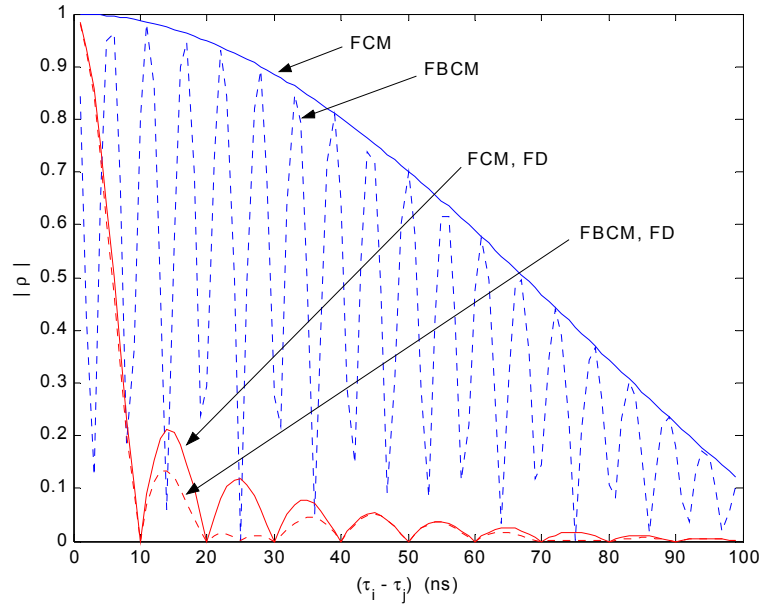


Figure 4.10: Correlation coefficients of FCM and FBCM with and without frequency diversity, with parameters $M = 9$, $\Delta f = 1\text{MHz}$, $(\theta_i - \theta_j) = 0$, $f_c = 1\text{GHz}$, $L = 13$, and $\Delta F = 100\text{MHz}$.

4.5 Summary and Conclusions

In this chapter, we have presented super-resolution TOA estimation techniques. The super-resolution spectral estimation algorithms are applied to the TOA estimation applications on the basis that the frequency representation of the multipath radio propagation channel model can be viewed as the harmonic signal model, which is well known in the spectral estimation field. After forming the signal model based on the frequency-domain channel response, the MUSIC super-resolution TOA estimation algorithm is derived in the same way as in the spectral estimation applications.

In the TOA estimation applications, the super-resolution algorithm is used to convert the measurement data, which is the estimate of the channel frequency response, from frequency domain to time domain to estimate the arrival time of the DLOS signal in contrast to the spectrum estimation applications, where the super-resolution algorithms are used to convert time-domain measurement data of a random signal to frequency domain to estimate the spectrum of the signal. Thus in spectrum estimation applications, more measurement data can be obtained by simply extending the observation time of the random signal, while in the TOA estimation applications increasing the length of the measurement data means an increase in the signal bandwidth. With longer measurement data, the correlation matrix can be estimated more accurately, which leads to the better performance of the super-resolution algorithm. The practical limitation on the available signal bandwidth poses a limitation on the length of the channel measurement data in the TOA estimation applications. Thus in this chapter several techniques are presented, including the forward-backward estimation of correlation matrix, eigenvector method, and diversity techniques, which can be used to improve the performance of the super-resolution TOA estimation algorithms when the length of the frequency-domain channel measurement data is short.

Also in this chapter, the effects of the forward estimation of correlation matrix, the forward-backward estimation of correlation matrix, the frequency diversity techniques, the FCM with frequency diversity, and the FBCM with frequency diversity techniques are analyzed with the correlation coefficients. The detailed derivation of the correlation coefficients is presented in the appendix of this chapter. From the analysis

we can conclude that the forward-backward estimation method has better decorrelation effects, which leads to the better performance of the super-resolution TOA estimation techniques, and diversity techniques, especially the frequency diversity technique, further improve the decorrelation effects of the correlation matrix. Two diversity combining schemes, *i.e.*, the GDCS and CMDCS diversity combining schemes, are proposed for the super-resolution TOA estimation techniques. It is shown that the CMDCS is computational superior than the GDCS, and the CMDCS is well suited for the frequency diversity techniques, which can significantly improve the decorrelation effects of the correlation matrix of the channel measurement data.

In the next chapter we compare and evaluate the performance of various super-resolution TOA estimation techniques presented in this chapter with the computer simulations based on empirical frequency-domain channel measurement data.

Appendix 4.A Derivation of Correlation Coefficients

In order to keep the main content of this chapter concise and easy to follow, the detailed derivation of the correlation coefficients in (4.16), (4.17), (4.25), (4.26), and (4.27) is presented in this appendix.

4.A.1 Correlation Coefficients using Forward Estimation Method

The parameter correlation matrix of the multipath channel model is defined in (4.5) as

$$\mathbf{A} = E\{\mathbf{a}\mathbf{a}^H\}. \quad (4.A.1)$$

while the parameter vector \mathbf{a} is defined in (4.5). Thus using the forward estimation method defined in (4.13), the (i, j) th element of the correlation matrix \mathbf{A} can be obtained as

$$\begin{aligned} A_{ij} &= E\{\alpha_i \alpha_j^*\} \\ &= \frac{1}{M} \sum_{k=0}^{M-1} (\alpha_i e^{-j2\pi(f_0+k\Delta f)\tau_i}) \times (\alpha_j e^{-j2\pi(f_0+k\Delta f)\tau_j})^* \\ &= \frac{1}{M} \alpha_i \alpha_j^* e^{-j2\pi f_0(\tau_i-\tau_j)} \sum_{k=0}^{M-1} e^{-j2\pi k\Delta f(\tau_i-\tau_j)} \\ &= \frac{1}{M} \alpha_i \alpha_j^* e^{-j2\pi f_0(\tau_i-\tau_j)} \frac{1 - e^{-j2\pi M\Delta f(\tau_i-\tau_j)}}{1 - e^{-j2\pi\Delta f(\tau_i-\tau_j)}} \\ &= \alpha_i \alpha_j^* e^{-j2\pi f_0(\tau_i-\tau_j)} e^{-j\pi(M-1)\Delta f(\tau_i-\tau_j)} \frac{\sin[M\pi\Delta f(\tau_i-\tau_j)]}{M \sin[\pi\Delta f(\tau_i-\tau_j)]} \end{aligned} \quad (4.A.2)$$

and it easily follows that

$$A_{ii} = |\alpha_i|^2 \quad (4.A.3)$$

where $\alpha_i = |\alpha_i| e^{j\theta_i}$ as defined in (4.1). From the definition of the correlation coefficient between i th and j th parameters, defined as [Red87], we can easily obtain that

$$\rho_{ij}^{(\text{FCM})} = \frac{A_{ij}}{\sqrt{A_{ii}A_{jj}}} = Ke^{-j\phi}, \quad (4.A.4)$$

where

$$K = \frac{\sin[M\pi\Delta f(\tau_i - \tau_j)]}{M \sin[\pi\Delta f(\tau_i - \tau_j)]}$$

$$\phi = -(\theta_i - \theta_j) + 2\pi f_0(\tau_i - \tau_j) + \pi(M-1)\Delta f(\tau_i - \tau_j).$$

4.A.2 Correlation Coefficients using Forward-backward Estimation

Method

The forward-backward correlation matrix is defined in (4.14),

$$\hat{\mathbf{R}}_{xx}^{(\text{FB})} = \frac{1}{2}(\hat{\mathbf{R}}_{xx} + \mathbf{J}\hat{\mathbf{R}}_{xx}^*\mathbf{J}) \quad (4.A.5)$$

where $\hat{\mathbf{R}}_{xx}$ and $\mathbf{J}\hat{\mathbf{R}}_{xx}^*\mathbf{J}$ are forward and backward correlation matrices, respectively.

The backward correlation matrix can be equivalently calculated using (4.13) with the data vector

$$\mathbf{x} = [x(L-1) \quad x(L-2) \quad \dots \quad x(0)]^H \quad (4.A.6)$$

which is reversed version of the original data vector defined in (4.5), so that the element of the parameter vector \mathbf{a} defined in (4.5) becomes

$$\alpha_k' = \alpha_k^* e^{j2\pi(f_0 + (L-1)\Delta f)\tau_k}. \quad (4.A.7)$$

Thus using the backward estimation method, the (i, j) th element of the parameter correlation matrix can be obtained as

$$\begin{aligned}
A_{ij}^{(B)} &= \frac{1}{M} \sum_{k=0}^{M-1} (\alpha_i^* e^{j2\pi(f_0+k\Delta f+(L-1)\Delta f)\tau_i}) \times (\alpha_j^* e^{j2\pi(f_0+k\Delta f+(L-1)\Delta f)\tau_j})^* \\
&= \frac{1}{M} \alpha_i^* \alpha_j e^{j2\pi(f_0+(L-1)\Delta f)(\tau_i-\tau_j)} \sum_{k=0}^{M-1} e^{j2\pi k\Delta f(\tau_i-\tau_j)} \\
&= \frac{1}{M} \alpha_i^* \alpha_j e^{j2\pi(f_0+(L-1)\Delta f)(\tau_i-\tau_j)} \frac{1 - e^{j2\pi M\Delta f(\tau_i-\tau_j)}}{1 - e^{j2\pi\Delta f(\tau_i-\tau_j)}} \quad (4.A.8) \\
&= \alpha_i^* \alpha_j e^{j2\pi(f_0+(L-1)\Delta f)(\tau_i-\tau_j)} e^{j\pi(M-1)\Delta f(\tau_i-\tau_j)} \frac{\sin[M\pi\Delta f(\tau_i-\tau_j)]}{M \sin[\pi\Delta f(\tau_i-\tau_j)]} \\
&= A_{ij}^* e^{j2\pi(L-1)\Delta f(\tau_i-\tau_j)}
\end{aligned}$$

where A_{ij} is given by (4.A.2). Then the (i, j) th element of the parameter correlation matrix using the forward-backward estimation method can be obtained as

$$A_{ij}^{(FB)} = \frac{1}{2} (A_{ij} + A_{ij}^{(B)}). \quad (4.A.9)$$

Finally the correlation coefficient between i th and j th parameters can be determined by

$$\begin{aligned}
\rho_{ij}^{(FBCM)} &= \frac{A_{ij}^{(FB)}}{|\alpha_i| |\alpha_j|} \\
&= \frac{1}{2} (K e^{-j\phi} + K e^{j(\phi+\psi)}) \quad (4.A.10) \\
&= K \cos(\phi + \psi/2) e^{j\psi/2}
\end{aligned}$$

where

$$\psi = 2\pi(L-1)\Delta f(\tau_i - \tau_j),$$

and K and ϕ are the same as in (4.A.4).

4.A.3 Correlation Coefficients with Frequency Diversity

For frequency diversity, we assume the carrier frequency is uniformly distributed as given in (4.24). The elements of the parameter correlation matrix are derived as follows:

$$\begin{aligned}
 A_{ij}^{(\text{FD})} &= E\{\alpha_i \alpha_j^*\} \\
 &= \frac{1}{\Delta F} \int_{f_c - \Delta F/2}^{f_c + \Delta F/2} \alpha_i \alpha_j^* e^{-j2\pi f_0(\tau_i - \tau_j)} df_0 \\
 &= \alpha_i \alpha_j^* e^{-j2\pi f_c(\tau_i - \tau_j)} \frac{\sin[\pi \Delta F(\tau_i - \tau_j)]}{\pi \Delta F(\tau_i - \tau_j)}
 \end{aligned} \tag{4.A.11}$$

and the correlation coefficient is easily obtained:

$$\begin{aligned}
 \rho_{ij}^{(\text{FD})} &= \frac{A_{ij}^{(\text{FD})}}{|\alpha_i| |\alpha_j|} \\
 &= \frac{\sin(\pi \Delta F(\tau_i - \tau_j))}{\pi \Delta F(\tau_i - \tau_j)} e^{j[(\theta_i - \theta_j) - 2\pi f_c(\tau_i - \tau_j)]} \\
 &= \text{sinc}(\pi \Delta F(\tau_i - \tau_j)) e^{j[(\theta_i - \theta_j) - 2\pi f_c(\tau_i - \tau_j)]},
 \end{aligned} \tag{4.A.12}$$

where the *sinc* function is defined as $\text{sinc}(x) = \sin(x)/x$.

The correlation coefficients of forward estimation methods, given in (4.26) are easily obtained by noticing that

$$\begin{aligned}
 &\rho_{ij}^{(\text{FCM, FD})} \\
 &= E\{\rho_{ij}^{(\text{FCM})}\} \\
 &= E\left\{K e^{-j[-(\theta_i - \theta_j) + 2\pi f_c(\tau_i - \tau_j) + \pi(M-1)\Delta f(\tau_i - \tau_j)]}\right\} \\
 &= E\left\{e^{-j2\pi f_c(\tau_i - \tau_j)}\right\} K e^{-j[-(\theta_i - \theta_j) + \pi(M-1)\Delta f(\tau_i - \tau_j)]} \\
 &= e^{-j2\pi f_c(\tau_i - \tau_j)} \frac{\sin[\pi \Delta F(\tau_i - \tau_j)]}{\pi \Delta F(\tau_i - \tau_j)} K e^{-j[-(\theta_i - \theta_j) + \pi(M-1)\Delta f(\tau_i - \tau_j)]} \\
 &= K' e^{-j\phi'}
 \end{aligned} \tag{4.A.13}$$

where

$$K' = K \frac{\sin(\pi \Delta F(\tau_i - \tau_j))}{\pi \Delta F(\tau_i - \tau_j)} = K \operatorname{sinc}(\pi \Delta F(\tau_i - \tau_j))$$

$$= \left| \rho_{ij}^{(\text{FD})} \right| \left| \rho_{ij}^{(\text{FCM})} \right|$$

$$\phi' = -(\theta_i - \theta_j) + 2\pi f_c(\tau_i - \tau_j) + \pi(M-1)\Delta f(\tau_i - \tau_j)$$

and the statistical expectation $E\{\cdot\}$ is performed with respect to the uniformly distributed carrier frequency f_0 , which is defined in (4.24). Similarly, the correlation coefficients of forward-backward estimation methods, given in (4.27) are obtained as follows,

$$\begin{aligned} & \rho_{ij}^{(\text{FBCM, FD})} \\ &= E\{\rho_{ij}^{(\text{FBCM})}\} \\ &= E\left\{K \cos(-(\theta_i - \theta_j) + 2\pi f_c(\tau_i - \tau_j) + \pi(M-1)\Delta f(\tau_i - \tau_j) + \psi/2) e^{j\psi/2}\right\} \\ &= \frac{Ke^{j\psi/2}}{2} E\left\{e^{-j[-(\theta_i - \theta_j) + 2\pi f_c(\tau_i - \tau_j) + \pi(M-1)\Delta f(\tau_i - \tau_j) + \psi/2]} \right. \\ & \quad \left. + e^{j[-(\theta_i - \theta_j) + 2\pi f_c(\tau_i - \tau_j) + \pi(M-1)\Delta f(\tau_i - \tau_j) + \psi/2]} \right\} \\ &= Ke^{j\psi/2} \frac{\sin(\pi \Delta F(\tau_i - \tau_j))}{\pi \Delta F(\tau_i - \tau_j)} \cos(\phi' + \psi/2) \\ &= K' \cos(\phi' + \frac{\psi}{2}) e^{j\psi/2}. \end{aligned} \tag{4.A.14}$$

where K' and ϕ' are the same as in (4.A.13), and ψ is the same as in (4.A.10).

Chapter 5

Performance Evaluation Based on Channel Measurements

In the previous chapters we have presented the traditional TOA estimation techniques, developed for the single-path AWGN channels, and the super-resolution TOA estimation techniques as well as the diversity techniques developed on the basis of the frequency-domain representation of the multipath radio propagation channel models. The super-resolution techniques can increase the resolution of the time-domain channel response in multipath channels, which helps to accurately estimate the arrival time of the DLOS signal, and thus improves the performance of the TOA estimation in indoor multipath radio propagation channels for geolocation applications. In Chapter 4, the performance of various super-resolution and diversity techniques has been evaluated and compared theoretically by comparing the correlation coefficients of the estimated channel parameter correlation matrix since better decorrelation effect in the channel parameter correlation matrix leads to better performance of the super-resolution techniques. However, there is no theoretical way to quantitatively compare the performance of various super-resolution techniques, and the super-resolution techniques

with the traditional TOA estimation techniques. As a result, in this chapter we further investigate the performance of super-resolution and diversity techniques for TOA estimation applications by the computer simulations based on the measured frequency-domain response of indoor radio propagation channels. In this chapter, the channel measurement system and measurement scenarios are described first in Section 5.1, followed by a description of the performance evaluation methodology in Section 5.2 that is employed in our research. Then various super-resolution techniques are evaluated and compared based on computer simulation results in the rest of this chapter. For reference purposes, a description of the measurement sites and scenarios are presented in Appendix 5.A, and the cumulative distribution functions of the ranging errors with different TOA estimation techniques are presented in Appendix 5.B.

5.1 Frequency-Domain Channel Measurement

The frequency response of indoor radio propagation channel can be directly measured with a frequency-domain channel measurement system reported in [How90, Pah95]. Figure 5.1 shows the block diagram of the frequency-domain channel measurement system. The main component of the measurement system is a network analyzer that generates a swept frequency signal and analyzes the resulting received signal to estimate the amplitude and phase fading effects of the radio propagation channel of interest at each specific frequency. The network analyzer is controlled by a laptop through the HP's version of a general purpose instrumentation bus (GPIB). The laptop initializes the network analyzer preceding each measurement, and collects the

data at the completion of each measurement. The magnitude and phase of the measured channel frequency response are stored for each measurement. A variety of signal processing techniques can be applied to the frequency-domain channel measurement data collected with this measurement system to obtain the time and frequency responses of the radio propagation channel, to estimate various channel characteristics, and to conduct statistical channel modeling as presented in [How92, Pah05].

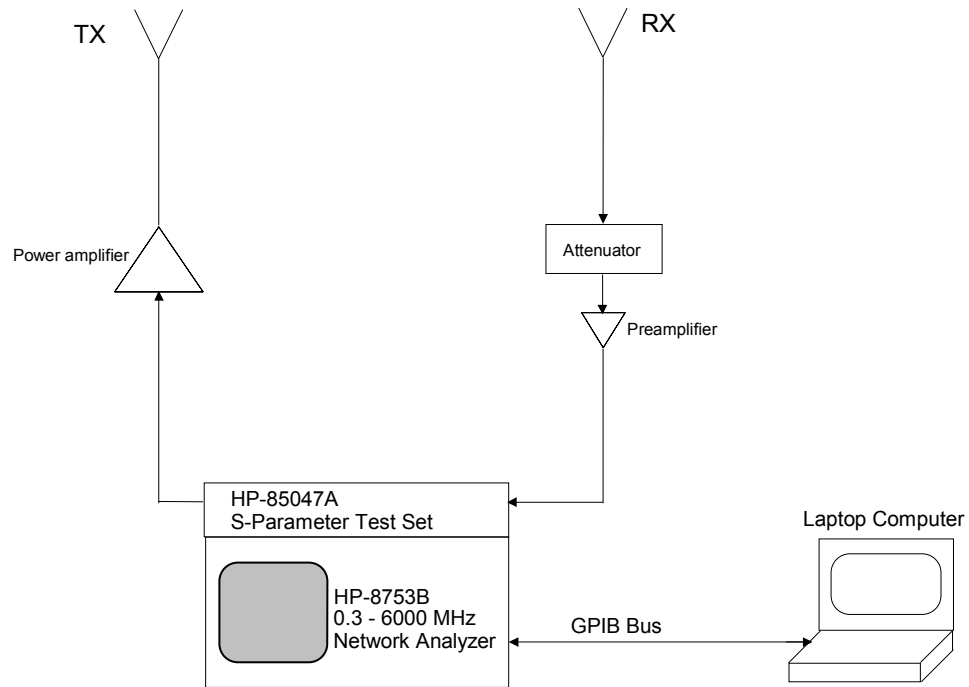


Figure 5.1: Block diagram of the frequency-domain channel measurement system.

The indoor radio propagation channel measurement data reported in [Ben99], collected with the measurement system shown in Fig. 5.1, is used in our research to evaluate the performance of super-resolution TOA estimation techniques as explained in details in the next section. The magnitude and phase measurements of radio

propagation channel were performed at the center frequency 1 GHz with a bandwidth of 200 MHz. The measurements were conducted at three different buildings that represent highly likely places for deployment of indoor geolocation systems, including a manufacturing building at the Norton Co., Worcester, MA, a modern academic building, the Fuller Laboratory at WPI, and a residential house, the Schussler House at the WPI. Thirty locations were selected at each site for measurement at the places where indoor geolocation systems will be likely used. At each receiver location, four consecutive snapshots of radio propagation channel were taken while preventing movement around the vicinity of the antennas of the transmitter and receiver. During the measurement, the transmitter antenna was fixed at one location while the receiver antenna was moved around. The measurement locations were distributed so as to include three different radio propagation scenarios, that is, indoor-to-indoor, outdoor-to-indoor, and outdoor-to-second floor communications. For each measurement location, the physical distance between the antennas of the transmitter and receiver were determined and recorded either directly or indirectly from the blueprint of the building floorplans. The detailed description of measurement sites and measurement locations are presented in Appendix 5.A. After the measurement process, the frequency domain measurement data were calibrated to remove the effects of the system and antenna gains and delays as described in the reference [How90].

5.2 Performance Evaluation Method

The super-resolution TOA estimation techniques are developed on the basis of the frequency-domain representation of the multipath radio propagation channel model, which can be equivalently viewed as the harmonic signal model that is well known in parametric spectral estimation field. As presented in Section 4.2 and 4.3, the input of the super-resolution algorithm in the TOA estimation is the estimated discrete channel frequency response. The frequency response of indoor radio propagation channel can be directly measured with a network analyzer as described in Section 5.1. Thus in this thesis, we evaluate the super-resolution TOA estimation techniques with empirical frequency-domain channel measurement data as the input of the algorithm, without concerning about issues in the channel frequency response estimation in the practical implementation of the TOA estimation systems. The techniques and performance of channel frequency response estimation, *i.e.*, the first functional block in Fig. 4.1, deserves a separate study and is beyond the scope of this thesis.

The purpose of the performance evaluation in this chapter is to compare various TOA estimation techniques, and to evaluate and benchmark the performance of super-resolution techniques in realistic indoor application environments. As we discussed in Chapter 3, the CRLB presented therein is derived for the single-path AWGN channels and it is the variance of the ML delay estimate in the neighborhood of its true value. However, in multipath channels the CRLB is not directly applicable because dramatically large TOA estimation errors occur when the DLOS path is undetectable. The effects of channel characteristics on the performance of the TOA estimation has not

yet been well studied and modeled. There are no suitable indoor multipath radio propagation channel models available in the literature for the performance evaluation of the TOA estimation techniques. Consequently, in designing TOA estimation techniques for multipath channels, the performance evaluation is usually conducted by studying the resolution of the estimation techniques based on computer simulations with a simple equal-gain two-path channel model as used in [Pal91]. In addition to the resolution of the estimation techniques, the radio channel characteristics such as multipath fading and shadow fading among others have tremendous effects on the performance of the TOA-based ranging systems in real application scenarios as we discussed in Chapter 3. The two-path channel model does not incorporate any of the complex characteristics of indoor radio propagation channels. Therefore, while the two-path channel model is useful in preliminary study of the multipath-resolving capability of the TOA estimation techniques, it is impossible to compare the traditional TOA estimation techniques and the super-resolution techniques, and to provide performance benchmarks in real application environments with the simple two-path model. In indoor environments, the performance of the TOA estimation techniques can be measured and benchmarked more appropriately by the computer simulations based on empirical channel measurement data, by conducting field measurement using prototype systems, or by using the ray-tracing software to simulate the site-specific indoor radio propagation channels. The performance study based on these methods reveals much more realistic statistical results than the resolution study of the estimation techniques with the simple two-path channel model. On the other hand, as noted in the beginning of this section,

the frequency-domain channel measurement data can be readily incorporated in the super-resolution TOA estimation techniques. As a result, in this chapter we evaluate the performance of various TOA estimation techniques, including traditional techniques, super-resolution techniques, and diversity techniques, through computer simulations based on empirical frequency-domain indoor radio propagation channel measurement data, which can be obtained with the frequency-domain channel measurement system presented in Section 5.1. Such a measurement-based simulation method can be employed in practice to conveniently establish empirical performance benchmarks when designing the TOA estimation systems.

Extensive channel measurement data are collected at spatially widely distributed locations where indoor geolocation systems are most likely deployed and used. During the measurement, the physical distance between the transmitter and receiver antennas of the measurement system is measured either directly or indirectly from the blueprint of building floorplans, to determine the expected TOA for each measurement location. Through the computer simulations based on channel measurement data, the statistical results of ranging errors are determined such as mean, standard deviation (STD), and cumulative distribution function (CDF). Various TOA estimation techniques are compared based on these statistical simulation results obtained from the same set of measurement data described in Section 5.1 and Appendix 5.A. It is important to note that due to the site specific nature and the complexity of indoor radio propagation channels, as presented in Chapter 2 and 3, the computer simulations based on different set of channel measurement data may reveal varying statistical results so that the

quantitative performance comparison of different TOA estimation techniques is meaningful only with the same set of measurement data.

The signal bandwidth is one of the key factors affecting the accuracy of the TOA estimation in the multipath propagation environments as presented in Chapter 3 and the reference [Pah02]. Therefore, in this chapter we compare different TOA estimation techniques with various bandwidths to observe the effect of signal bandwidth. To study the performance of the TOA estimation using signals of various bandwidths, in our simulations we use only a segment of each frequency-domain measurement data to reflect the band-limitation effects. For example, with a 1 MHz frequency-domain sampling interval, a data segment of 21 samples of each measurement data, centered at 1 GHz, is used in the simulations for a signal bandwidth of 20 MHz.

In the following sections, various performance evaluation results are presented, which are obtained from the channel measurement data based simulations that are outlined in this section, to evaluate and to benchmark the performance of various TOA estimation techniques in indoor application environments.

5.3 Performance of Super-resolution Techniques

The purpose of this section is to compare the performance of various super-resolution TOA estimation techniques presented in Section 4.2 and 4.3 with the measurement data based simulations outlined in Section 5.2. As discussed in Section 5.2, instead of estimating from the received signal as shown in Fig. 4.1, the channel

frequency response is directly obtained using the frequency-domain channel measurement system shown in Fig. 5.1. A sample measured channel frequency response is shown in Fig. 5.2, which is obtained at the center frequency of 1 GHz with a frequency bandwidth of 200 MHz and a frequency sampling interval of 1 MHz. The super-resolution TOA estimation algorithm shown in Fig. 4.2 is implemented to estimate the TOA. In this section the input data correlation matrix \mathbf{R}_{xx} is estimated using the forward estimation technique given in (4.13) and the forward-backward estimation technique given in (4.14) while in Section 5.5 and 5.6 the correlation matrix is estimated using the diversity techniques given in (4.12) together with the forward and forward-backward estimation techniques. In our simulations, as discussed in Section 4.3.2 the length of segments $L = 2N/3$, which is defined in (4.13), and the total number of the multipath components L_p is determined using the MDL criteria given in (4.20) and (4.21) for forward and forward-backward estimation methods, respectively.

As we discussed earlier in Section 4.3.3, the Eigenvector (EV) method is a variant of the MUSIC method and it is preferred when the correlation matrix is estimated from a limited number of data samples. To compare the performance of the EV and MUSIC methods, both algorithms are applied to the same set of the measured data described in Section 5.1 and Appendix 5.A, with the forward-backward estimation of the correlation matrix. In Section 4.3.1, we have theoretically analyzed the forward (FCM) and forward-backward (FBCM) estimation techniques for super-resolution TOA estimation through the decorrelation effects in the estimated correlation matrix. Since there is no analytical way to quantitatively relate the improvement in the accuracy of the

TOA estimation to the correlation matrix estimation techniques, in this section we also compare these two methods using statistical simulation results.

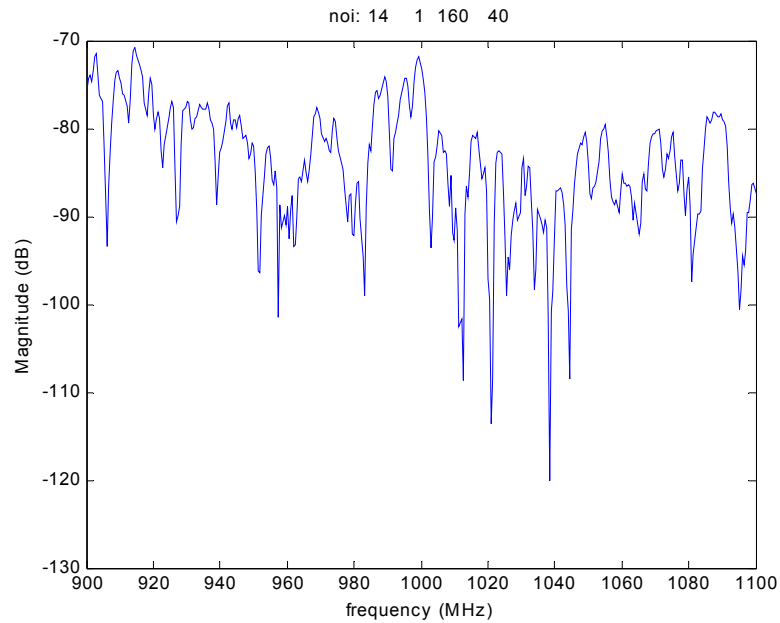


Figure 5.2: Frequency-domain channel measurement data obtained using the measurement system in Fig. 5.1.

Figure 5.3 presents the mean of the ranging errors versus signal bandwidth using various super-resolution TOA estimation techniques. The vertical line corresponds to plus and minus one standard deviation about the mean. To clearly relate the results to geolocation applications, time delay τ is converted to distance d by the relation $d = c \times \tau$, where $c = 3 \times 10^8$ m/s is the constant speed-of-light in free space. The results for different techniques are slightly shifted in the x -axis for better observation. From the results in Fig. 5.3, we can observe that both mean and standard deviation of the

ranging errors decrease as the bandwidth increases for all techniques. The statistical performance of the MUSIC and EV algorithms with the FBCM, *i.e.*, MUSIC/FBCM and the MUSIC/FCM, is very close to each other. However, the EV method has slightly better performance than the MUSIC for low signal bandwidth in terms of smaller standard deviation of estimation errors. Without further comparison of the MUSIC and EV algorithms, in the following we use the EV algorithm for further investigation of the FCM, FBCM, and the diversity techniques.

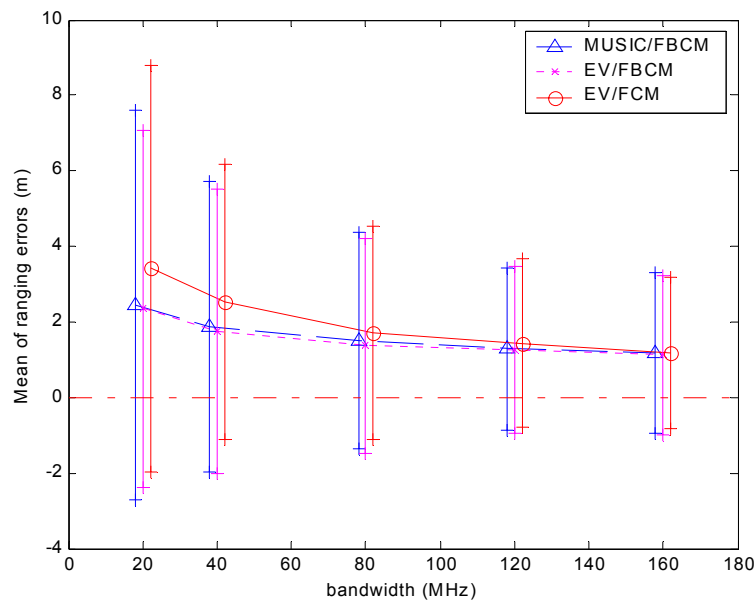


Figure 5.3: Mean of ranging errors using the MUSIC and EV algorithms with the forward (FCM) and forward-back (FBCM) estimation of correlation matrix. The vertical line corresponds to plus and minus one standard deviation of the ranging errors about the mean.

Figure 5.3 also presents the simulation results for the EV algorithm with the FCM (EV/FCM). Comparing the EV/FBCM and the EV/FCM, it is clear that the FBCM based method performs much better than the FCM based method in terms of smaller mean and standard deviation of the estimation errors for the same simulation scenarios, which is consistent with the analysis in Section 4.3.1. For example, the EV/FBCM has about 1 m's smaller mean and about 2 m's smaller standard deviation than the EV/FCM for a bandwidth of 20 MHz. It is also noted that both techniques have similar performance when the signal bandwidth is large, *e.g.*, when the bandwidth is larger than 120 MHz.

5.4 Comparison of Super-resolution and Conventional Techniques

In order to demonstrate the usefulness of the super-resolution technique, we compare its performance with two conventional time delay estimation techniques. In the first of the other two techniques, the frequency-domain channel response is converted directly to time domain using the inverse Fourier transform (IFT) and then the propagation delay of the DLOS signal is detected. Since indoor radio propagation channels have limited multipath delay spread and here we are only interested in the arrival time of the DLOS signal, partial time-domain channel response will suffice for the TOA estimation. If partial time response is desired when converting the frequency response to time domain, the chirp-z transform (CZT) is preferred that provides flexibility in the choice of time-domain parameters with the cost of longer

computational time as compared with the IFFT [Ulr86]. The time-domain resolution with the CZT is the same as with the inverse FFT. On the other hand, a proper window function is needed to avoid leakage and false peaks by reducing the sidelobes of the time-domain response, which is resulted from finite bandwidth, with the cost of reduced time-domain resolution. In our simulations, we employ the CZT with the Hanning window to convert frequency channel response to time domain, though on the figures of our simulation results such a technique is still denoted by IFT.

The second technique uses the traditional cross-correlation technique with the direct-sequence spread-spectrum (DSSS) signals, designated as DSSS/xcorr on the figures of the simulation results. To simulate the DSSS signal-based cross-correlation technique using the frequency-domain channel measurement data, the frequency response of a raised-cosine pulse with a rolloff factor of 0.25 is first applied to the frequency channel response as a combined response of the band-limitation pulse-shaping filters of the transmitter and the receiver. Then the resultant frequency response is converted to time domain using the inverse Fourier transform for the TOA estimation. The use of such a simulation technique is easily justified since the delay profile obtained using the DSSS signal-based ranging technique is the channel impulse response convolved with the pulse shape of a single chip of the spread spectrum signal. Interested readers can refer to the references [Rap96, Cox72] for more detailed discussion on this issue.

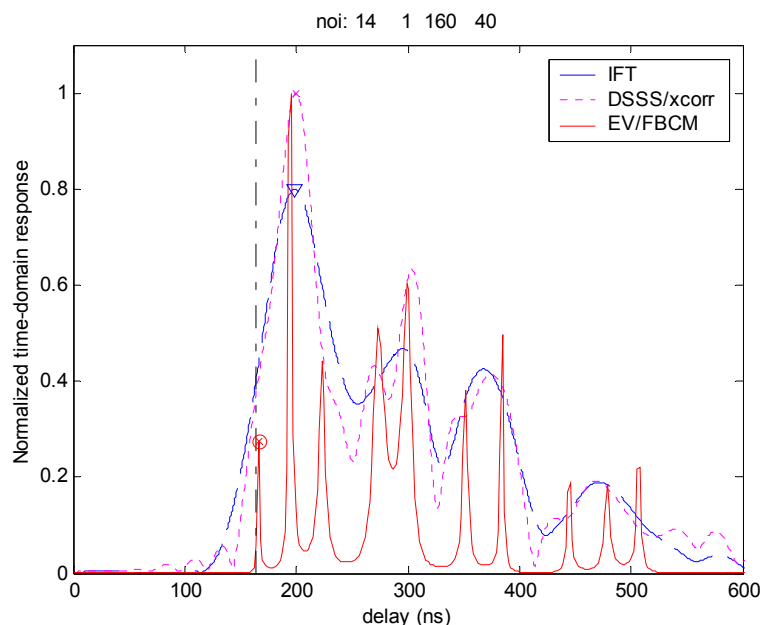


Figure 5.4: Normalized time-domain channel responses obtained using three different techniques. The vertical dash-dot line denotes the expected TOA. The estimated TOA is marked on the time-domain channel response for each of the three techniques.

Figure 5.4 shows the normalized time-domain channel responses obtained from the simulations using three different techniques, *i.e.*, the IFT and DSSS/xcorr techniques described in this section and the EV/FBCM described in Section 5.3, using a sample frequency-domain channel measurement data with a bandwidth of 40 MHz. The vertical dash-dot line on the figure denotes the position of the expected TOA (obtained by measuring physical distance between the transmitter and receiver antennas) and the estimated TOA is marked on the time-domain channel response for each of the estimation techniques. We can clearly observe that the EV/FBCM super-

resolution technique shows much higher time-domain resolution than the other two techniques and it accurately detects the arrival time of the DLOS path with 2.7 ns estimation error, while the other two show much larger estimation errors of about 35 ns.

Figure 5.5 presents the mean and the standard deviation of ranging errors versus signal bandwidth using the same techniques as in Fig. 5.4. Figure 5.6 presents the probabilities of the channel measurement locations where the absolute ranging errors are smaller than 3 m. From these results we can observe significant difference between the super-resolution technique and the other two TOA estimation techniques, especially when the signal bandwidth is relatively small. With a signal bandwidth of 20 MHz, the mean of ranging errors with the super-resolution technique is about 2 m's smaller than that of the DSSS/xcorr technique, and about 4 m's smaller than that of the IFT technique. On the other hand, with 20 MHz bandwidth, using the super-resolution technique we can estimate distance within 3 m's accuracy at about 25% more locations than by using the other two techniques. It is also noted that the performance difference decreases as the signal bandwidth increases.

From the simulation results presented above, we can conclude that in general, the super-resolution technique has the best performance and it is especially preferred when the signal bandwidth is small. On the other hand, it should also be noted from the simulation results that while using the super-resolution technique and larger bandwidth can improve the statistical performance of the TOA estimation, it cannot eliminate large estimation errors at some locations. For example, from Fig. 5.6 we can observe that even with a bandwidth of 160 MHz there are still around 15% of the total measurement

locations showing larger than 3 m's ranging errors. This is because of the high probability no-LOS (NLOS) situation in indoor environments between the transmitter and receiver antennas that we discussed previously in Section 3.3. The large TOA (or distance) estimation errors due to the NLOS condition need to be dealt with in the positioning process to achieve high positional accuracy in indoor geolocation systems as presented in Section 3.3 and Section 2.4.

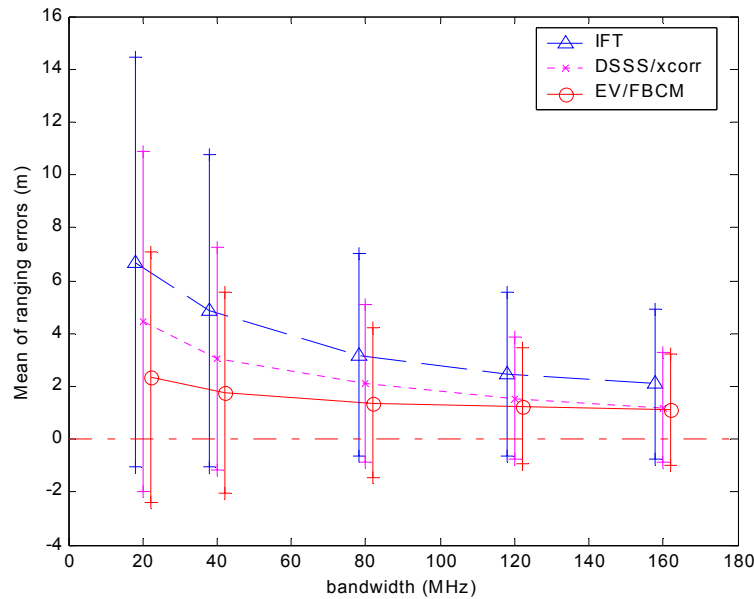


Figure 5.5: Mean of the estimation errors using three different techniques. The vertical line corresponds to plus and minus one standard deviation.

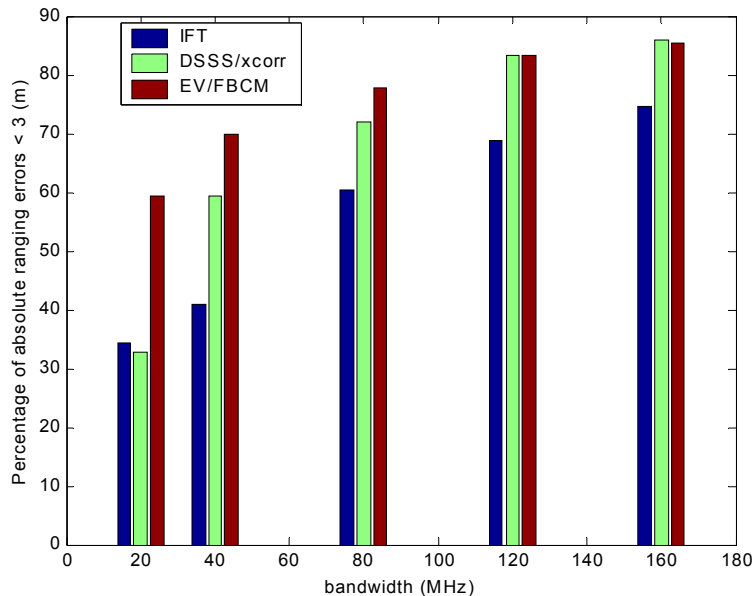


Figure 5.6: Percentages of the measurement locations where absolute ranging errors are smaller than 3 meters with three different TOA estimation techniques.

The exact comparison of our simulation results with the CRLB presented in Section 3.2 is not possible because our simulation results show the mean and standard deviation of the TOA estimation errors over a larger number of different locations but the CRLB is the lower bound of the TOA estimation errors caused by additive white noise at one location. However, since the CRLB is the lower bound of the variance of TOA estimation errors about the true time delay, the existence of the NLOS situations, which is apparent from our simulation results, makes it impossible to benchmark the performance of the TOA estimation techniques in indoor environments with the CRLB. For the same reason, the TOA estimation in the multipath indoor radio propagation channels has non-zero mean of estimation errors, that is, the estimation is biased as

shown in the Fig. 5.5; and the variance of the TOA estimation errors is much larger than the CRLB obtained with the single-path AWGN channel shown in Fig. 3.2.

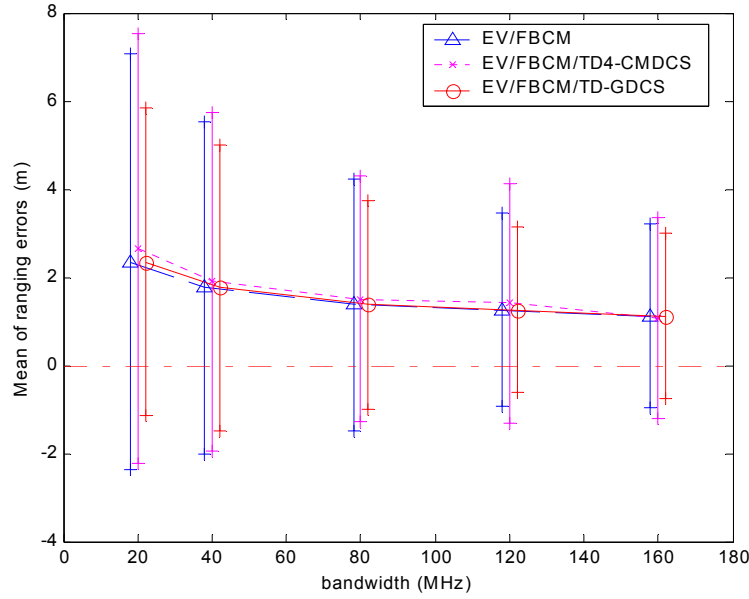


Figure 5.7: Mean and standard deviation of ranging errors without time diversity (EV/FBCM), with time diversity using the CMDCS (EV/FBCM/TD4-CMDCS) and GDCS schemes (EV/FBCM/TD-GDCS).

5.5 Effects of Time Diversity

In Section 4.4 we have discussed diversity techniques for the TOA estimation applications, including time, space, and frequency diversities. In this section we study the effects of time diversity with the two diversity combining schemes that we presented in Section 4.4, *i.e.*, the GDCS and CMDCS diversity combining schemes. In our channel measurement data based simulations, the time diversity is simulated by

running simulations with the four snapshots of the channel frequency response collected consecutively at each location while stopping movement in the vicinity of the transmitter and receiver antennas during the measurement. This represents the situation in which the system is used for quasi-stationary applications with four time diversity branches.

Figure 5.7 shows simulation results for the EV/FBCM technique with time diversity using two different diversity combining schemes, *i.e.*, using the CMDCS (EV/FBCM/TD4-CMDCS) and using the GDCS (EV/FBCM/TD-GDCS). The simulation results for the EV/FBCM method without time diversity are also presented on the figure as a reference for comparison and it is referred to as non-diversity method in the following. From the results, we can observe that there is no significant difference in the mean of the ranging errors with the three techniques for all bandwidth values. But the CMDCS based method has slightly worse performance in terms of larger standard deviation of ranging errors than the non-diversity method, which justifies the analysis and conclusion in Section 4.4 that the CMDCS diversity combining scheme is not suitable for the time diversity techniques. However, the GDCS based method has consistently better performance than the non-diversity method for all bandwidth values in terms of smaller standard deviation of ranging errors. For example, as compared with the non-diversity technique the GDCS based method has 1 m's smaller standard deviation of ranging errors with 20 MHz bandwidth, and about 0.5 m's smaller standard deviation with 40 MHz bandwidth. Therefore, the same as in Section 4.4 we can conclude that the GDCS diversity combining scheme can be used in time diversity

systems to improve the performance of the TOA estimation, while the CMDCS diversity combining scheme is not suitable for the time diversity technique. In the next section, we evaluate the performance of frequency diversity techniques with simulation results.

5.6 Effects of Frequency Diversity

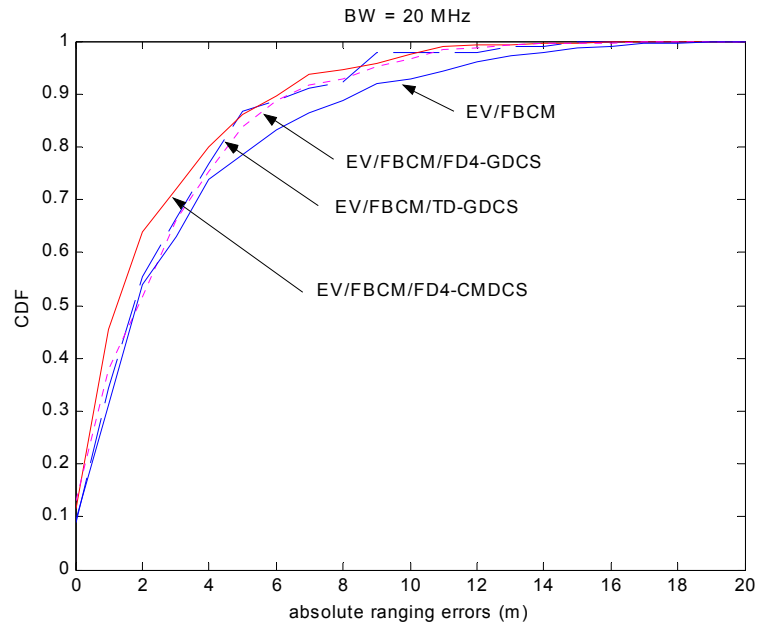
Through the analysis of the correlation coefficients of the estimated channel parameter correlation matrix, it is shown in Section 4.4 that the CMDCS diversity combining scheme is well suited for the super-resolution TOA estimation techniques with frequency diversity technique. The frequency diversity with the CMDCS can significantly reduce the correlation coefficients of the estimated channel parameter correlation matrix, and thus improves the performance of the super-resolution algorithms. But the theoretical quantitative relation between the improvement in the TOA estimation results and the parameters of frequency diversity technique, such as the number of the diversity branches, is not known. Therefore, in this section we evaluate the effect of frequency diversity on the super-resolution TOA estimation techniques with the channel measurement data based simulation results.

The use of frequency diversity technique is simulated by running simulations with a number of different segments of data samples from one snapshot of the frequency-domain channel response in a way similar to the data segmentation method used in (4.13). Each frequency-domain channel measurement data, *i.e.*, each snapshot of the frequency-domain channel response, is divided into a number of equally spaced

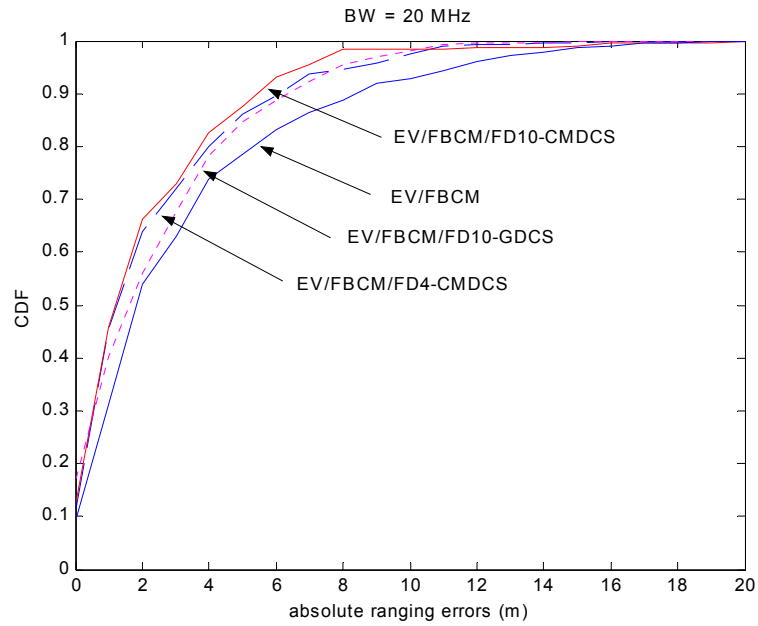
segments, so that each segment of the data has different center frequency. Since the measurement data at each location are of 200 MHz bandwidth, to avoid overlapping among diversity segments, the effect of frequency diversity is evaluated only for a bandwidth of 20MHz in this section. But it should be noted that in real implementation, overlapping segments can be used for frequency diversity. In our simulations, the overlapping is avoided only in order to avoid the correlation between measurement noises in the overlapping segments since the segments are obtained from the same snapshot of the frequency-domain channel response. Four equally spaced segments are first used for each measurement data sequence to compare the frequency and time diversity techniques using the same number of diversity branches. Both the GDCS and CMDCS diversity combining schemes are used for the EV/FBCM with frequency diversity, *i.e.*, the EV/FBCM/FD4-GDCS and the EV/FBCM/FD4-CMDCS as shown in Fig. 5.8a, and the results are compared with that of the non-diversity technique EV/FBCM and the time-diversity technique EV/FBCM/TD-GDCS. Since we only have simulation results for one bandwidth values, here we could use the cumulative distribution function (CDF) of the absolute ranging errors for comparison, which provides much more performance information than the mean and the standard deviation measures. From Fig. 5.8, we can observe that all three diversity techniques perform better than the non-diversity technique EV/FBCM and the CMDCS-based frequency diversity technique EEV/FBCM/FD4-CMDCS has the best performance.

In order to examine the effects of the number of diversity branches, we increase the number of diversity branches to 10, which is the maximum number of segments of

20 MHz bandwidth that we can achieve from 200 MHz channel measurement data without overlapping segments. The simulation results of the GDCS and the CMDCS based frequency diversity techniques with 10 diversity branches are compared, *i.e.*, the EV/FBCM/FD10-GDCS and the EV/FBCM/FD10-CMDCS in Fig. 5.8b, respectively, with that of the non-diversity technique EV/FBCM and the frequency diversity technique EV/FBCM/FD4-CMDCS, the latter of which has the best performance in Fig. 5.8a. From the results, it is clear that the EV/FBCM/FD10-CMDCS technique has the best performance and even the EV/FBCM/FD4-CMDCS technique has slightly better performance than the EV/FBCM/FD10-GDCS technique, although it has a smaller number of diversity branches. Consequently, from the simulation results we can conclude that frequency diversity techniques can significantly improve the ranging performance and for frequency diversity, the CMDCS diversity combining scheme is strongly preferred to the GDCS scheme by considering the computational superiority, discussed in Section 4.4, that the CMDCS-based super-resolution techniques has over the GDCS-based super-resolution techniques.



(a)



(b)

Figure 5.8: Cumulative distribution function of the absolute ranging errors for a bandwidth of 20MHz with frequency diversity.

5.7 Summary and Conclusions

The super-resolution TOA estimation technique needs to first estimate channel frequency response and then convert the channel frequency response to time domain to estimate the arrival time of the first peak of the time-domain pseudospectrum. Therefore, the empirical frequency-domain channel measurement data can be very conveniently integrated into the super-resolution techniques to study the performance of the TOA estimation in indoor environments. In this chapter we have evaluated the performance of various super-resolution TOA estimation techniques, which are presented in Chapter 4, with the computer simulations based on a set of measured channel frequency response. The indoor radio propagation channel measurement data is collected with a frequency-domain channel measurement system.

From our simulation results, it is clearly observed that the super-resolution techniques can significantly improve the performance of the TOA estimation in indoor multipath channels as compared with the conventional techniques including the direct IFT and the DSSS signal-based cross-correlation techniques. The improvement techniques can further improve the TOA estimation performance, including the EV method, the forward-backward estimation of the correlation matrix, time diversity techniques, and frequency diversity techniques. Two diversity combining schemes, *i.e.*, the GDCS and CMDCS schemes, are studied for the time and frequency diversity super-resolution techniques. The simulation results show that for the time diversity techniques the GDCS diversity combining scheme is preferred while for the frequency diversity techniques the CMDCS is strongly preferred.

It is also observed from the simulation results presented in this chapter that the signal bandwidth has great impacts on the performance of the TOA estimation techniques in the multipath indoor radio propagation channels. For each of the techniques, the larger the bandwidth is, the better the performance. This observation is consistent with our analysis presented in Chapter 3. Also the super-resolution TOA estimation techniques and the improvement methods for the super-resolution techniques all provide significant performance improvement when the signal bandwidth is small, but as the bandwidth increases there tends to be less significant difference between different estimation techniques. It is also noted that because of the possibility of the NLOS condition between the transmitter and receiver antennas in indoor environments, using the super-resolution technique and the large signal bandwidth cannot eliminate the large ranging errors at some locations. The large TOA estimation errors due to the NLOS condition need to be dealt with in the positioning process, which follows the process of the TOA estimation, to achieve good performance of the location finding systems. It is worth to mention that due to the site specific nature and the complexity of indoor radio propagation channels, the simulations based on channel measurement data may reveal varying statistical results so that quantitative performance comparison between different TOA estimation techniques is meaningful only with the same set of measurement data.

There is no suitable multipath channel model available in the literature for the performance evaluation of the TOA estimation techniques in indoor environments. The CRLB derived for the traditional applications is not applicable for indoor applications

due to the existence of the NLOS situation, which can be easily verified with our simulation results. The results obtained from the empirical channel measurement data based simulations provide an insight into the achievable performance in realistic indoor application environments. The measurement data based simulation methods presented in this chapter can be used in practice to conveniently establish the performance benchmarks of the TOA estimation systems in indoor application environments.

In the next chapter we conclude this thesis with a summary of conclusions, and discussions of future work.

Appendix 5.A Measurement Sites and Scenarios

Descriptions of the measurement sites and measurement scenarios are presented in this section for the ease of reference, more details can be found in [Ben99c]. The measurements were conducted at three different buildings, including a manufacturing building at the Norton Co., Worcester, MA, a modern academic building, the Fuller Laboratory at WPI, and a residential house, the Schussler House at WPI. Thirty locations were selected at each site for measurement, including indoor-to-indoor, outdoor-to-indoor, and outdoor-to-second floor communication scenarios.

5.A.1 Descriptions of Measurement Sites

Norton company is a manufacturer of welding equipment and abrasives for grinding machines. The building selected for measurement is Plant 7 that is a large building with dimensions on the order of a few hundred meters. This building is connected to a five floor brick building and to another manufacturing floor through a long corridor. The rest of Plant 7 is mainly surrounded by open areas and small buildings. The building is used for manufacturing abrasives and inside the building are huge ovens, grinding machines, transformers, cranes and other heavy machinery. The building includes a set of partitioned offices with brick external walls, metallic windows and doors attached to the main huge open manufacturing area with steel sheet walls of a height of around seven meters and small metallic windows close to the ceiling. In addition to the fluorescent lights, many utility pipes and metallic support beams hang from the ceiling. A snapshot of the interior view of the building is shown in Fig. 5.A.1.



Figure 5.A.1: A snapshot of Plant 7, Norton Co., Worcester, MA.

Fuller Laboratories at WPI is a modern building that houses the Computer Science department at WPI and has been selected as the site for measurements related to office areas. The dimensions of this building are on the order of a few tens of meters. It is surrounded on two sides by older WPI buildings (the Atwater Kent Laboratories and the Gordon Library) and by roads on the other two sides. One of the road is an internal WPI campus road on the other side of which is the Salisbury Laboratories. The other road is a main road with an open park on the other side. The external walls of Fuller Laboratories are made of brick with some aluminium siding on two sides, metallic window frames and doors. Within the building are several computer labs, department offices, offices of faculty and graduate students, lecture halls, and classrooms. The walls are made of sheetrock and in some offices, soft partitions divide the room into cubicles. Most of the rooms have furniture such as tables, chairs and desks as well as computers. Some conference rooms have glass walls mounted in metallic frames. Figure 5.A.2 shows an exterior view of the building.



Figure 5.A.2: A snapshot of the Fuller Laboratories, WPI, Worcester, MA.

Schussler house is a part of the residences available at WPI for visitors. This is a fairly big residential house with wooden exterior walls and sheetrock interior walls. The house is however very old and some portions of the external walls are made of stone as shown in Fig. 5.A.3. The house is located in a fairly open area with a few buildings of similar features located nearby. Some trees and a parking lot surround other sides of the house. Inside, there are several rooms that are furnished (with couches, tables, chairs etc.). Some rooms have brick fireplaces. Rooms have dimensions on the order of a few meters.



Figure 5.A.3 A snapshot of Schussler house, WPI, Worcester, MA.

5.A.2 Descriptions of Measurement Scenarios

Building layouts with transmitter and receiver locations at the three different measurements sites are illustrated in Fig. 5.A.4, Fig. 5.A.5, and Fig. 5.A.6. Thirty locations are selected at each site for measurement including indoor-to-indoor, outdoor-to-indoor, and outdoor-to-second floor scenarios. Four consecutive snapshots of the radio channel were taken at each receiver location while preventing movement around the vicinity of the antennas of transmitter and receiver. During the measurement, transmitter was fixed at one location while receiver was moved around. For each measurement location, the physical distance between the antennas of transmitter and receiver were determined either directly or indirectly from the blueprint of the building floorplans.

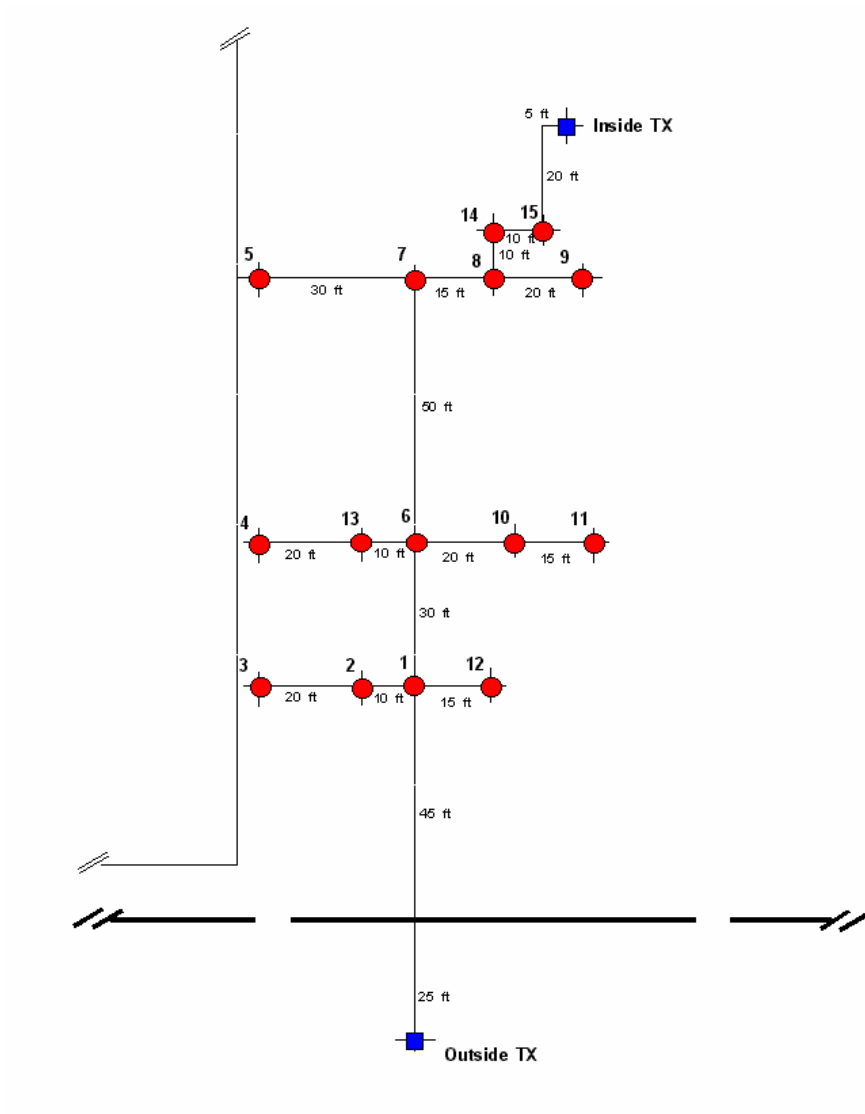
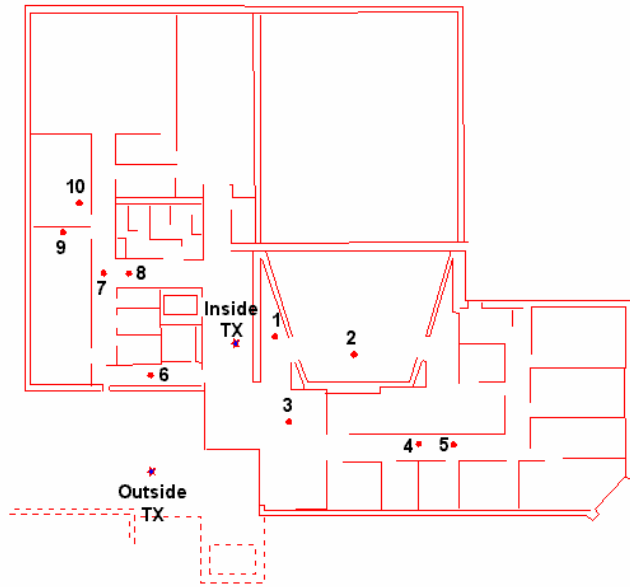
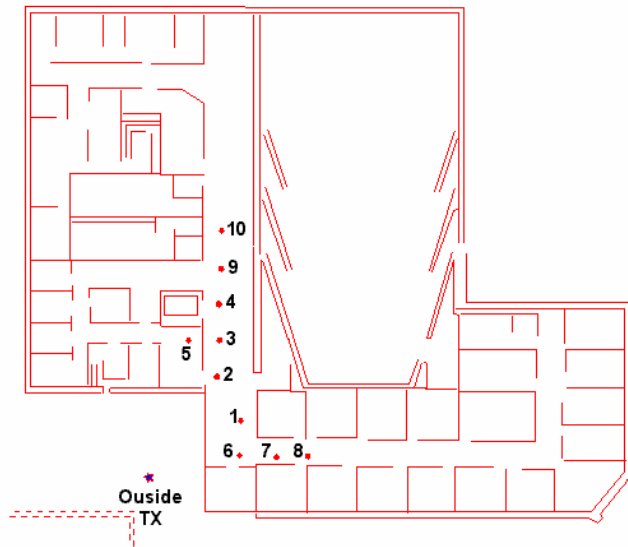


Figure 5.A.4: Building layout with transmitter and receiver locations at the ground level of Plant 7, Norton Co., Worcester, MA.

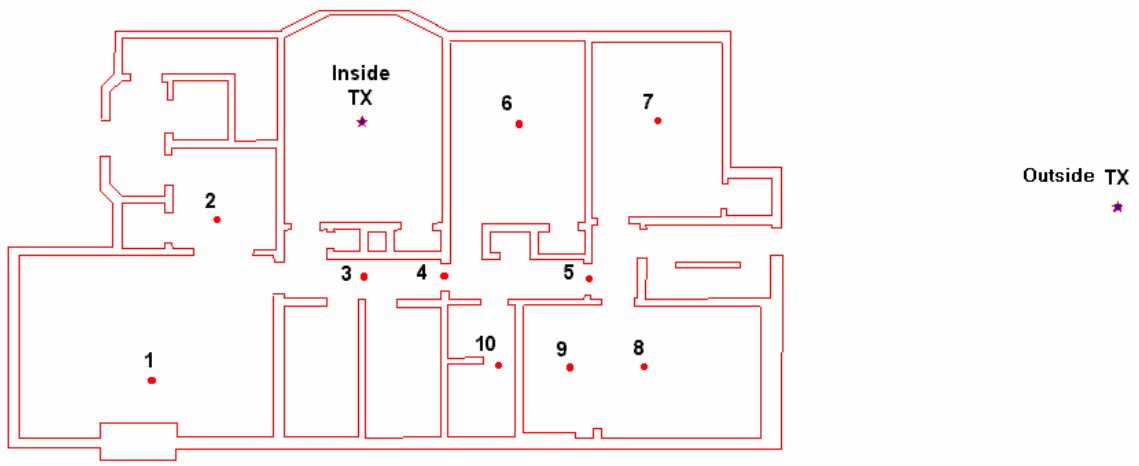


(a)

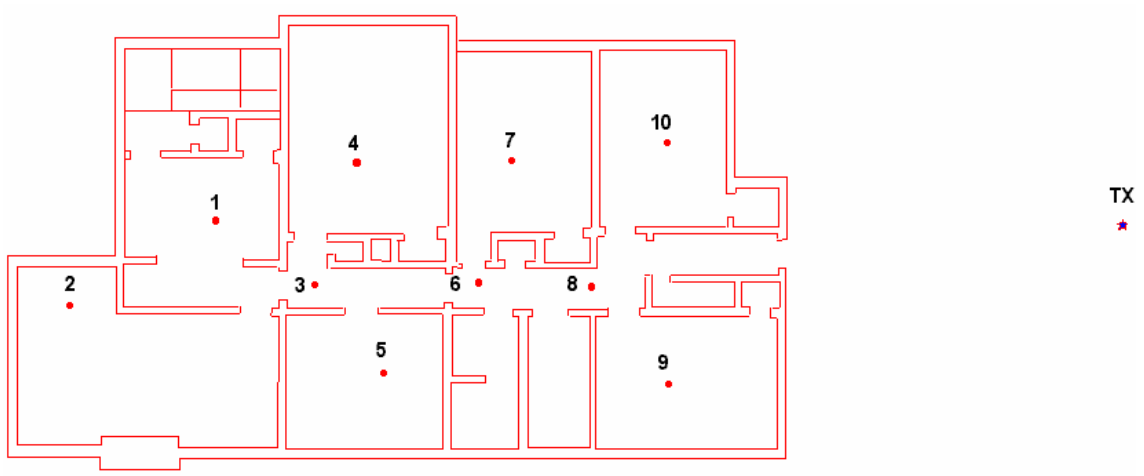


(b)

Figure 5.A.5: Building layout with transmitter and receiver locations at Fuller Laboratories, WPI, (a) for indoor-to-indoor and outdoor-to-indoor scenarios, (b) for outdoor-to-second floor scenarios.



(a)



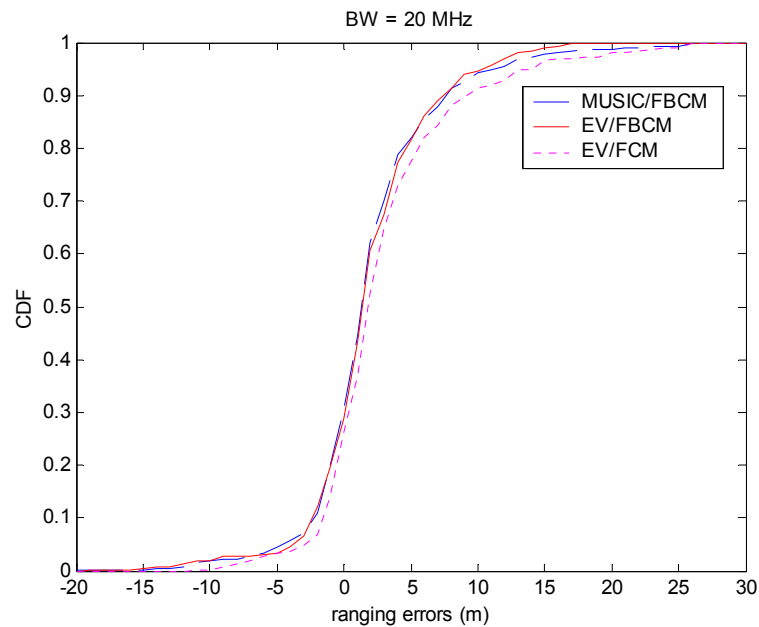
(b)

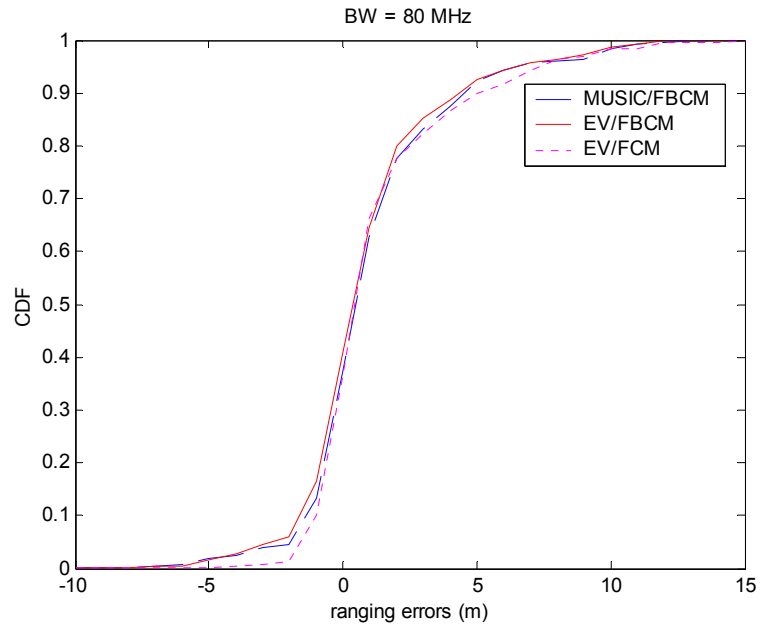
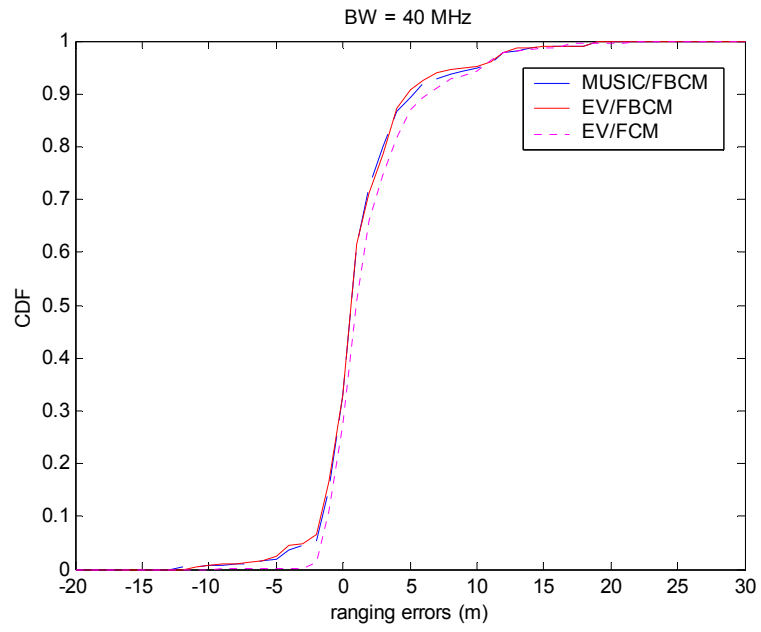
Figure 5.A.6: Building layout with transmitter and receiver locations at Schussler house, WPI, (a) for indoor-to-indoor and outdoor-to-indoor scenarios, (b) for outdoor-to-second floor scenarios.

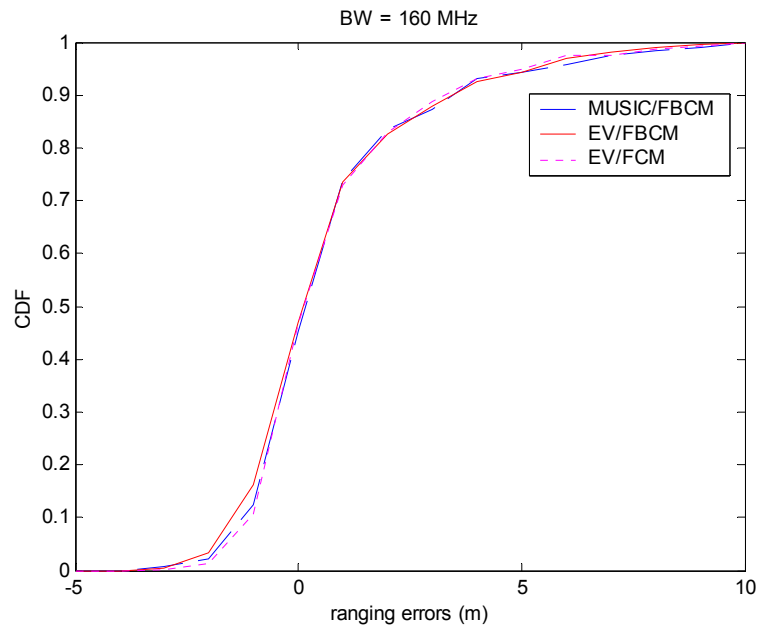
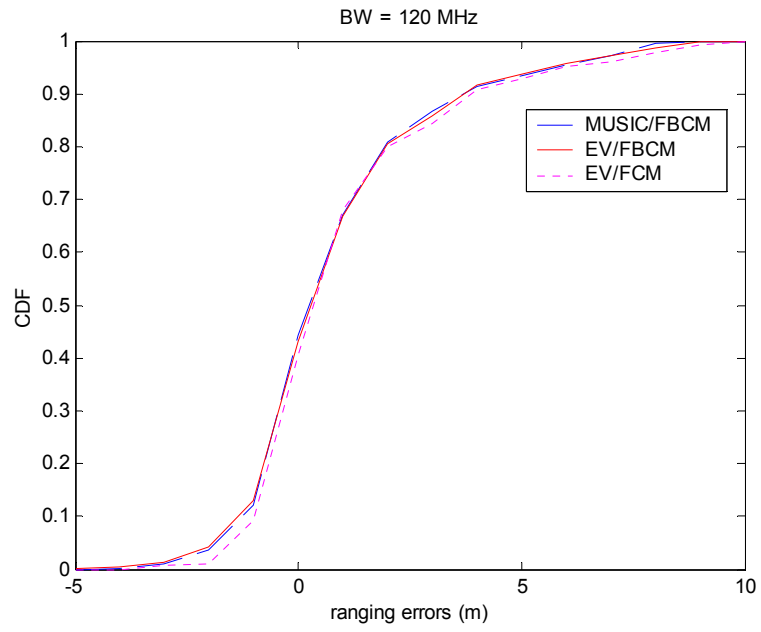
Appendix 5.B Cumulative Distribution Functions of the Ranging Errors

In this appendix, the cumulative distribution functions (CDF) of the ranging errors with different TOA estimation techniques are presented for the reference purposes. The results are organized in subsections to match the results presented in Section 5.3, Section 5.4, Section 5.5, and Section 5.6, respectively. Each figure illustrates the CDF of several TOA estimation techniques for a specific value of signal bandwidth as noted in the title and the legend of the figure.

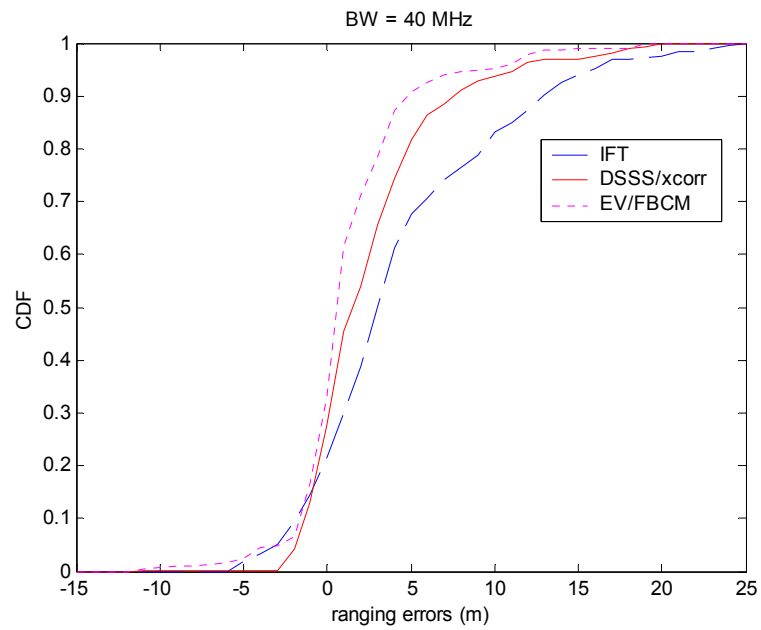
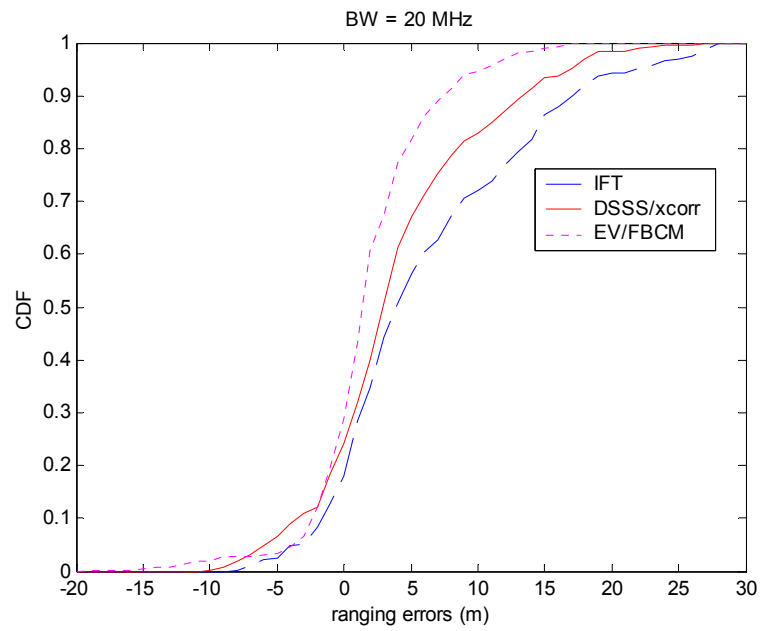
5.B.1 Performance of Super-resolution Techniques

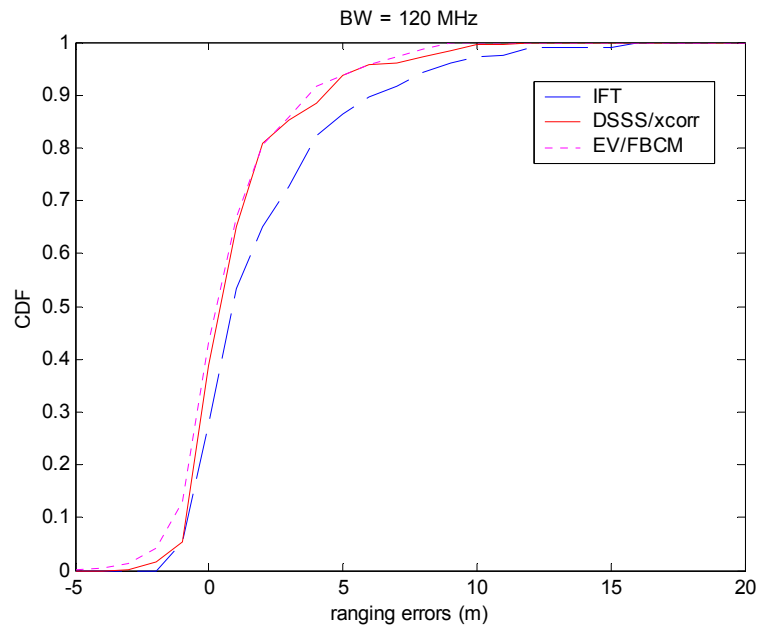
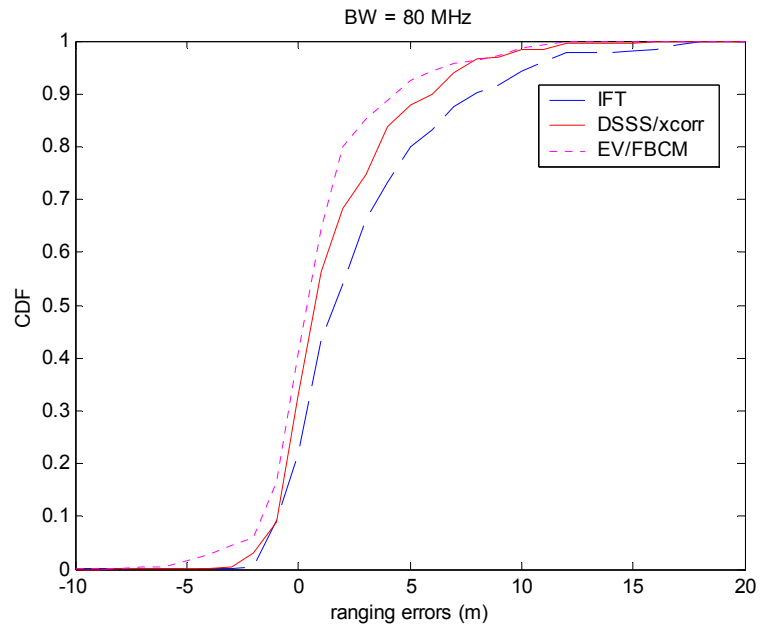


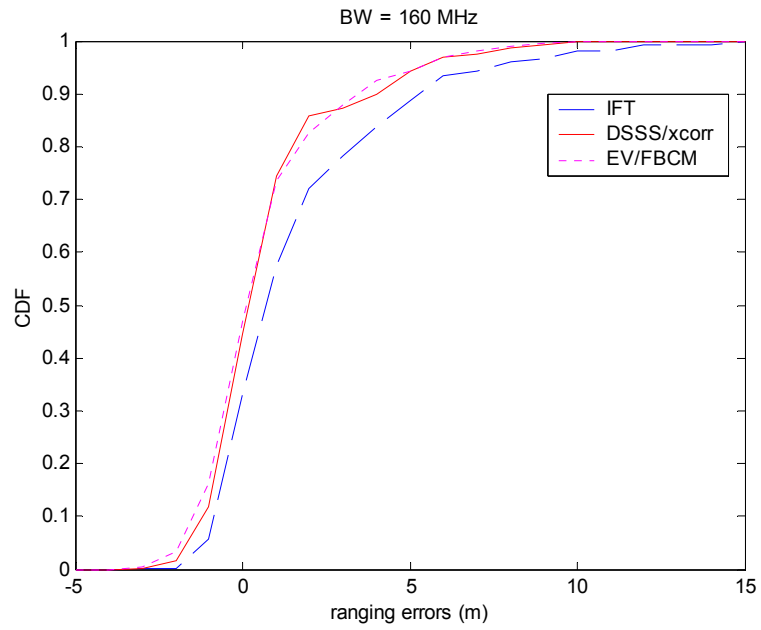




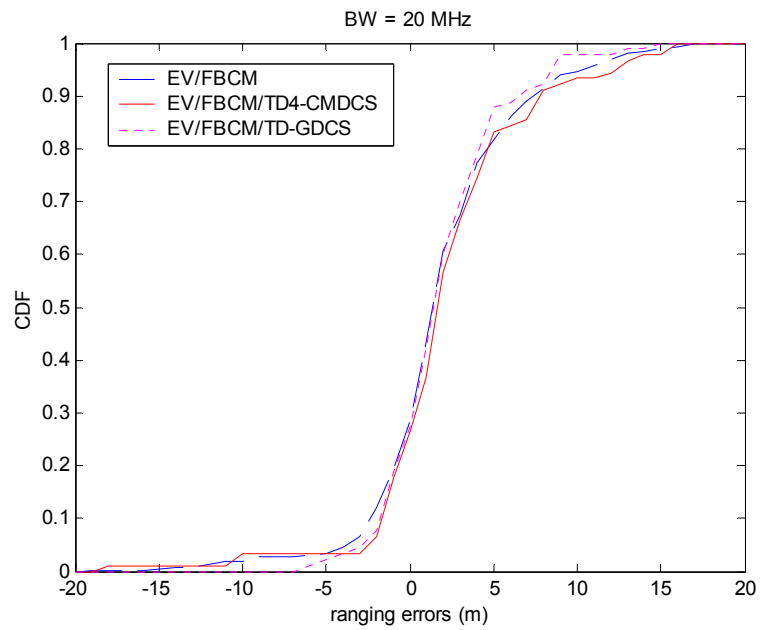
5.B.2 Comparison of Super-resolution and Conventional Techniques

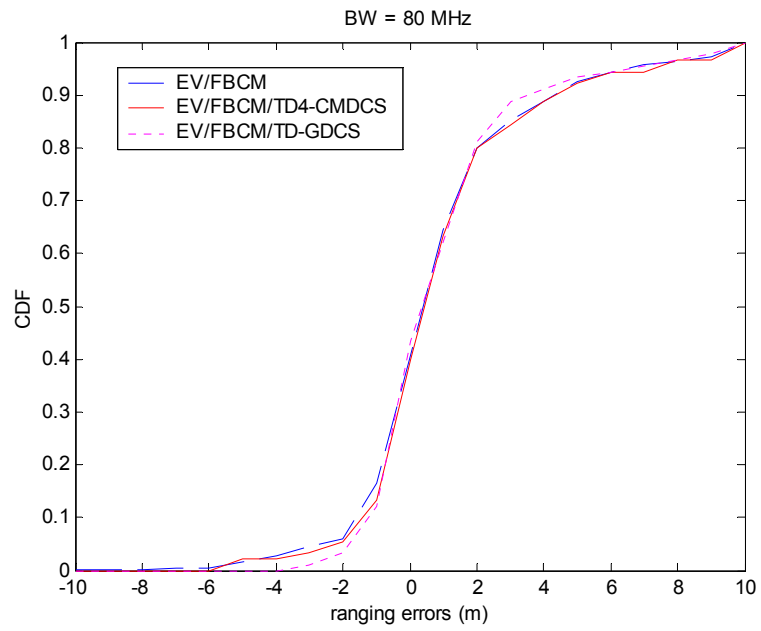
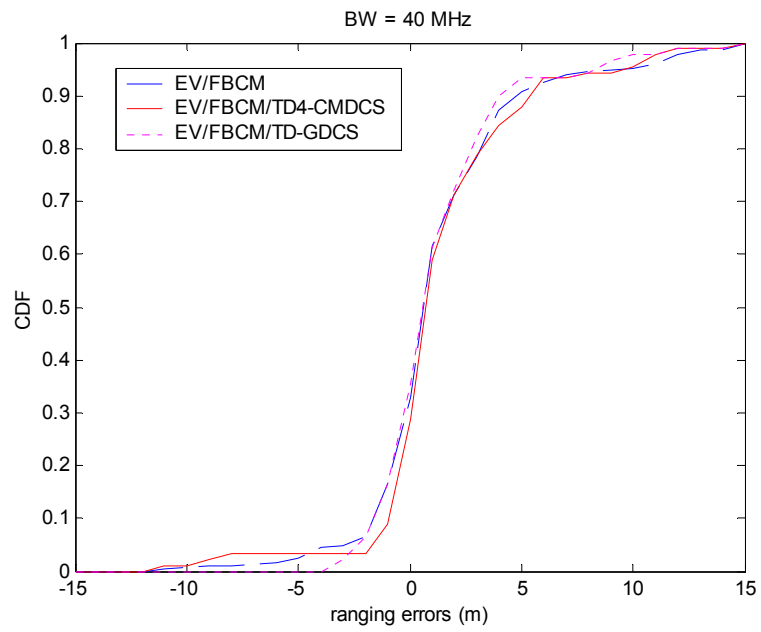


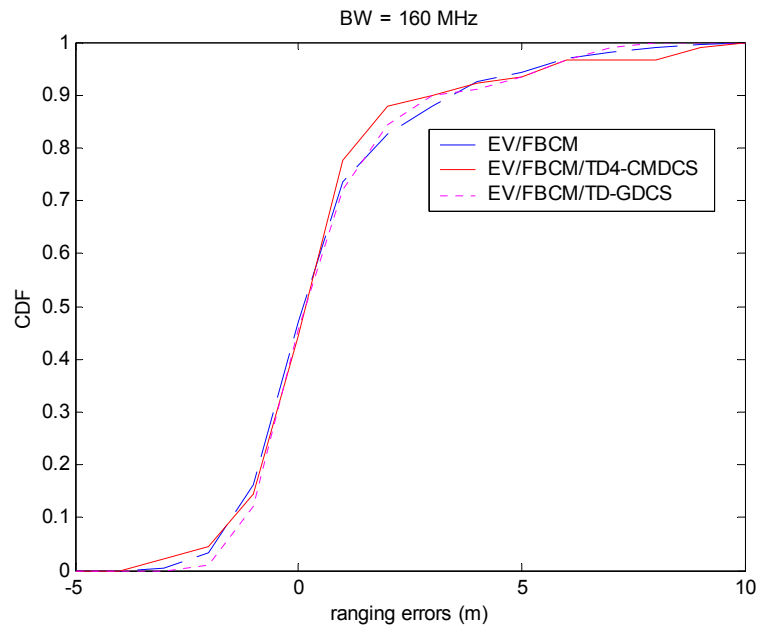
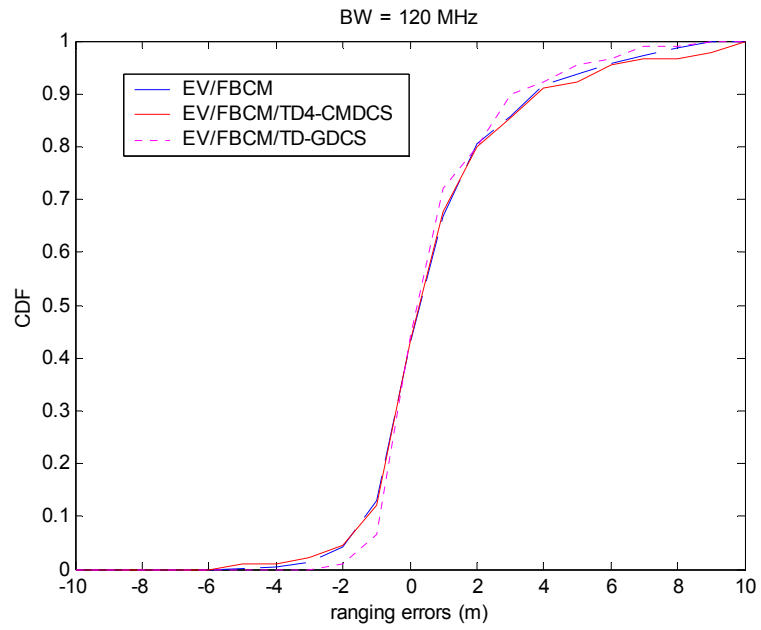




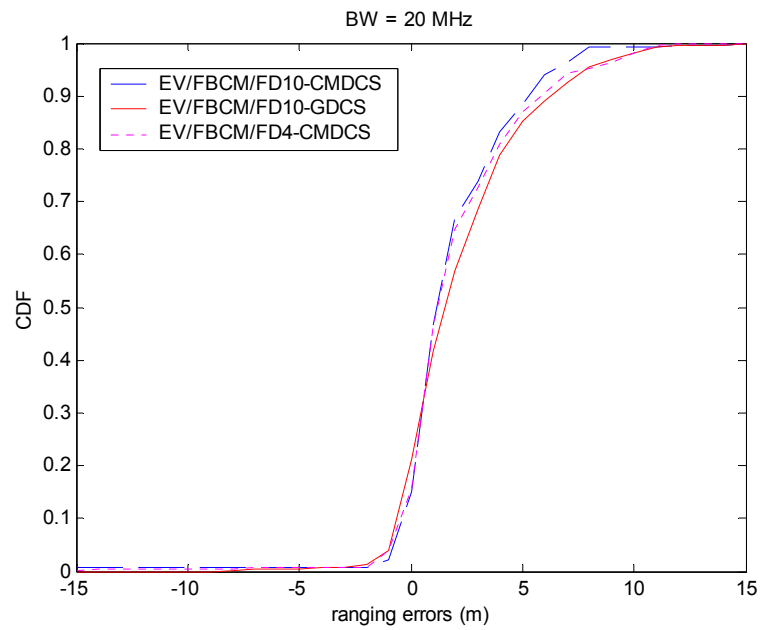
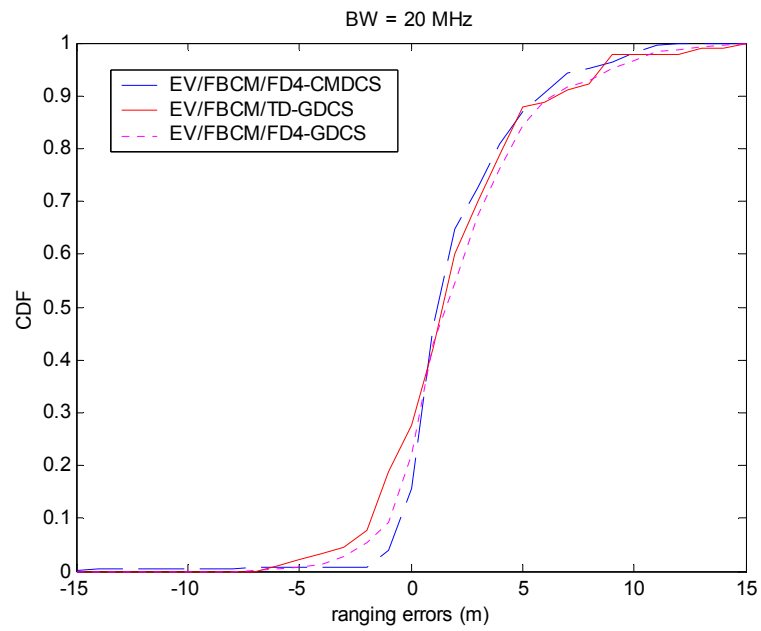
5.B.3 Effects of Time Diversity







5.B.4 Effects of Frequency Diversity



Chapter 6

Conclusions and Future Work

6.1 Conclusions

In this section we briefly summarize the conclusions drawn from our research work presented in this thesis. More detailed discussions can be found in the previous chapters, especially in the last section of each chapter, which specifically summarizes and concludes each chapter.

In recent years, there are great interests in the location-based applications and the location-awareness of mobile wireless systems in indoor areas, which necessitate accurate location estimation in indoor environments. The traditional geolocation systems such as the GPS cannot provide accurate location estimation in indoor environments, so that the indoor geolocation is emerging as a new important research field. In this thesis, we have presented an in-depth study of the location finding systems and techniques, especially the TOA estimation techniques, for indoor applications. The original work presented in this thesis has made contributions in various aspects of this emerging field, which provides a basic foundation for the design and performance evaluation of the indoor geolocation systems.

An overview of a wide variety of the technical issues involved in the design and performance evaluation of the indoor location finding systems have been presented. It is shown that a large amount of research opportunities exist in this new field. First, there is a need for the measurement and modeling of the multipath indoor radio propagation channels for the design and performance evaluation of various location sensing techniques. Second, we need to design new location sensing techniques for the accurate estimation of various location metrics to overcome the challenges caused by the complex indoor radio propagation channels, and new positioning algorithms to compensate for the erroneous estimations of location metrics, to fuse multiple location metrics, and to exploit the unique features of indoor applications. Third, we also need to study the system architectures and the practical deployment methods for the location sensor infrastructure networks in the ad hoc indoor application environments.

The maximum-likelihood TOA estimation technique is studied in details, which was derived for the traditional location finding applications such as the GPS, sonar, and radar. It is shown that in indoor multipath environments due to the complex channel characteristics, dramatically large estimation errors may occur with the traditional TOA estimation techniques, and the CRLB derived for the traditional applications is no longer applicable. The alternative time delay-based location metric TDOA is briefly studied. It is shown that in indoor environments the TOA is more appropriate than the TDOA due to an ambiguity in the TDOA estimation in the multipath channels. The issues involved in the practical measurement of the TOA with spatially separated mobile units are discussed, and the techniques for synchronizing and coordinating the

remotely located transmitter and receiver are studied. A non-synchronized TOA/TDOA measurement method is designed for overlaying geolocation functionality onto the existing wireless networks without significant modification to the existing system infrastructures and signaling formats.

The MUSIC super-resolution spectral estimation algorithm is applied to the TOA estimation applications, on the basis that the frequency representation of the multipath channel model can be viewed as the harmonic signal model. The super-resolution TOA estimation techniques require the estimation of channel frequency response. The practical limitation on the available signal bandwidth poses a limitation on the length of the channel measurement data in the TOA estimation applications. Therefore several techniques are presented to improve the performance of the super-resolution TOA estimation techniques when the channel measurement data is short in length, including the Eigenvector method, the forward-backward estimation of correlation matrix, and diversity techniques. The decorrelation effects of the channel parameter correlation matrix are analyzed for the forward and forward-backward correlation matrix estimation methods and for the frequency diversity techniques. From the analysis we can conclude that the forward-backward estimation method has better decorrelation effects, which leads to the better performance of the super-resolution TOA estimation techniques, and diversity techniques, especially the frequency diversity technique, further improve the decorrelation effects of the correlation matrix. Two diversity combining schemes are proposed for the super-resolution TOA estimation techniques, including the GDCS and CMDCS diversity combining schemes. It is

shown that the CMDCS is computational superior than the GDCS, and the CMDCS is well suited for the frequency diversity techniques, which can significantly improve the decorrelation effects of the correlation matrix.

Since the super-resolution TOA estimation techniques require the estimation of channel frequency response, the empirical frequency-domain channel measurement data can be conveniently employed to study the performance of the super-resolution TOA estimation techniques. Thus, various TOA estimation techniques presented in this thesis are evaluated with the computer simulations based on a set of the measured channel frequency response collected in typical indoor application environments. From our simulation results, it is clearly observed that the super-resolution techniques can significantly improve the performance of the TOA estimation in indoor multipath channels as compared with the conventional techniques including the direct IFT and the DSSS signal-based cross-correlation techniques, and the improvement techniques can further improve the TOA estimation performance, including the EV method, the forward-backward estimation of correlation matrix, and the time and frequency diversity techniques. Also, it is shown that for the time diversity techniques the GDCS diversity combining scheme is preferred while for the frequency diversity techniques the CMDCS is strongly preferred.

From the simulation results it is observed that the larger the signal bandwidth, the better the performance of the TOA estimation techniques in the multipath indoor radio propagation channels. Also, the super-resolution TOA estimation techniques and the improvement methods for the super-resolution techniques all provide significant

performance improvement when the signal bandwidth is small, but as bandwidth increases there tends to be less significant difference between different estimation techniques. It is noted that because of the possibility of the NLOS condition between the transmitter and receiver antennas in indoor environments, using the super-resolution technique and large signal bandwidth cannot eliminate the large ranging errors at some locations.

There is no suitable multipath channel model available in the literature for the performance evaluation of the TOA estimation techniques in indoor environments. The CRLB derived for the traditional applications is not applicable for indoor applications due to the existence of the NLOS situation, which can be easily verified with our simulation results. The results obtained from the empirical channel measurement data based simulations provide an insight into the achievable performance in the realistic indoor application environments. The measurement data based simulation methods presented in this chapter can be employed in practice to conveniently establish the performance benchmarks of the TOA estimation systems in indoor application environments.

6.2 Future Work

As we discussed in Chapter 2, the indoor geolocation is a new research field where many research topics remains to be investigated, including channel measurement and modeling, design of new location sensing techniques and positioning algorithms, study of the practical deployment method for the ad hoc location sensor infrastructure, and *etc.* Since the emerging indoor location-based applications are largely diversified in terms of application environments, application scenarios, accuracy requirements, and system requirements among many other considerations, it is foreseeable that a single technology or system could not fit for the requirements of all location-based applications. This makes the research in the field of indoor geolocation more complicated and more interesting.

The following two specific projects can be conducted as a continuation of the research work on the super-resolution TOA estimation techniques that are presented in this thesis. First, more channel measurement data could be collected to do more site-specific and application-specific performance evaluation of the super-resolution TOA estimation techniques. In this thesis, the channel measurement data used in the performance evaluation simulations were collected from several different buildings for several different application scenarios, but due to the limited number of the measurement data for each measurement scenario, in this thesis the performance evaluation is conducted without classifying the measurement data into different measurement scenarios. It will be interesting and important to study and compare the

performance of the TOA estimation techniques in different application environments and different application scenarios.

Second, study and compare the TOA estimation techniques in terms of performance and implementation complexity. The complexity of the super-resolution TOA estimation techniques may limit its use in some applications. Therefore, it is important to study the implementation complexity and the tradeoffs between the performance and the cost of the practical implementation through theoretical studies and the implementation of a prototype system.

Bibliography

- [Bah00] P. Bahl and V. Padmanabhan, "RADAR: an in-building RF-based user location and tracking system," *IEEE INFOCOM*, Israel, Mar. 2000.
- [Bac97] J. Bacon, J. Bates, and D. Halls, "Location-oriented multimedia," *IEEE Personal Communications*, pp. 48-57, Oct. 1997.
- [Ban02] S. Banerjee, S. Agarwal, *et al.*, "Rover: Scalable location-aware computing," *IEEE Computer*, pp. 46-53, Oct. 2002.
- [Ben99a] J. Beneat, K. Pahlavan, and P. Krishnamurthy, "Radio channel characterization for indoor and urban geolocation at different frequencies," *IEEE PIMRC*, Osaka, Japan, Sep. 1999.
- [Ben99b] J. Beneat, K. Pahlavan, and P. Krishnamurthy, "Radio channel characterization for geolocation at 1 GHz, 500 MHz, 90 MHz and 60 MHz in SUO/SAS," *IEEE MILCOM*, 1999.
- [Ben99c] J. Beneat, P. Krishnamurthy, M. Marku, and K. Pahlavan, "Short range geolocation and telecommunication channel measurement and modeling at 1GHz, 500MHz, 90MHz, and 60MHz," *DARPA SUO SAS Open Review 6*, Washington, Jan. 1999.
- [Ber99] H.L. Bertoni, *Radio Propagation for Modern Wireless Systems*, Prentice Hall PTR, 1999.

- [Bey01] W. Beyene, "Improving time-domain measurements with a network analyzer using a robust rational interpolation technique," *IEEE Trans. MTT*, vol. 49, no. 3, pp. 500-508, Mar. 2001.
- [Caf98] J. Caffery and G. Stuber, "Subscriber location in CDMA cellular networks," *IEEE Trans. VT*, vol. 47, no. 2, pp. 406-416, May 1998.
- [Caf99] J. Caffery, *Wireless Location in CDMA Cellular Radio Systems*, Kluwer Academic Publishers, 1999.
- [Dum94] L. Dumont, M. Fattouche and G. Morrison, "Super-resolution of multipath channels in a spread spectrum location system," *Electronics Letters*, vol. 30, no. 19, pp. 1583-1584, 15th Sep. 1994.
- [Fon01] R. Fontana, "Advances in ultra wideband indoor geolocation systems," *The Third IEEE Workshop on WLAN*, Boston, MA, Sep. 2001.
- [Has02] M. Hassan-Ali and K. Pahlavan, "A new statistical model for site-specific indoor radio propagation prediction based on geometric optics and geometric probability," *IEEE Trans. Wireless Comm.*, vol. 1, no. 1, pp. 112-124, Jan. 2002.
- [How90] S. Howard and K. Pahlavan, "Measurement and analysis of the indoor radio channel in the frequency domain," *IEEE Trans. IM*, vol. 39, no. 5, pp. 751-755, Oct. 1990.
- [How92] S. Howard, K. Pahlavan, "Autoregressive modeling of wide-band indoor radio propagation," *IEEE Trans. Comm.*, vol. 40, no. 9, pp. 1540-1552, Sep. 1992.
- [Iee99] IEEE, *ANSI/IEEE Std 802.11 Wireless LAN Medium Access Control and Physical Layer Specifications*, The Institute of Electrical and Electronics Engineers, Inc., 1999.

- [Jak94] W. Jakes, *Microwave Mobile Communications*, IEEE Press, 1994.
- [Joh82] D. Johnson and S. DeGraaf, "Improving the resolution of bearing in passive sonar arrays by eigenvalue analysis," *IEEE Trans. ASSP*, vol. ASSP-30, no. 4, pp. 638-647, Aug. 1982.
- [Kap96] E. Kaplan, *Understanding GPS: Principles and Applications*, Artech House Publishers, 1996.
- [Kri96] H. Krim and M. Viberg, "Two decades of array signal processing research," *IEEE Signal Processing Magazine*, pp. 67-94, July 1996.
- [Kri99] P. Krishnamurthy, *Analysis and Modeling of the Wideband Radio Channel for Indoor Geolocation Applications*, Ph.D. Dissertation, Worcester Polytechnic Institute, 1999.
- [Lan80] S. Lang and J. Mclellan, "Frequency estimation with maximum entropy spectral estimators," *IEEE Trans. ASSP*, vol. ASSP-28, no. 6, pp. 716-724, Dec. 1980.
- [Li00a] X. Li, K. Pahlavan, M. Latva-aho, and M. Ylianttila, "Indoor geolocation using OFDM signals in HIPERLAN/2 wireless LANs," *IEEE PIMRC*, London, Sep. 2000.
- [Li00b] X. Li, K. Pahlavan, M. Latva-aho, and M. Ylianttila, "Comparison of indoor geolocation methods in DSSS and OFDM wireless LAN systems," *IEEE VTC Fall*, Boston, Sep. 2000.
- [Li01a] X. Li and K. Pahlavan, "Indoor super-resolution TOA measurement in frequency-domain," *The Third IEEE WLAN Workshop*, Boston, Sep. 2001.
- [Li01b] X. Li and K. Pahlavan, "Super-resolution TOA estimation with diversity for indoor geolocation," accepted for publication in *IEEE Trans. Wireless Comm.*, to appear.

- [Li02] X. Li, K. Pahlavan, and J. Beneat, "Performance of TOA estimation techniques in indoor multipath channels", *IEEE PIMRC*, Portugal, Sep. 2002.
- [Lib99] J. Liberti and T. Rappaport, *Smart Antennas for Wireless Communications: IS-95 and Third Generation CDMA Applications*, Prentice-Hall, 1999.
- [Lo94] T. Lo, J. Litva, and H. Leung, "A new approach for estimating indoor radio propagation characteristics," *IEEE Trans. AP*, vol. 42, no. 10, Oct. 1994.
- [Man94] T.G. Manickam, R.J. Vaccaro, and D.W. Tufts, "A least-squares algorithm for multipath time-delay estimation," *IEEE Trans. SP*, vol. 42, no. 11, Nov. 1994.
- [Man00] D. Manolakis, V. Ingle, and S. Kogon, *Statistical and Adaptive Signal Processing*, McGraw-Hill Co., Inc., 2000.
- [Mor95] G. Morley and W. Grover, "Improved location estimation with pulse-ranging in presence of shadowing and multipath excess-delay effects", *Electronic Letter*, vol. 31, pp 1609-1610, Aug., 1995.
- [Mor98] G. Morrison and M. Fattouche, "Super-resolution modeling of the indoor radio propagation channel," *IEEE Trans. VT*, vol. 47, no. 2, pp. 649-657, May 1998.
- [Pah95] K. Pahlavan and A. Levesque, *Wireless Information Networks*, John Wiley and Sons, 1995.
- [Pah98] K. Pahlavan, P. Krishnamurthy, and J. Beneat, "Wideband radio channel modeling for indoor geolocation applications," *IEEE Comm. Mag.*, vol. 36, no. 4, pp.60-65, April 1998.
- [Pah00a] K. Pahlavan, X. Li, M. Ylianttila, R. Chana, and M. Latva-aho, "An overview of wireless indoor geolocation techniques and systems," *MWCN*, Paris, France, May 2000.

- [Pah00b] K. Pahlavan, X. Li, M. Ylianttila, and M. Latva-aho, "Wireless data communication systems," *Wireless Communication Technologies: New Multimedia Systems*, Edited by R. Kohno, S. Sampei, and N. Morinaga, Kluwer Academic Publishers, 2000.
- [Pah00c] K. Pahlavan, X. Li, and J. Beneat, "LANs from office to home - Future directions in home networking", Keynote Speech, *MWCN*, Paris, May 2000.
- [Pah02a] K. Pahlavan and P. Krishnamurthy, *Principles of Wireless Networks – A Unified Approach*, Prentice Hall, 2002.
- [Pah02b] K. Pahlavan, X. Li, and J. Makela, "Indoor geolocation science and technology," *IEEE Comm. Mag.*, pp. 112-118, Feb. 2002.
- [Pah02c] K. Pahlavan, J. Beneat, and X. Li, "Trends in wireless indoor networks," *Wiley Encyclopedia of Telecommunications*, Edited by J. Proakis, John Wiley and Sons, 2002.
- [Pal91] M. Pallas and G. Jourdain, "Active high resolution time delay estimation for large BT signals," *IEEE Trans. SP*, vol. 39, no. 4, pp. 781-788, Apr. 1991.
- [Pro95] J. Proakis, *Digital Communications*, Third Edition, McCraw-Hill, Inc., 1995.
- [Qua81] A. Quazi, "An overview on the time delay estimation in active and passive systems for target localization," *IEEE Trans. ASSP*, vol. ASSP-29, no. 3, Jun. 1981.
- [Rae97] H. Raemer, *Radar Systems Principles*, CRC Press, Inc., 1997.
- [Rap96] T. Rappaport, *Wireless Communications Principles and Practice*, Prentice Hall PTR, 1996.
- [Red87] V. Reddy, A. Paulraj, and T. Kailath, "Performance analysis of the optimum beamformer in the presence of correlated sources and its behavior under

- spatial smoothing,” *IEEE Trans. ASSP*, vol. ASSP-35, no. 7, pp. 927-936, Jul. 1987.
- [Saa97] H. Saarnisaari, “TLS-ESPRIT in a time delay estimation,” *Proc. IEEE 47th VTC*, pp. 1619-1623, Sep. 1997.
- [Sal87] A. Saleh and R. Valenzuela, “A statistical model for indoor multipath propagation,” *IEEE JSAC*, vol. SAC-5, no. 2, Feb. 1987.
- [Sch81] R. Schmidt, *A Signal Subspace Approach to Multiple Emitter Location and Spectral Estimation*, Ph.D. dissertation, Stanford Univ., Stanford, CA, 1981.
- [Son94] Han-Lee Song, “Automatic vehicle location in cellular communications systems,” *IEEE Trans. VT*, vol. 43, No. 4, pp. 902-908, Nov. 1994.
- [Tek98] S. Tekinay, E. Chao, and R. Richton, “Performance benchmarking for wireless location systems,” *IEEE Comm. Mag.*, vol. 36, no. 4, pp. 72-76, Apr. 1998.
- [Tin00] R. Tingley, *Space-time Parameter Estimation and Statistical Modeling of the Indoor Radio Channel*, Ph.D. dissertation, Worcester Polytechnic Institute, Worcester, MA, 2000.
- [Tin01] R. Tingley and K. Pahlavan, “Time-space measurement of indoor radio propagation,” *IEEE Trans. Instrumentation and Measurements*, vol. 50, no. 1, pp. 22-31, Feb. 2001.
- [Tuf82] D. Tufts and R. Kumaresan, “Estimation of frequencies of multiple sinusoids: making linear prediction perform like maximum likelihood,” *Proc. of the IEEE*, vol. 70, no. 9, pp. 975-989, Sep. 1982.
- [Ulr86] B. Ulriksson, “Conversion of frequency-domain data to the time domain,” *Proc. of the IEEE*, vol. 74, no. 1, pp. 74-76, Jan. 1986.

- [Van68] H. van Trees, *Detection, Estimation, and Modulation Theory, Part I. Detection, Estimation, and Linear Modulation Theory*, Jonh Wiley & Sons, Inc., 1968.
- [Wan01] R. Want and B. Schilit, "Expanding the horizons of location-aware computing," *IEEE Computer*, pp. 31-34, Aug. 2001.
- [Wax85] M. Wax and T. Kailath, "Detection of signals by information theoretic criteria," *IEEE Trans. ASSP*, vol. ASSP-33, no. 2, pp. 387-392, Apr. 1985.
- [Wer98] J. Werb and C. Lanzl, "Designing a positioning system for finding things and People Indoors," *IEEE Spectrum*, vol. 35, no. 9, pp. 71-78, Sep. 1998.
- [Wil88] R. Williams, S. Prasad, A. Mahalanabis, and L. Sibul, "An improved spatial smoothing technique for bearing estimation in a multipath environment," *IEEE Trans. ASSP*, vol. 36, no. 4, pp. 425-432, Apr. 1988.
- [Win98] M. Win and R. Scholtz, "On the performance of ultra-wide bandwidth signals in dense multipath environment," *IEEE Comm. Letters*, vol. 2, no. 2, pp. 51-53, Feb. 1998.
- [Xu94] G. Xu, R. Roy, and T. Kailath, "Detection of number of sources via exploitation of centro-symmetry property," *IEEE Trans. SP*, vol. 42, no. 1, pp. 102-112, Jan. 1994.
- [Yam91] H. Yamada, M. Ohmiya, Y. Ogawa, and K. Itoh, "Superresolution techniques for time-domain measurements with a network analyzer," *IEEE Trans. AP*, vol. 39, no. 2, pp. 177-183, Feb. 1991.
- [Yan94] G. Yang, *Performance Evaluation of High Speed Wireless Data Systems Using a 3D Ray Tracing Algorithm*, PhD Dissertation, Worcester Polytechnic Institute, 1994.